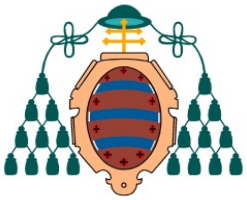

Programa de doctorado

Minería, Obra Civil y Medio Ambiente y Dirección de Proyectos

"Recuperación de terrenos contaminados por actividades mineras y metalúrgicas mediante procedimientos de separación física"

"Remediation of mining and metallurgy Brownfields by means of Physical Separation Procedures"

TESIS DOCTORAL

Carlos Sierra Fernández

Oviedo 2013

“I know of no genius but the genius of hard work”.

Joseph Mallord William Turner

“There is much pleasure to be gained from useless knowledge”.

Bertrand Russell

Abstract

This research develops techniques for the sustainable treatment of contaminated soils, by means of physical separation technologies. The current challenge lies in the promotion of technological solutions for treating contaminated soils, rather than sending them to landfills. The experimental tests were performed in soils of 3 contaminated sites located in the Provinces of Asturias and Linares.

The study was begun with an initial characterization of the soils, including grain-size fractioning, texture, liberation degree determination and chemical analyses. This information was complemented with edaphological, geochemical and mineralogical information of the aforementioned study sites.

Laboratory-scale experiments were conducted to determine the effectiveness and limitations of three specific mineral dressing procedures, namely, classification, gravity concentration and magnetic separation. To this end, three apparatus, viz. hydrocycloning lab-scale plant (C700 Mozley), the C800 Mozley laboratory mineral separator; and the OUTOTEC Laboratory WHIMS 3X4L were tested.

Moreover, the thesis developed and applied two theoretical formulations for the determination of the optimal concentration conditions, during a soil washing operation. The first formulation, a new expression based on attributive analysis, was used for the evaluation and selection of optimal parameters in classification tests, by means of hydrocycloning; whilst the second, based on Shulz separation efficiency, was employed to evaluate the performance of a magnetic separation operation.

Resumen

El objetivo de esta investigación es el desarrollo de técnicas para el tratamiento de suelos contaminados a través de las tecnologías de separación física. El desafío actual radica en la promoción de soluciones tecnológicas para el tratamiento de suelos contaminados que eviten enviarlos a vertedero. Esta tecnología fue probada en los suelos de tres emplazamientos contaminados distribuidos entre las provincias de Asturias y Linares (España).

El estudio se inició con una caracterización inicial de los suelos, incluyendo fraccionamiento granulométrico, determinaciones de la textura y del grado de liberación, así como análisis químicos. Esta información fue complementada con la edafología, geoquímica y mineralogía de los sitios de estudio mencionados.

A continuación, se realizaron experimentos a escala de laboratorio para determinar la efectividad y las limitaciones de tres procedimientos específicos: clasificación, concentración por gravedad y separación magnética. Con este fin se probaron tres equipos a escala de laboratorio: la planta de hidrociclones (C700 Mozley), el separador C800 Mozley, y el equipo de separación magnética de alta intensidad (3X4L WHIMS Outotec).

Además, la tesis desarrolla y aplica dos formulaciones teóricas para la determinación de las condiciones óptimas de concentración, durante una operación de lavado de suelos. La primera, es una nueva expresión basada en el análisis atributivo que se utilizó para la evaluación y selección de los parámetros óptimos en los ensayos de clasificación por medio de hidrociclonado; mientras que la segunda, basada en la eficiencia de separación Shulz, se empleó para evaluar el rendimiento de una operación de separación magnética.

Acknowledgements

I acknowledge the work of all those who have been supportive towards me during all these years at the University of Oviedo, namely, my colleagues, friends and/or professors, but particularly that of the following individuals:

First of all, I would like to express my deepest and sincerest **Gratitude** to my supervisor, Associate Professor José Luis R. Gallego, at the Department of Mining Exploitation and Prospecting at the aforementioned University, for his continual advice, guidance, encouragement, understanding and motivation throughout the course of this thesis.

I am likewise grateful to Associate Professor Juan Maria Menéndez Aguado, of the same Department, for his assistance and patient guidance during the experimental work.

I am in debt to my colleges Eduardo Rodríguez, Dimas Fernández, Ramón Villa, Diego Menéndez and Sergio Gutiérrez for their friendship during all these years and to all the co-authors of the research papers, to all of whom I am most thankful, for their support and diligence in answering my numerous questions. It has been an honour working with all of you.

My appreciation also extends to Professor Guy Mercier and Professor Jean-François Blais for their mentoring and wise advice during my research stay at the INRS-ete in Quebec. Likewise, I would like to express my *remerciement* to his entire team for making me feel at home, though I was more than 5000 km away from it.

Finally, I take this opportunity to express my profound and heartfelt gratitude to my beloved mother and to my father, who encouraged me to complete this thesis before his early death. I cannot forget my maternal grandmother for imbibing ethics during my childhood, unquestionably influencing me to be the person I am today.

Preamble

The context of reconversion that has occurred and continues to occur at different locations in the European territory has led to the abandonment of industrial activity and promoted new development patterns, based mainly on the services sector. This process has generated the emergence of a high number of wastelands, which, in several cases, have high levels of contamination. Many of these sites, particularly those located in urban or periurban areas, are now known by the term "Brownfields", having in common significant levels of pollution in soils. The accumulation of synthetic chemicals in these sites can damage the quality of "soils" in the immediate areas, leading to undesirable risks in living organisms that come into contact with them.

In this regard, it is important to point out that some confusion could arise regarding the use of the word "soil" when applied to these sites. This is because the term is usually understood with relation to an edaphic definition that describes it as a biologically active medium composed of layers of organic and inorganic materials. This contrasts with the state in which they are usually found in Brownfields after years of human activities. In this respect, the term regolith, introduced by Merrill, G. P. (1897) in his manual *Rocks, rock-weathering and soils:* "the entire mantle of unconsolidated material, whatever its nature or origin", could be more appropriate. This is the sense in which many authors unconsciously use the word "soil" when they refer to Brownfields and this is the one used in this thesis.

There are a number of technologies available for the elimination of pollutants from Brownfields, depending on the nature of both the pollutant and the soil. The simplest division establishes different methodologies based on the organic or inorganic nature of the contaminant. In this sense, soil washing is an ex situ decontamination process based on mineral processing technologies, applicable to both organic and inorganic pollutants, which pretends to concentrate the pollutants into a smaller fraction of soil. This proposal will apply different technologies of soil

washing tested at laboratory scale to soils contaminated with heavy metals in an attempt to improve the treatment conditions applicable to them.

Concerning its structure, this thesis has been written up as a compendium of published research papers and has been finally structured into 5 chapters. The introduction, entitled "Introduction to Brownfields and Soil washing", pretends to establish an initial contact with the problems of soil pollution in its social and technical aspects, briefly describing the principles of soil washing technology. The following three chapters correspond to three research papers recently published in the Journal of Hazardous Materials, whilst the fourth corresponds to the one submitted to the same journal in the same thematic. "Conclusion" summarizes, organises and discusses in conjunction the information collected in the previous chapters. Finally, an Appendix has been included with all the papers in the original format in which they were published and it contains the lines of code of the software COS developed for this thesis.

February 2013

Carlos Sierra

MAS, MSCE, MSEV, ME, GE, PGCE

Author´s contribution to the published work

Regarding the authorship, the introductory chapter of the thesis was entirely conducted by the student and includes fragments of his hand-outs for a lecture at the CIEMAT in Madrid. The redaction of all the research papers, the field work, the manipulations of the soil samples, the development of operating protocols and the laboratory experiments were also carried out by the student, supervised by the rest of the authors. The chemical analyses were subcontracted to Actlabs (Canada); SEMEDX, XRD analyses and the magnetic measures were performed at the Scientific and Technical Services the University of Oviedo and interpreted by the author, with the assistance of the technicians. The equations for the optimization of the upgrading are an original idea of the author and the software that automates the calculations of attributive analysis was developed with the invaluable support of Sergio Gutiérrez, Juan Maria Menéndez, and José Luis R. Gallego.

Aim and Objectives

Throughout this research, the author has pursued the **aim** of developing techniques for the sustainable treatment of contaminated soils, by means of physical separation technologies (one of the usual focus of soil washing). The challenge lay in promoting technological solutions for treating contaminated soils, rather than sending the contaminated soil to landfills. This technology was applied to three contaminated sites located in the regions of Asturias and Andalucía (Spain) to test its usefulness in heavy metal removal in order to determine if it could be incorporated into sustainable policy considerations. Thus, the specific **objectives** of this thesis were as follows:

- To introduce a bibliographic compilation on the social, economic and legal aspects of the Brownfields, as well as on the most common soil washing technologies for their remediation.
- To initially characterize the soils of the Brownfield areas, including grain-size fractioning, texture, liberation degree determination and chemical analyses, in order to identify the soil fractions in which the contaminants were bound. This information was complemented with edaphological, geochemical and mineralogical information of the aforementioned study sites.
- To perform laboratory-scale experiments to determine the effectiveness and limitations of three specific mineral dressing procedures: classification, gravity concentration and magnetic separation. To this end, three apparatus: a hydrocycloning lab-scale plant (C700 Mozley), the C800 Mozley laboratory mineral separator and the OUTOTEC Laboratory WHIMS 3X4L were used.
- To develop and apply two theoretical formulations for the determination of the optimal operating conditions for a soil washing concentration operation: the first, based on attributive analysis, is valuable for the evaluation and selection of optimal conditions based on chemical parameters; and the second, based on Shulz separation efficiency, determines the optimal concentration conditions, based on the magnetic properties of the separated materials.

CHAPTER I: "Introduction to Brownfields and soil washing"

1. Concept of "Brownfield"

The term Brownfield has several nuances and its definition varies according to the laws of the respective country. Thus, according to the network CABERNET [1], in Spain, there is no legal definition for this term, except the one given by the Public Environmental Management Company Basque (IHOBE), which defines it as “industrial ruins and potentially contaminated sites”; in the UK, government agencies talk about a "previously developed land that is or was occupied by a permanent structure (excluding agricultural or forestry buildings)"; the German Ministry of the Environment defines it as "inner city areas for renewal and redevelopment"; in France, as "previously developed areas that are temporarily or permanently abandoned after the cessation of activity and need to be recovered for future use, "therefore not requiring the presence of contamination at the site”; and in Poland it is defined as" areas degraded due to diffuse contamination of soil”.

Notwithstanding the foregoing, the origin of the term lies in the United States´ regional planning slang and was first introduced in 1992 in the Congress to refer to lands that had been abandoned and were unproductive, due to the presence of contaminants [2, 3]. Currently, the federal government defines Brownfield, according to the Small Business Liability Relief and Brownfields Revitalization Act of 2002 [4], as: "That real property in which expansion, development or reuse may be compromised due to the perception of the existence or the actual existence of environmental pollution".

The difference between Brownfield, in the original sense of the term (collected by the North American law) and contaminated land is subtle; in fact, all Brownfields are contaminated lands in some way or the other. In order to clarify this, let us, for instance, consider the different types of pollution generated by the petroleum industry. In this sense, the pollution generated during phases of exploration, as well as by transportation by ships, would seldom generate Brownfields, being more likely to generate spills during the life time of the facilities. On the other hand, a former

petrochemical plant, which is out of service and abandoned and which would have generated pollution in the soil, represents a clear example of a Brownfield.

2. Origin and extent of Brownfields

Brownfields are generated by processes called obsolescence; these can be physical, when the abandonment has deteriorated the structures, leaving many of them in a dilapidated condition; functional, when, as a result of technological advances, the facilities do not meet the purpose for which they were designed; internal, for example, when an exploitation is abandoned as a result of the depletion of the exploited resource [5].There is a third type, economical, when the location of the land makes it more viable for other uses, but these do not generate Brownfields due to their rapid replacement of one use by another [6].

Heavy industry, including old steel industries, petrochemicals, chemicals, explosives and fertiliser factories, in addition to military installations and mining, are the main sources of Brownfields. Minor Brownfields are also located in former commercial facilities, as in the case of petrol stations and warehouses; or in transport infrastructures, such as car parks, bus stations, abandoned railroad facilities, etc.

The 2007 update document of the European Environment Agency (EEA) [7] indicates that, typically, the industrial sector is the source of contamination in soils, followed by the service sector and the petroleum industry (Figure 1.1). The same report details that the most typical contamination is caused by heavy metals, mineral oils and polycyclic aromatic hydrocarbons[1].

[1]The U.S. has developed a specific program for the treatment of the sites with very high pollution levels: The Superfund Program.

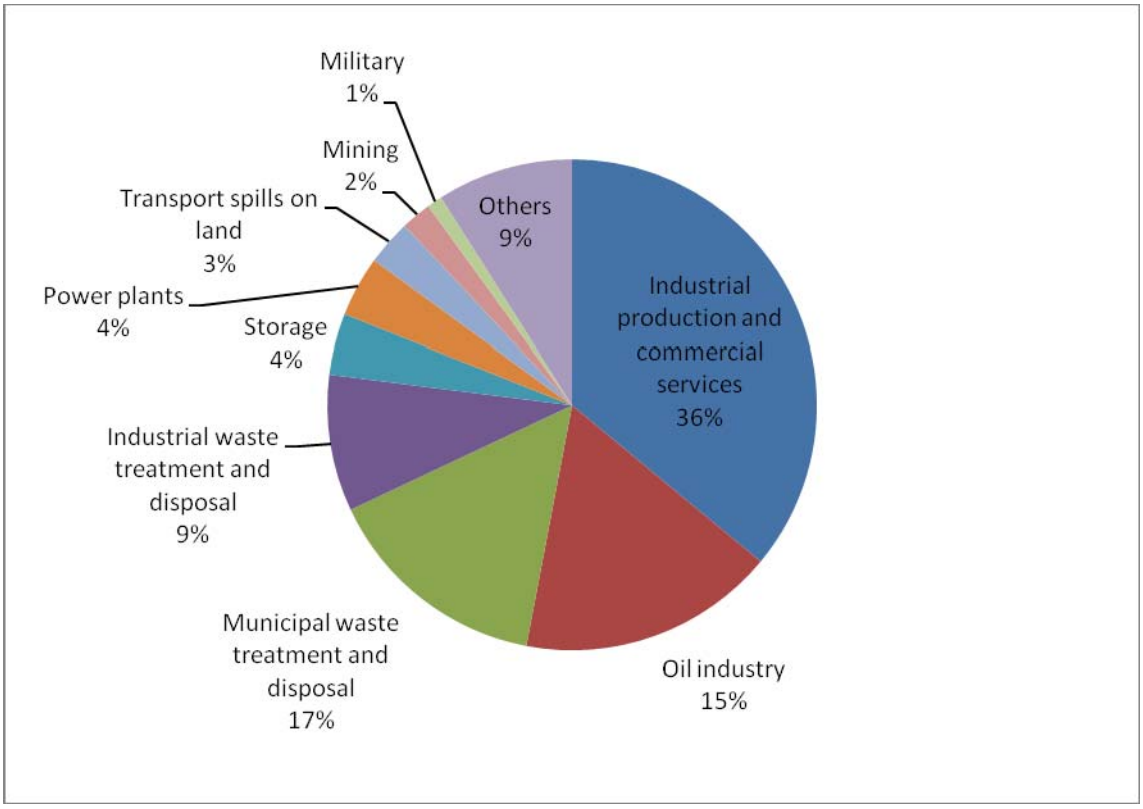

Figure 1. 1 Sources of pollution in the UE (EMain sources of pollution in the UE (EEA).

On the contrary, other activities, generally considered to be sources of contamination, are mining, sourcing of copper, nickel, arsenic, selenium, iron and cadmium contamination; and the military, typically contributing with petroleum by-products and heavy metals (this fact contrasts with the extraordinary importance of the U.S. Department of Defence, frequently reported as the world's biggest polluter) barely represents 1% of the total contamination [7, 8].

From the point of view of size, it is difficult to establish a range of sizes. Thus, in the US, sites below 1 Ha are not considered Brownfields; while, in Europe, the definition is more flexible and variations in the average size range from the smaller sizes of 0.2 Ha (Netherlands, Switzerland, France, and Belgium) to the 250 Ha of some Polish sites, according to the network CABERNET [1].

No comprehensive studies have been conducted regarding the total extent of these areas degraded by pollution in Spain; however, data from other European countries are available. For instance, Germany has 128,000 Ha, the UK 65,700 Ha and France 20,000 Ha [1]. Cases in Germany, where the absorption of the former GDR industry in the early 90s created enormous environmental remediation costs, are especially noteworthy and so are the cases in the US, where the aforementioned EPA's Superfund program has identified and organised hundreds of Brownfields remediation from the 80s, many of which have been associated with the military industry.

3. Advantages of Brownfields Redevelopment

The city planning in Europe has gone through several stages, evolving from the reconstruction stage that took place after the Second World War to the revitalization stage of the 60s, in which the peripheral and suburban growth of cities was developed, to the renewal stage of the 70s, which marked the beginning of a specific interest in the environment. It continued in the 80s, with the development stages and a greater involvement of the private sector and ended in the 90s with the regeneration period, when the currently prevailing concept of sustainable development was introduced [9].

The regeneration of Brownfields is of great interest to the landowner from the environmental point of view, as he is interested in reducing the potential environmental liabilities resulting not only from direct damage generated in the Brownfields itself, but also the damage from the migration of contaminants to adjacent properties. The latter can affect people through drinking water; dust inhalation; or the surrounding natural environment, as aquifers, wetlands or the wildlife. However, despite all these benefits, it is usually the possibility of increasing the market value of the real property, which is ultimately responsible for the interest in decontamination [9].

The recovery of these contaminated sites (in both developed and developing countries) involves a series of improvements to society, among which these three groups have been clearly pointed out by authors like [10, 11, 12, 13, and 14] and these can be summarized as follows:

-**Economic**: Consequence of the jobs created by the regenerating activity or the opportunities for the restoration of existing industrial activity, as it presents an important incentive for developing countries and can be considered an aid for economic development. In this sense, soil clean-up in industrialised nations may help alleviate the rising price of industrial land (now inactive due to the financial crisis). This presented a major problem associated with the exponential growth of housing prices; finally, the existence of cheap land acts as a vital catalyst in the settlement of new industries.

-**Environmental and health**: The release of soil improves the citizens' quality of life, by eliminating hazardous pollutants, which can affect not only soils but also superficial water and groundwater, thereby posing a risk to human health, by increasing the number of diseases and reducing life-expectancy. It also reduces the incursion of the cities in the surrounding urban spaces and vice versa.

-**Urban Planning**: Brownfields redevelopment serves as a renovation of the entire city. The pioneer examples, namely, British cities, such as Bristol and Liverpool, with attractive contributions to urban policy, and in some cases preserving the industrial heritage in integrating the new spaces, must be highlighted.

-Social: The restoration of Brownfields usually causes benefits for the communities, because they are often located in depressed areas that can generate social conflicts and delinquency.

4. Redevelopment of Brownfields and its difficulties

The reclamation project of a Brownfield involves various parties responsible for the viability of the project [15]:

- Municipal representatives
- Representatives of the Local Authority
- The Promoter

- An environmental consultant

- Representatives of the affected community

Many aspects, such as the need for environmental advice from an administration, may hinder the remediation of the site. However, the main responsible for the development of these areas is the promoter and the economic balance he establishes between the value of the remediated land and the value of the land after being recovered. If the balance is negative, the promoter will tend not to execute its purpose or select "clean sites" (green fields) to carry out his investment. This is an undesirable situation, as it involves both the loss of the ability to retrieve a soil and the environmental disadvantages resulting from the development of a green area [16, 17]. In cases where the developer opts for a clean site, the environmental impact could be reduced if he selects a Greyfield (obsolescent site without contamination, generally representing the sea of asphalt in the surroundings of a city) for his purposes. Despite all this, the lack of land in urban areas, together with interest from various administrations as well as the affected communities, has made it possible to reclaim many of these sites in the last few years.

Regarding their redevelopment, aspects such as market conditions, the location of the Brownfield, its size, (economies of scale therefore makes that small sites are often ignored) play a decisive role on their treatment [9]. According to this, Brownfields can be classified into four categories [18]:

• Sites with sufficient market demand, which can be treated without subsidies or incentives.

• Locations that have a certain potential, if they are provided with appropriate assistance or incentives.

• Places that have a very limited market potential even after decontamination

• Locations that are currently operating, but at risk of becoming Brownfields, after the activity is terminated.

Other factors limiting the redevelopment of the brownfields include:

The promoter´s fears regarding the restoration operations, as they can promote, the dispersion of pollutants; in this case, liability exemptions for those who desire decontamination would be reasonable.

The complexity of the legislation on this topic; hence, a simplification of the legislation or unification among countries can be a step forward towards a more efficient decontamination effort. In this regard, the Thematic Strategy for Soil Protection [19] promotes the creation of a Framework Directive at the European level, for unification of criteria.

The limited availability of existing information regarding these contaminated sites makes the decontamination tasks more difficult, as it could be favoured by a more thorough inventory, enabling different countries to make a more efficient use of resources. Similarly, information regarding previous cases of treatment of Brownfields is not generally made public and coordination of the acquired knowledge between private enterprise and scientific community is not usually optimal.

Finally, once the decontamination work has begun, the main factor that could endanger the restoration of a Brownfield is the unexpected presence of contamination that may increase costs and, thus, paralyze the project; hence, an exhaustive characterization of the area before starting the process of decontamination is critical.

5. Local and global examples

Some of the worldwide examples of Brownfields have been appalling, due to the magnitude of the health problems they generate or have generated. In this regard, the periodic classification published by the Blacksmith Institute [20] is of great interest, listing the ten most polluted places on the planet, describing locations or sometimes entire areas where decontamination has become essential due to the high mortality rates of the population and low life expectancy (in many cases close to that of the Middle Ages). Some representative examples in the mining and heavy industry context are listed below.

5.1 Mining Brownfields

One of the emblematic cases is the case of the Kabwe (Zambia) mine, where, 250,000 people are now being affected, as a result of the exploitation of lead for about 90 years in the last century. Kabwe pollution comes from a surface covering of mining waste, residues from the concentrator and mud from the refinery and smelter slag. The lead contaminated soil is transported as sediment by surface runoff during the rainy season; the phenomenon is coupled with the emission of particles due to the wind, which results in lead being easily inhaled or ingested by the population. Currently, the Copperbelt project has received funding from the World Bank and is responsible for dealing with this problem [20].

Other examples of rehabilitation of Brownfields in mining areas, in this case at the European level, can be seen in the old coal mines of Quierschied in Saarland and in the former iron plant of Duisburg, Nordrhein - Westfalen, Germany (already completed).

The first one, with an extension of approximately 115 Ha, interesting industrial heritage and evidences of contamination in soils and waters, has received public investment worth around 40 million Euros. Decontamination has fundamentally comprised phytoremediation and removal of contaminated material. One of the main features of this project was the ability to obtain financing from the private sector, which contributed 35 million Euros in addition to the public investment. In this regard, an interesting initiative comes from the construction of a solar power plant of 8.2 MW, which allows the sale of carbon bonds and the recovery part of the investment [5].

The second one has an area of 250 hectares and with a similar interesting industrial heritage along with the considerable amount of 17 million Euros of public investment; however, it differs from the former due to major pollution in soils and in the variety of remediation techniques that have been employed, including phytoremediation, seals, inertisation and removal of waste. In this case, the restored buildings were given to private companies for their operation. Nevertheless, most of the funding has been public [5, 21, and 22].

Interesting nationwide examples are:

Figure 1.2 Ancient mining and metallurgy Brownfield at: La Soterraña (Asturias), left; Linares (Jaen), right.

The mining district of Linares (Andalucía, Spain) is an old mining and metallurgy area devoted to the beneficiation of Pb from galena (PbS), since Roman times (figure 1.2). The activity was expanded greatly during the nineteenth and early twentieth century, until the installations were dismantled at the beginning of the 90s. Anomalous concentration of trace elements has been detected in the entire area, causing a threat to human health and the environment [23].

The former Asturian mercury mining (until the end of the 1970) left us notable examples, such La Soterraña (figure 1.2). This is an ancient mining area exploited since the middle of the XIX century, wherein cinnabar (HgS), which was accompanied by orpiment (As_2S_3), realgar and pararealgar (AsS), As-enriched pyrite and marcasite (FeS_2), and arsenopyrite (FeAsS), in a gangue of quartz and calcite, was exploited. Together with these mining activities, mineral dressing and metallurgy were also carried out intermittently. The process consisted of a milling steep, which was followed by roasting, to obtain Hg vapour, which was then condensed. These activities caused not only the accumulation of a substantial amount of waste, but also a halo of contamination, due to the emissions from the chimneys [24].

5.2 Industrial Brownfields

The case of Sumgayit in Azerbaijan is noteworthy, where more than 40 factories generated several different types (pesticides, aluminium, detergents, and mercury) of chemical contamination, affecting about 275,000 people by increasing cancer incidence rates and doubling the average of Azerbaijan. The site has also been collected in the study of the Blacksmith Institute [20]. According to the Institute, it received funding from the World Bank, the UK and even from Japan. Despite the closure of many of the facilities after the decline of the Soviet Union, the site still faces several challenges concerning the treatment of the existing contamination.

Figure 1.3 Former industrial complexes in Asturias: Ensidesa (Avilés), left; and Nitrastur (Langreo), right.

The most representative industrial remediation in Europe took place in East London in case of the 2012 Olympics celebration. Decontamination operations included bioremediation, stabilization, immobilization, thermal desorption, dredging and soil washing. Thus, more than 1.5 million tons of contaminated soils were treated in the biggest soil washing operation ever conducted in the UK [25]. The pollution was caused by oil, gasoline, lead, arsenic and cyanides. More than 80 per cent of the soils were cleaned by soil washing and bioremediation, with more than 90 per cent of demolition materials were recycled [26].

In Asturias, we highlight the cases of the former Steel Factory of ENSIDESA in Avilés and Nitrastur Factory (figure 1.3):

The former covers a total area of 110 hectares, wherein significant amounts of various types of waste, were abandoned. This pollution included temporary dumping areas, leakages, demolition debris, fuel deposits, electricity transformers, etc. A new industrial area for new medium and heavy industries was built on the released land. This involved the construction of new access roads, internal roads and utility networks [27].

The latter is a former industrial complex located in Langreo (Spain, devoted to the production of fertilizers, among ammonium and sulphate nitrates. Since its closure in 1997, this factory has been partially demolished and it is currently in an advanced state of abandonment. The total surface of the affected site is 70,000m^2, more than half of which corresponds to landfills between 4 and 5m deep, comprised of pyrite ashes in addition to other iron and steel-type debris [28]. Projected by the engineer Carlos FernándezCasado, it is one of the largest abandoned industrial sites in Spain with an area of 200,000 m^2.

6. Technical aspects in the recovery of Brownfields

The following points should be considered when performing a Brownfield redevelopment:

- The initial phase of the work may require a small study of the "industrial archaeology", based on interviews with some of the former workers and the collection of information on industrial processes taking place in the area.
- Sampling campaign must be representative, with a considerable number of in-field samples being taken. Making a well-detailed site investigation will prevent sudden surprises later on in the remediation stage.

- In this respect, analytical techniques of "in situ screening" can be useful, allowing for very important analytical expenditure savings, providing the location of batches and guiding all the subsequent analytical work. The most common techniques are the portable X-ray fluorescence for analysis of heavy metals and portable chromatographs or simple gas meter in the case of organics.

- If the site is very large (several ha), a detailed hydro geological study must be performed, using geophysical techniques if there are underground structures (collectors, piping, etc.)

- A detailed risk-analysis should be performed, considering several scenarios based on future land.

- In some cases, given the legal implications that may be involved, true environmental forensics should be conducted, limited not only to the quantification of the contaminants in the different areas but also to the determination of their origin, age and evolution.

- In any case, obtaining a conceptual model of the site and understanding the underground movement of the pollutants are very important in these cases. This model also needs to be translated into graphs and informative reports to make it accessible to all the involved parties.

6.2 Selection of the remediation technology

Nowadays, multiple technologies are being employed in the treatment of contaminated soils. In general terms, these are usually classified in accordance with the location of the soil during the treatment in in-situ, and ex-situ. The former encompasses the decontamination works taking place at the same site where the polluted soil was originally found; whilst the latter designates those that take place after excavating the soil. In the second case, soil treatment can take place on-site, that is to say, in the same Brownfield, or off-site, that is transferring them to another location [29].

While selecting technologies for site recovery, the fundamental problems faced are the costs. Thus, the size and complexity of pollution tend to be coupled with costly operations that, nonetheless, must be confronted. One of the important thumb rules is that, the use of landfills (except for pure waste) must be avoided.

In general, **corrective actions for contaminated soils** can be classified as follows [29]:

- Isolation / containment,
- "Transfer" to a landfill or
- Pollutant Removal

Thus, we can choose between two options: recovering the soil or destroying it. While the first option was the most common in the past, the current legislation in a majority of countries prefers the latter. In this respect, a wide range of technologies, including thermal, physical, chemical and biological ones can be selected for this purpose [29]. The most common techniques of each of these groups are shown in the table 1.1 below.

Table 1. 1 Decontamination techniques classification.

Physicochemical	Biological	Thermal
Vapour extraction	Biodegradation in situ	Incineration
Air injection	In situ bio stimulation	Thermal desorption
Aeration	Bioventing	

Water pumping	Bio slurping
Soil Washing	On-site ex-situ biodegradation
Electrokinetic treatment	Landfarmig
In situ chemical treatments	Bio cells
Permeable reactive barriers	Composting

The presence of housing or residential areas near the site, which is very common, may influence the selection of one of these techniques, because some of them may involve significant inconveniences for the local communities (dust, noise, emissions of gases). That is the case, for example, in thermal desorption.

The use of long-term passive remediation techniques to refine the result of the decontamination is highly recommended. In fact, the usual pattern of such work involves beginning with an initial soil washing combined with soil bioremediation of and/or thermal desorption, followed by a second phase of natural attenuation and/or phytoremediation.

6. Soil washing: physical separation and chemical extraction

Soil washing is a broad term that usually refers to two kinds of cleaning technologies, namely, physical separation and chemical extraction, although other terms, such as soil recycling or volume reduction are usually applied [30].

Thus, physical separation is a particle separation process that removes the contaminants from the soil, by concentrating them into a minor volume exploiting the differences between the characteristics of metal-bearing particles and soil particles (size, density, hydrophobic surface properties, magnetism), in a way similar to the treatment of mineral ores. On the other hand, chemical extraction is a procedure that desorbs and makes soluble the metals contained in the soil, by means of chemical reagents, thus resembling a hydrometallurgical procedure.

There are several parameters controlling the efficiency of the physical separation process *viz*. particle size distribution, particulate shape, clay content, humic content, heterogeneity of soil matrix, difference in density between soil matrix and metal contaminants and magnetic properties [30, 31, and32], However, the two main parameters to consider before starting a physical separation project in a soil are: liberation degree and proportion of fines and the volume of soil to be treated.

The first indicates the percentage of a particular phase that occurs as free particles in relation to the total of that phase that appears in free and locked forms [33]. The second is important because an elevated proportion of fines can affect the soil washing process. This is because a significant portion of it is usually performed by size classification. Thus, if the entire soil is silted or clayed, it indicates that most of the pollutants can be sorbed to these fractions, in which case chemical extraction is preferred. If a physical soil washing process is to be chosen, it is important to consider the volume of soil to be treated, because soil washing can be a cost-effective alternative only if this volume is significant [34].

6.2 Physical soil washing technologies

Physical separation of pollutants in soils uses the technology applied by the mineral processing to obtain the desired minerals from their ores. A summary of the technologies used for this thesis are shown in table 1.2.

Table 1. 2 Classification of the main physical separation procedures used for soil washing purposes: Adapted from [30, 31].

	Size washing	Washing by sedimentation velocity	Gravity washing	Magnetic washing
Fundamentals	Several open diameters: passage of particles of different size	Different ratios of sedimentation due to size, shape or density	Separation due to density differences	Magnetic susceptibility
Advantages	High level of continuous processing with simple and inexpensive equipment.	High level of continuous processing with simple and inexpensive equipment	High level of continuous processing with simple and inexpensive equipment	Recovery of a wide variety of materials when used on soil with very different properties.
Limitations	Dry processes produce dust	Difficult process when high proportions of clay, silt and humic materials	Difficult process when high proportions of clay, silt and humic materials	The process involves high operating costs

Equipment	Screens and trommels	Hydrocyclones	Shaking tables, spirals and jigs	Magnetic separators

The unit operations involved are: attrition scrubbing, classification, gravity concentration, froth flotation, magnetic separation and electrostatic separation.

The description of all the apparatus used in soil washing plants exceeds the limits of this introduction. Consequently, merely an overview has been provided and should the reader desire to get more information regarding this field, he should refer himself to a mineral processing book [33, 35] or a review of soil washing technologies [30].

6.2.1 Classification

As stated above, the natural tendency of the contaminants is to concentrate on the finer fractions of the soil, given the higher specific surface of the clay particles and the organic matter. Thus, if these fractions are separated, the concentration of pollutants in the soil can be reduced with a significant decrease in volume of up to 95% of the original soil. In this regard, classification is a process of separation of the grains on the basis of their velocity in a fluid under the action of the forces of gravity or centrifuge. This process is mainly dependant on the size of the particle and also on its density and shape.

When the objective of the classification is the separation of the grains on the basis of their dimensions, in this case, operating on diluted pulp is recommended. Conversely, when the contrast between the different masses of the particles needs to be enhanced, the device should be operated with a pulp as dense as possible**.** Most common size classifiers used in soil washing are the log washer, spiral classifiers, rake classifiers and hydrocyclons. The last one has been used in the experimental of this thesis.

Hydrocycloning

A hydrocyclone (figure 1.4) is a device that applies centrifugal force to a liquid mixture, promoting the separation of the particles in a water suspension, by establishing a force balance between the centripetal force and the resistance of the fluid. This ratio is low in case of light and fine particles and high in case of dense and coarse particles.

Figure 1.4 Hydrocycloning lab-scale plants at the laboratory of mineral processing the Campus of Mieres (Asturias, Spain).

A Hydrocyclone uses a tangential injection flow process, transforming the velocity of the incoming liquid into rotary motion, which enhances the centrifugal forces resulting in moving solid particles outwards. Heavy components move outward and downward in a spiral path towards the underflow discharge (sedimentation tank), whilst light components move upwards towards the axis of the hydrocyclon, wherein a vortex has been created and are discharged at the top.

This is a compact separation unit with easy operation and installation, small dimensions, cheap maintenance, offering versatility in its configuration.

6.2.2 Gravity concentration

Gravity concentration is a method that separates particles based on their gravity, according to their relative movement in a viscous fluid, generally air or water.

When this separation method is chosen, a significant difference in the density between the clean soil fractions and the metal bearing fractions is a must. In order to assess the effectiveness of an eventual separation operation, the concentration criterion has been established (Wills), thus:

$$C.C = \frac{D_h - D_f}{D_l - D_f}$$

Where D_h denotes the density of the heavy soil fractions, D_l is the density of the light fractions and D_f is the density of the fluid medium.

It has generally been established that the higher the C.C for a given group of particles, the better the performance of a separation operation. Table 1.3 represents the minimum possible C.C for a concentration to take place, as a function of the particle grain size. This limit is higher in case of the smallest grain sizes (for instance 2.5 for a grain size of 100 μm) and smaller for the coarser ones. In practical terms, this can be traduced to mean that density difference between particles must be at least $1 g/cm^3$ for satisfactory separation [30, 36].

However, this threshold is dependent on the size of the particles that are to be separated. In general, the larger the size the better the performance of the gravity separation [37]

Table 1. 3 Variation of the limit for the concentration criterion as a function of the grain size [37].

Concentration criterion (C.C.)	Suitability to gravity separation
> 2.5	Easy down to 75 µm
1.75-2.5	Possible down to 150 µm
1.5-1.75	Possible down to 1,7 mm
1.25-1.5	Possible down to 6,35 mm
<1.25	Impossible

There are several mechanisms by which gravity concentration can take place [38]:

1-**Density**

This kind of separation takes place as a consequence of the differences in the buoyancy forces acting on the particles in free-fall in a fluid medium. According to these forces, some will tend to sink whilst others will float. A common example is heavy medium separation.

2- **By flowing film**

This kind of separation relies on the fact that a laminar flow has different velocities, depending on the depth from the free surface of the film, zero at the bottom and maximum at it; according to this, lighter particles are dragged by the flow, while the heavier ones will tend to accumulate.

3- **Stratification**

The components of the soil are separated on the basis of alternative updrafts and downdrafts that classify the miners in the vertical plane, according to their density. The most common example is the jig.

4- **Shaking**

The particles tend to stratify due to the asymmetric acceleration caused by the oscillating or orbital movement of a board in which they lie. Typical examples of this type of separation (that is coupled with the flowing separation) are the shaking table and the Bartles-Mozley separator.

If a concentration operation lies outside the aforementioned criteria, it does not necessarily mean that separation is impossible, but rather that separation is not possible in simple g devices, such as Jigs, tables, sluices, spirals; nevertheless, if the conditions of the concentration are changed, for instance, by introducing Multiple 'g' devices, the separation can still take place. In this regard, the MGS concentration is an interesting device, which enables separation, as stated above, of particles larger than 1 mm in size and a difference of density of more than 1 g/cm^3 [30].

Another alternative is to increase the density of the medium fluid. In this case, there is an improved separation (see concentration criterion), as the lighter phases tend to float in the medium whilst the heavy phases sink.

Gravity separation yields are the worst when it is used to treat particles with either a narrow density distribution or a wide granulometric distribution [30]. Consequently, close feeding granulometrics is preferable for reducing the size effect and enhancing the specific gravity separation.

C-300 Mozley Miner al separator

In this thesis, an experimental apparatus, the C-300 Mozley Mineral separator (figure 1.5)**,** has been used in order to separate the finest fractions of the soil by means of gravity concentration procedures. The operating principle of this system appears to be the same as the one in the concentration in stationary table (governed by the principle of the thin flowing film) to which an orbital movement has also been added, incorporating an acceleration that is responsible for the asymmetric intermittent advance of solids on the board.

Figure 1.5 C-300 Mosley Mineral Separator.

The order of deposition of particulate matter from upstream to downstream, under the effect of this principle is:

1. Fine heavy particles

2. Large particles and fine light heavy

3. Light large particles

If an asymmetrical acceleration is added to the previously described principle, the particles of the board are subjected to 3 forces, one due to the acceleration of the board; the second caused by friction between the board and the particle (the simple action of this phenomenon is capable of separating minerals); and the third as a consequence of friction among particles.

In consequence, this new orbital motion enhances the separation of the particles by gravity (Newton´s second law), rather than by grain size (Stokes´ Law), as is the case in thin film separation.

From the above, it would appear that the concentration in this device depends on the following parameters:

- The slope of the board
- The thickness of the sheet (or fluid flow ratio)
- The coefficients of friction between the different particles and the board.
- The density of the particles
- The shape of the particles
- The relationship between the acceleration of the board and time taken to complete a cycle.
- The roughness of the board (fixed for this separator)
- The viscosity of the fluid (fixed: water)

6.2.3 Magnetic separation

Minerals present in soils can have their origin in the parent rocks, be formed as a consequence of the alteration of the parent rock during the formation of the soil or produced from human activities. In case the magnetic background is not excessive, some magnetic measurements show a strong correlation between the magnetic properties of the soil and the pollutant content [39, 40, and 41].

It can be assumed that this correlation is based on a) the common origin that many pollutants share with the magnetic particles, as a consequence of anthropogenic activities. This is, for instance, the case in ashes originating in coal power plants, having Fe and other heavy metals in their composition, b) the presence of Fe and Mnoxyhydroxides that are chemically active and preferentially adsorb other metals on their surface.

The Magnetic separation procedure has been widely used for the concentration of mineral ores and in soil washing to remove pollutants from contaminated soils [42, 43], in order to protect the crushers and mills from the metal fragments that may be present in the soil or for the removal of certain phases present in the soil rich in contaminants of Mn, Cr, Sn, Zn.

This is a mechanical procedure that exploits the differences between the magnetic properties of the phases present in the soil, to separate them according to their magnetic susceptibility [44].

Based on this, materials with positive magnetic susceptibility are attracted by a magnetic field, whilst those with a negative value are weakly repelled from the magnet. Therefore, materials can be classified into 3 broad groups, based on whether they are attracted or repelled by a magnet.

Thus, substances with a highly positive magnetic susceptibility, which can be easily separated by means of low intensity magnetic separators, are usually termed “magnetic”. This classification includes the ferri- and ferro-magnetic materials and is characterised by their capacity to multiply the magnetic flux density (B) within them [44, 45]. Those substances with a lower positive magnetic

susceptibility need a high intensity magnetic separation in order to be trapped from a mixture containing diamagnetic particles and, in consequence, are usually termed “weakly magnetic”. This includes the para- and antiferro-magnetic materials, which barely increase the magnetic flux density in their surroundings [46]. Finally, the last group designates materials with a slightly negative magnetic susceptibility, as “non-magnetic”, which, in consequence, cannot be separated by means of magnetic separation. These materials weaken the magnetic field in their presence [46] and although all materials show some degree of diamagnetism, these generally exhibit a weak effect that can be ignored or a small correction to a large effect. All these properties, other than diamagnetism, which is present in all substances, have their origin in the interactions of unpaired electrons at the molecular level.

Thus, a substance is ferromagnetic if all of its unpaired electrons are aligned, thereby causing a positive contribution to the net magnetization. On the contrary, if some of the unpaired electrons reduce the net magnetization, to wit, if they are partially anti-aligned (anti parallel, or paired off in opposite directions), the substance is termed as ferri magnetic [45]. The magnetic properties of these two kinds of materials disappear above a temperature termed as the Curie temperature; if these materials are cooled down again, the initial magnetic properties are restored [46].

Ferromagnetism is found in elemental metals, such as Fe, Ni, Co and some of their alloys. Ferrimagnetism mainly occurs in ferrites and in magnetites.

Paramagnetism takes place only in the presence of an external magnetic field. In this case, unpaired electrons are randomly arranged. Atoms in these materials have some inner electron shells that are incomplete, causing their unpaired electrons to spin and orbit in a specific way, thus making the atoms a permanent magnet tending to align with the external magnetic field and thereby strengthening it. [46]. Typical examples of such types of ordering are Al, Na, hematite, goethite.

In antiferromagnetic materials, the magnetism due to magnetic atoms or ions oriented in one direction is cancelled out by the set of magnetic atoms or ions that are aligned in the reverse direction. The magnetic susceptibility of an antiferromagnetic substance is thermal dependent, thereby varying from the non-magnetic response at very low temperatures, up to a maximum called the Néel temperature, to finally decrease with the increasing temperature [S. Blundell].

Antiferromagnetism is characteristic of solids, for example, hematite, chromium, alloys such as Fe Mn (FeMn) and oxides, such as manganese oxide (MnO) and nickel oxide (NiO) [45].

Regarding soil contamination, it would be interesting to study the removal efficiency of the magnetic separation procedures in soils that have been burned. This is because in such a case, some minerals, such as hematite, goethite and limonite may have transformed into pseudomorphic magnetite that can be easily removed.

In the same line, selective magnetic coating is another interesting process used for the separation of inorganic pollutants from contaminated soils. The technology is based on the idea of promoting the selective adsorption of fine magnetic particles onto the pollutants, to then be easily trapped by magnetic separation [47].

Wet-High intensity magnetic separator

In this thesis, magnetic separation has been performed by means of WHIMS (OUTOTEC Laboratory, WHIMS 3X4L) (figure 1.6). In such types of devices, the feed passes through a separating chamber composed of soft Fe spheres. The magnetic field is created by a current passing through a coil that creates a magnetic field, which magnetizes the soft Fe spheres. Consequently, the particles of the initial feed are separated on the basis of their magnetic properties, thus, some remain attached to the balls in the chamber ("mags"); whilst others keep on the water stream passing through it ("non-mags").

In consequence, the forces acting on a particle that is being separated are, apart from those caused by the gravity, the drag forces (F_d) and the magnetic forces (F_m) [44].

Figure 1. 6 OUTOTEC Laboratory WHIMS 3X4L.

The former is proportional to the fluid viscosity (N), the particle diameter (d) and fluid velocity (V); and the latter to the magnetic susceptibility, the cube of the diameter of the particles (d), the applied magnetic field (B) and the magnetic field gradient dB/dx (which is proportional to the magnetization of the steal balls and inversely proportional to their diameter).

Or Mathematically expressed [48]:

$$F_d \propto NdV$$

$$F_m \propto X d^3 B \, dB/dx$$

This indicates that all the parameters have the same importance, except the diameter of the particles, which is the most important parameter.

6.3 Scale up of the results

In designing a soil washing plant (see figure 1.7 for an example on this kind of plant), many aspects must be considered; amongst them, the following aspects are emphasised [49, 50]:

The material above 150 mm is usually free of pollutants and is removed before the decontamination process starts. Equipment such as, trammels, screening hoopers, etc… are usually used at this stage. The rest of the metals are usually eliminated at the beginning of the soil washing process by eddy current magnetic separators.

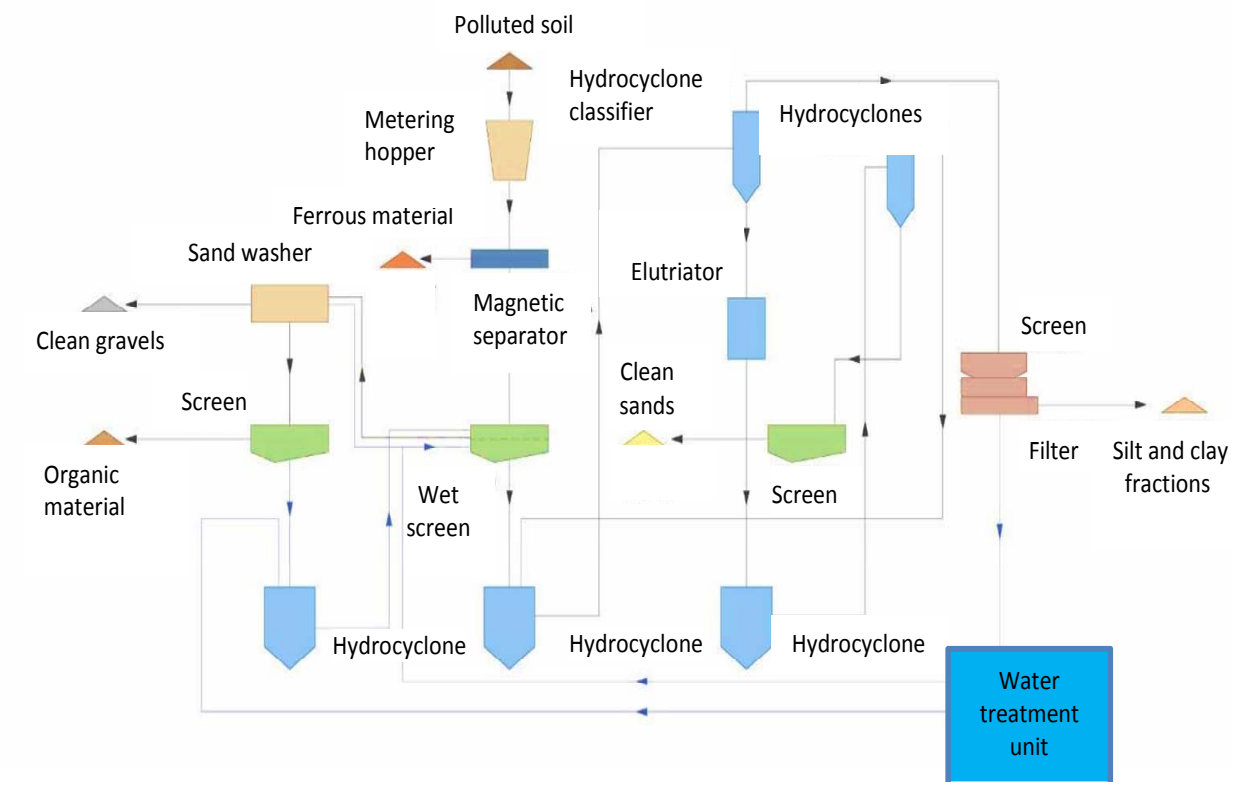

Figure 1.7 Schematic of a mobile soil washing plant (courtesy of Environmental Technologies Soldec).

Nevertheless, if the level of contamination in this fraction is high exceeding the target requirement, these fractions should be fragmented, in order to release the pollutants. In this case, primary crushers, such us jaw crusher or gyratory crushers; secondary crushers, such as roll or impact crushers; and even grinding by means of rod mills, ball mills, etc. could be necessary.

Following this stage, gravels, if liberated enough, are usually separated by dry screening and washing vibrating screening. Removing the small fractions attached to the larger grain sizes needs great attrition intensity, high pressure in the wash water, centrifugal acceleration and/or vibration [32, 51]. This steep is usually accompanied by intercalated desmiling units, such as logs and spirals classifiers. The addition of surfactants and dispersants, such as allophone solutions, hexametaphosphate, sodium nitrate, zirconium or even ultrasounds that help detach the fines from the sand, can become necessary at this stage.

The separation of the smallest fractions of the soil is the major objective in soil washing, since, as stated above, it is in the clay-size fractions where an important part of the pollution is expected to be accumulated, due to their high surface to volume ratio. In consequence, sands, which are expected to be clean, are typically separated by means of hydrocyclones from the silt and clay grain size fractions [52].

The process is continued with the removal of other contaminants, such as carbonaceous matter, slags, iron oxides or metal fragments, based on the different physical properties, but mainly on gravity separators.

Optionally, the finest particles could require the addition of flocculants and even chemical leaching or precipitation, in order to eliminate the pollutants therein. The water is usually removed by means of a filter press or a centrifuge.

Advantages and limitations

The **main advantages** of these methods are [30, 53]:

- Allows soils containing hazardous chemicals to be excavated and treated on-site.
- The system does not depend on external conditions
- The variety of possible treatments that allow for greater flexibility.
- The great number of different components that can be treated by the procedure.
- The procedure can be operated coupled with other technologies.
- It is relatively simple.

- It can be cost-effective.

On the contrary, these methods **do not work well when** [30, 53]:

- The pollutants are strongly bound to the soil grains or are not fully liberated.
- There is no strong difference in the physical properties between the natural soil and the contaminants.
- There is high variability in the chemical forms of the pollutant or the soil matrix.
- When contaminant concentrations are very hig.
- In soils with low contents of silt and clay (generally in excess of 30 to 50%).
- The soil has an elevated content in humic matter.

There is clearly a difference, in the author´s view, between mineral dressing physical soil washing: the existence of very high concentrations of clays and organic matter in soils.

The presence of clays is the essence of soil washing, which mainly relies on the separation of these phases; however, if an elevated percentage of declassified clays are present in the sand-size fractions after separation; this can seriously harm the performance of the processes. This is normally addressed by means of intense mechanical agitation or the addition of dispersants.

Regarding the organic matter, this can be easily separated by mechanical procedures, resulting in even more benefits, as will be shown in the ensuing chapters; however, it could be a problem when a physico-chemical treatment (froth flotation) is to be conducted. If need be, these problems could be prevented by a prior oxidation treatment, usually by simple combustion (controlling the temperature to prevent the formation of refractory materials, which could consist of low reactive to chemical

wash) or with a chemical oxidant, e.g. hydrogen peroxide. However, this is never performed, as it results in increasing the operation costs and usually worsens the performance of the flotation due to the formation of oxides.

References

[1] L. Oliver, U. Ferber, D. Grimski, K. Millar, P. Nathanail, The Scale and Nature of European Brownfields. In Proceedings of CABERNET: The International Conference on Managing Urban Land, Waterfront Hall Belfast, Northern Ireland, UK, 2005, Available at: www.cabernet.org.uk/resourcefs/417.pdf (accessed February 2013).

[2] U.S. Environmental Protection Agency (USEPA), Brownfield definition, Brownfields homepage, Available at: http://www.epa.gov/swerosps/bf/overview/glossary.htm (accessed February 2013)

[3] USEPA, Characteristics of sustainable brownfields projects, Washington DC, USA, Tech. Rep. EPA500-R-98-001G, 1998.

[4] Small Business Liability Relief and Brownfields Revitalization Act, Pub .L.No. 107-118, 115 stat. 2356.

[5] J. T. Riedel, Brownfields como oportunidad, Recuperación de sitios ambientalmente degradados en la periferia urbana, Facultad de Arquitectura, Diseño y Estudios Urbanos, Pontificia Universidad Católica de Chile, 2010.

[6] N. Green, Environmental constraints to brownfield redevelopment. Economic Development Quarterly, 8 (1994) 325–28.

[7] European Environment Agency, Overview of economic activities causing soil contamination in some WCE and SEE countries, 2009, Available at: http://www.eea.europa.eu/data-and-maps/figures/overview-of-economic-activities-causing-soil-contamination-in-some-wce-and-see-countries-pct-of-investigated-sites (accessed February 2013).

[8] J.S. Davis, “Is It Really Safe? That's What We Want to Know”: Science, Stories, and Dangerous Places, The Professional Geographer, 57 (2) (2005) 213–221.

[9] P. Roberts, H. Skyes, Current Challenges and Future Prospects, Urban Regeneration A Handbook, Sage Publications, London, 2000.

[10] M.R. Thomas, A GIS based decision support system for brownfield redevelopment. Landscape and Urban Planning, 58 (2002) 7-23.

[11] C.N. Brooks, A model for redeveloping complex, highly contaminated sites the Industri-plex Site in Woburn, Massachusetts. WIT Transactions on Ecology and the Environment, 94 (2006) 229-238.

[12] C. De Sousa, Brownfield redevelopment versus greenfield development: A private sector perspective on the costs and risks associated with brown-field redevelopment in the greater Toronto area, Journal of Environmental Planning and Management, 43(6) (2000) 831–53.

[13] C. De Sousa, Policy performance and brownfield redevelopment in Milwaukee, Wisconsin, The Professional Geographer, 57 (2) (2005), 312–327.

[14] G. Thornton, M. Franz, D. Edwards, G. Pahlen, P. Nathanail, The challenge of sustainability: incentives for brownfield regeneration in Europe, Environ. Sci.Policy, 10 (2007) 116–134.

[15] K. Wernstedt, L. Heberle, A. Alberini, P. Meyer, The Brownfields Phenomenon: Much Ado about Something or the Timing of the Shrewd? Resources for the Future, Discussion Paper 04–46, 2004, Available at: http://www.rff.org/documents/rff-dp-04-46.pdf (Accessed February 2013).

[16] D. Hara, Market Failures and the Optimal use of Brownfield Redevelopment Policy Instruments, Presentation to National Brownfields Redevelopment Strategy session, 37th Annual Meeting of the Canadian Economics Association. 2003, Available at http://economics.ca/2003/papers/0245.pdf (Accessed February 2013).

[17] Council for Urban Economic Development (CUED), Brownfields Redevelopment: Performance Evaluation, Washington, D.C., 1999.

[18] USEPA, Brownfields economic redevelopment initiative, Solid waste and Emergency Response (5101), EPA500-F-97-158,1997.

[19] Commission of the European Communities, Thematic Strategy for Soil Protection [SEC(2006)620][SEC(2006)1165]

[20] The Top Ten of The Dirty Thirty, The World's Worst Polluted Places, Blacksmith Institute, New York, 2007.

[21] P. Latz, Duisburg North Landscape Park. Anthos, 3 (1992) 27-32.

[22] P. Latz, Landscape Park Duisburg-Nord: the metamorphosis of an industrial site. In Manufactured Sites – Rethinking the Post-Industrial Landscape. Taylor & Francis, New York, 2001.

[23] J. Martínez, J. Llamas, E. de Miguel, J. Rey, M.C. Hidalgo, A.J. Sáez, Multivariate analysis of contamination in the mining district of Linares (Jaén, Spain), Appl.Geochem., 23 (2008) 2324–2336.

[24] J. Loredo, A. Ordóñez, R. Álvarez, Environmental impact of toxic metals and metalloids from the Muñón Cimero mercury-mining area (Asturias, Spain), J. Hazard. Mater., 136 (2006) 455–467.

[25] Environment Agency Wales, Case study – Land issues at the Olympic Park, Available at: http://www.environment-ency.gov.uk/cy/ymchwil/llyfrgell/cyhoeddiadau/115841.aspx (accessed February 2013).

[26] R. Black, Olympics shoot for green medal, BBC News, 2012, Available at: http://www.bbc.co.uk/news/science-environment-16853201 (accessed February 2013).

[27] R. Rio Ciruela , F.J. Fernandez Gonzalez,A. Ferrer Garcia, M. Perez Holguera, Inventario, caracterizacion y gestion de residuos peligrosos y suelos contaminados en el desmantelamiento de la antigua cabecera de Ensidesa (Avilés, Principado de Asturias). VI Congreso Nacional del Medio Ambiente, Madrid, 2003.

[28] E. Peláez, El desplome de Nitrastur, La Nueva España,01.02.2013, Available at: http://www.lne.es/nalon/2013/02/01/desplome-nitrastur/1362147.html (accessed February 2013).

[29] H.D. Sharma, K.R. Reddy, Geoenvironmental Engineering: Site Remediation, Waste Containment, and Emerging Waste Management Technologies, John Wiley & Sons, 2004.

[30] G. Dermont, M. Bergeron, G. Mercier, M. Richer-Laflèche, Soil washing for metal removal: a review of physical/chemical technologies and field applications, J. Hazard. Mater., 152 (2008) 1–31.

[31] USEPA, Contaminants and Remedial Options at Selected Metal-Contaminated Sites, EPA/540/R-95/512, Office of Research and Development, Washington, DC, 1995.

[32] C.W. Williford, Z. Li, Z. Wang, R.M. Bricka, Vertical column hydroclassification of metalcontaminated soils, J. Hazard. Mat. 66 (1999) 15–30.

[33] B.A. Wills, T.J. Napier-Munn, Mineral Processing Technology: An Introduction to thePractical Aspects of Ore Treatment and Mineral Recovery, 7th ed., Butterworth-Heinemann, Burlington, MA, 2006.

[34] R.A. Griffiths, Soil-washing technology and practice, J. Hazard. Mat., 40 (1995) 175–190.

[35] J. Drzymala, Mineral Processing, Foundations of Theory and Practice of Minerallurgy,Oficyna Wydawnicza PWr., 2007. Available at: www.ig.pwr.wroc.pl/minproc (accessed January 2013).

[36] A. Gosselin, D. Blackburn, M. Bergeron, Assessment Protocol of the Applicability of Ore-Processing Technology to treat Contaminated Soils, Sediments and Sludges, prepared for Eco-Technology Innovation Section Technology Development and Demonstration Program, Environment Canada, 1999.

[37] A. Gupta, D. Yan, Mineral Processing Design and Operation: An Introduction, Elsevier, Amsterdam, 2006.

[38] R.O. Burt, Gravity Concentration Technology, Developments in Mineral Processing, volume 5, Elsevier, Amsterdam, 1984.

[39] T. Magiera, Z. Strzyszcz, A. Kapicka, E. Petrovsky Discrimination of lithogenic and anthropogenic influences on topsoil magnetic susceptibility in Central Europe. Geoderma, 130 (2006) 299-311.

[40] D. Jordanova, N. Jordanova, V. Hoffmann, Magnetic mineralogy and grain-size dependence of hysteresis parameters of single spherules from industrial waste products. Physics of the Earth and Planetary Interiors, 154 (2006) 255–265.

[41] X. S. Wang, Y. Qin, Correlation between magnetic susceptibility and heavy metal in urban topsoil: a case study from the city of Xuzhou, China. Environ. Geol., 49 (2005) 10-18**.**

[42] R.A. Rikers, P. Rem, W.L. Dalmijn, Improved Method for Prediction of Heavy Metal Recoveries from Soil Using High Intensity Magnetic Separation (HIMS), Int. J. Miner.Process, 54 (1998) 165–182.

[43] L.R. Avens, L.A. Worl, K.J. de Aguero, D.D. Padilla, F.C. Prenger, W.F. Stewart, D.D.Hill, T.L. Tolt, Magnetic Separation for Soil Decontamination. Los Álamos National Lab. NM (USA), 1993.

[44] J. Svoboda, Magnetic Techniques for the Treatment of Materials, Kluwer Academic Publishers, 2004.

[45] B.D. Cullity, C.D. Graham, Introduction to Magnetic Materials, John Willey & sons, 2008.

[46]S. Blundell, Magnetism in Condensed Matter, Oxford Master Series in Physics, 2001.

[47] Bardos RP, Parsonage P. separation processes selective magnetic coating and bioleaching-biosorption, three approaches with potential for metal and radionuclide removal from contaminated soils. Proceedings of the Soil Decon '93: Technology Targeting Radionuclides and Heavy Metals, June 16 and 17, 1993,Gatlinburg, TN, ORNL-6769, Oak Ridge National Laboratory, Oak Ridge, TN, 1993.

[48] D.A. Norgran, M.J. Mankosa, Bench scale and pilot plant test for magnetic concentration circuit design, A. L. Mular, D. N. Halbe, and D. J. Barratt Eds. Mineral processing plant design, practice, and control: Proceedings. Editorial: Littleton: Society for Mining, metallurgy and exploration, New York, 2002.

[49] M.J. Mann, Full scale and pilot scale soil washing, J. Hazard. Mater., 66 (1998) 119–136.

[50] B. Yarar & Z. M. Dogan, eds., Mineral Processing Design, Proceedings, NATO Advanced Study Institute on Mineral processing Design, Bursa, Turkey, Martinus Nijhoff Publishers, 1987.

[51] M.A. Marino, R.M. Bricka, C.N. Neale, Heavy metal soil remediation; The effects of attrition scrubbing on a wet gravity concentration process, Environ. Progr., 16 (3) (1997) 208–214.

[52] R. Anderson, E. Rasor, Particle size separation via soil washing to obtain volume reduction, J. Hazard. Mater., 6 (1998) 89–98.

[53] Federal Remediation Technologies Roundtable (FRTR), Remediation Technologies Screening Matrix and Reference Guides, Version 4.0., Available at: http://www.frtr.gov/matrix2/top_page.html, March 2007. (accessed February 2013)

CHAPTER II: Analysis of soil washing effectiveness to remediate a brownfield polluted with pyrite ashes

C. Sierra, J.R Gallego., E. Afif, J.M. Menéndez-Aguado, F. González-Coto

Journal of Hazardous Materials (2010) 180, 602-608.

Abstract

Soil in a brownfield contaminated by pyrite ashes showed remarkably high concentrations of several toxic elements (Hg, Pb, Zn, Cu, Cd, As). Initially, we assessed various physical, chemical and mineralogical properties of this soil. The data obtained, and particularly multivariate statistics of geochemical results, were useful to establish the predominant role of the soil organic matter fraction (6%) and iron oxyhydroxides in the binding of heavy metals and arsenic. In addition, we studied the viability of soil washing techniques to reduce the volume of contaminated soil. Therefore, to concentrate most of the contaminants in a smaller volume of soil, the grain size fraction below 125 microns was treated by hydrocycloning techniques. The operational parameters were optimized by means of a factorial design, and the results were evaluated by attributive analysis. This novel approach is practical for the global simultaneous evaluation of washing effectiveness for several contaminants. A concentration factor higher than 2.2 was achieved in a separated fraction that contained less than 20% of the initial weight. These good yields were obtained for all the contaminants and with only one cycle of hydrocycloning. Hence full-scale soil washing is a plausible remediation technique for the study site.

Key words: soil pollution, pyrite ashes, hydrocycloning, soil washing.

1. Introduction

During recent decades, the closure of heavy industry across Europe has left large extensions of contaminated land [1,2]. As a result of the accumulation of pollutants derived from industrial activity over many years this land is currently not suitable for use. The recovery of these affected areas, especially when they have multi-component contamination and are situated in urban or peri-urban zones -`brownfields'- is of particular interest to economic and city-planning authorities [3].

In this context, a suitable remediation technique to reduce the initial volume of contaminated soil is the soil washing approach [4]. This technique involves concentrating polluting agents in a reduced volume fraction of the initial affected soil what generally results in the decontamination of the rest of the soil [5]. With this aim, particle size separation, gravity separation, attrition scrubbing and other processes are used, with or without chemical additives [6]. In the case of heavy metals, most approaches are based on the isolation of the finest fractions of the soil, due to - among other phenomena - the greater specific surface of argillaceous particles, the organic matter, and the oxyhydroxide gels, all of which bind heavy metals and other trace elements [7] These effects are related to the mobility of the metals, which is generally controlled by precipitation, diffusion, volatilization and dissolution of unstable minerals, in addition to other surface complexation processes [8]. Also, bioavailability and toxicity may vary according to pH, redox conditions (Eh) and changes in the land use pattern; however, given that soil washing requires excavation, all of these environmental parameters are more controllable than in ‘in situ’ treatments.

Most effective soil washing technologies apply physical processes to concentrate contaminants by exploiting differences in characteristics between the metal-bearing particles and soil particles (size, density, magnetism, and hydrophobic surface properties) [6]. The general strategy is based on well-known technologies commonly applied in the mineral processing industry to extract

the desired particles from mineral ores [9]. This technology is relatively simple to operate, often inexpensive, and highly versatile as it can be used in mobile plants (on-site treatments) or large-scale facilities (ex-situ treatments) [10].

The first step in the design of a full-scale washing treatment is a viability analysis, which involves several laboratory and analytical determinations to examine the main characteristics of the soil [7, 11]. In the second step, experiments on a pilot-scale can be performed in similar equipment to full-scale ones. Here we applied this work-plan to soil highly contaminated over many years by the industrial activity of a fertilizer factory. The main aims of the current study were the following:

- To integrate grain size distribution data with edaphological, geochemical and mineralogical information of the site in order to identify the soil fractions in which the contaminants were bound.

- To apply the information reported in the previous step to design and implement a physical separation study by means of hydrocycloning, thereby obtaining functional conclusions for the implementation of full-scale soil washing treatments.

- To develop and apply a theoretical formulation (attributive analysis) for the evaluation and selection of optimal parameters in the physical separation tests for our study site.

2. Experimental procedures

2.1 Site description and soil sampling

The study site is situated in the central zone of Asturias (Northern Spain), where a number of industrial and mining facilities have been closed in recent decades, thus generating several 'brownfields'. In this area, the climate is Atlantic (European) with an annual average precipitation and evapotranspiration of 1,130 and 667 mm respectively, and an annual average temperature of 13 ºC. The soil moisture regime is Udic, with adequate soil moisture for most of the growing season except for a one-month drought in the summer.

The soil samples analyzed were collected from the area surrounding a derelict fertilizer factory. Since its closure in 1997, this factory has been partially demolished and it is currently in an advanced state of abandonment. The total surface of the affected site is 70,000 m^2, more than half corresponding to landfills between 4 and 5 m deep comprised of pyrite ashes in addition to other iron and steel-type debris. The other plots of ground consist of natural soils however, these have been polluted as a result of decades of fertilizer manufacture, spills of waste and furnace emissions. Concretely, the pyrite ashes, comprising mainly oxides and hydroxides of iron and other metals, were produced as a by-product of toasting sulphur ores. These ores were industrially transformed to produce sulphuric acid and were subsequently used to manufacture ammonium sulphate fertilizer.

After initial "in situ" determinations and observations (data not shown), we identified several areas of natural soil distributed in the study site. We then carried out a double sampling campaign on these soils to perform a multi-element characterization to determine contamination. In the first case, samples were collected at 21 points randomly located in the natural soil areas, from a depth between 0 and 30 centimetres using a Dutch auger; formerly we ruled out deeper sampling following

information of a previous campaign of exploratory core sampling. Three subsamples of 0.5 kg were obtained and then mixed to obtain composite samples, which were packaged in inert plastic bags. In the second case, a "macrosample" of about 50 kg (from one of the 'hot points' found in the first sampling, see results) was taken from superficial soil with a shovel. In all the cases, the soil `in situ' was passed through a 2-cm mesh screen to remove rocks, gravel and other large material.

2.2 Geochemical characterization

The soil samples taken in the first campaign were dried at room temperature. The soil was then disaggregated by a roller and subsequently sieved through a 4-mm screen. Materials with a grain size greater than 4 mm were vigorously washed and rubbed off to recover fine particles adhered to the gravels and pebbles, which, once cleaned up, were excluded from the study. Given that fine-grained fractions are the most interesting in environmental geochemistry, and especially in toxicology (see [12] and references therein), grain-size particles below 4 mm were then quartered by means of a channel separator to obtain about 20 g of representative fractions, which were passed through a sieve of 125 microns. For chemical analysis, representative 1-g sub-samples were leached by means of an 'Aqua regia' digestion (HCl + HNO_3). The digested material was analyzed in duplicate for total concentrations of major and trace elements (Ca, Mg, K, Na, Al, Fe, S, Cu, Pb, Zn, Cd, Ni, Mn, As, Sr, Sb, La, Cr and Hg) by Inductively Coupled Plasma – Optical Emission Spectroscopy (ICP-OES) at the accredited laboratory Actlabs int., Ancaster (Ontario, Canada).

Descriptive statistics and cluster analysis were used to study the geochemical association of elements in the samples. Concretely, clustering was undertaken following the Ward-algorithmic method, which maximizes the variance between groups and minimizes it between members of the same group [13]. To show clustering results, a dendrogram obtained with the statistical software SPSS v15.0 was used [14]. Groups of elements with a similar geochemical behaviour were identified using values of the statistical distance between them (squared-Euclidean distance was selected).

2.3 Grain, mineralogical and pedology soil study

The 50-kg sample was wet-sieved in 100-g batches by means of a standardized series of Restch screens, in agreement with the norm ASTM D-422-63. Two main fractions (0-125 microns, 125-4000 microns) were obtained and used for ICP-OES analyses (see above). Particularly, in order to homogenize conditions for chemical attack, samples with a grain size higher than 125 microns were ground using a vibratory disc mill (RS 100 Retsch) operated at 400 rpm for 40 s to reduce grain size to below 125 microns. Samples finer than 125 microns did not require grinding and their grain-size distribution was examined in depth using a Laser Dispersion Particle Analyser (Beckman Inc. Coulter). Finally, several batches of this fine fraction were used for the hydrocycloning tests.

Texture was determined by the pipette method after a disaggregating treatment with two dispersants: sodium hexametaphosphate and sodium carbonate [15]. Regarding mineralogical and pedological characterization, the composition of the silicate clay minerals (< 2 μm particle-size fraction) was estimated by means of a diffractometer (Philips X Pert Pro, incorporating databases of the International Centre for Diffraction Data). The pH was measured in a suspension of soil and water (1: 2.5) in H_2O with a glass electrode and the electrical conductivity was measured in the same extract (diluted 1:5). Organic matter was determined by the ignition method (400ºC). Exchangeable cations (Ca, Mg, K and Na) extracted with 1 M NH_4Cl, and exchangeable aluminium extracted with 1 M KCl were determined by atomic absorption/emission spectrophotometry [16] in a AA200 Perkin Elmer analyzer; the effective cation exchange capacity (ECEC) was calculated as the sum of the values of the latter two measurements (sum of exchangeable cations and exchangeable Al).

2.4 Experiments of physical separation

2.4.1. Experimental design

There are several approaches available to study the soil washing of the separated fine fraction (< 125 microns). However, taking in consideration the most habitual equipment at soil remediation plants [6, 10], we used a hydrocycloning lab-scale plant (C700 Mozley) with capacity to operate hydrocyclones from 10 to 50 mm in diameter. In this apparatus, an in-flow slurry (feed) is tangentially pumped inside the cyclone where the centrifugal forces merge with the thickness and density of the particles. This system determines whether an individual particle flows through by the apex (underflow) or the upper part (overflow) of the hydrocyclone. The lighter and finer particles generally flow through the overflow.

The solid concentration of the feeding slurry used in our experiments was constant (20% per weight) whereas the underflow diameters and different working pressures were combined in a factorial test (see Results). In all cases, after reaching a stationary regime, samples from the underflow and overflow were taken in borosilicate flasks. They were then weighed and later dried in an oven at low temperature (45ºC to minimize loss of Hg and As via volatilization) to obtain dry weight and representative subsamples for ICP-OES analyses.

Having completed the multi-element analyses, for each test and for each element we defined recovery as the percentage of the total element contained in the overflow or in the underflow with respect to the total concentration in the feed slurry (a recovery of 90% of a given element in the overflow implies that 90% of the initial concentration was recovered in the overflow and 10% is 'lost' in the underflow). In addition, the ratio of concentration for each test was defined as the ratio of the weight of the feed to the weight of the concentrates in the overflow or in the underflow.

2.4.2 Attributive analysis

Ideally, in a soil washing procedure the aim is to concentrate a given contaminant in a smaller volume of soil than the initial one, i.e. to maximize its recovery and to reduce the ratio of concentration of that fraction. However, here we simultaneously addressed several contaminants and therefore required a method to adjust the selection of recoveries and ratios of concentration in order to achieve good results for a group of contaminants rather than a single one. Therefore, we chose a methodology based on attributive analysis [17]. In our case, a merit index was obtained, which facilitates the classification of the quality of the results of the distinct tests. This approach offers the advantage that it takes into account all the results obtained and allows the selection of the optimal test. Considering a number 'n' of tests with distinct operational conditions, the procedure was as follows.

- First, we defined R^i (%) as the ratio of concentration in the test 'i'. In the 'n' tests performed, i.e. within the R^i, the test with the minimum ratio of concentration was identified and this parameter was labelled Rmin (%).

- For a given element, e.g. Hg, conditions for concentration (i.e. recovery greater than ratio of concentration) were identified in each test. These conditions can occur in the overflow or in the underflow. For both cases, we labelled each recovery as Rec^i_{Hg} (recovery of Hg in test 'i'). One test showed maximum recovery of Hg and this value was labelled $Recmax_{Hg}$ (%).

- Taking into account the set of values and parameters defined, the index of merit Q^i_{Hg} for Hg was defined for each test 'i' following the expression:

$$Q^i_{Hg} = \frac{R\min}{R^i} + \frac{Rec^i_{Hg}}{Recmax_{Hg}} \quad (1)$$

The expression (1) can be generalized for multi-element contamination as the sum of Q^i for diverse elements (in this particular case we considered Hg, As, Cu, Cd, Pb and Zn, based on the results of the sampling characterization). However, all the polluting agents do not have the same relevance in the washing process as they are not present in equal concentrations in the initial soil, nor the objective to achieve for each one of them in the remediation project is the same. Thus, we defined a weighting factor 'A' for each contaminant, e.g. Hg:

$$A_{Hg} = \frac{Co_{Hg}\,(\text{ppm})}{RV_{Hg}\,(\text{ppm})} \qquad (2)$$

Where Co_{Hg} it is the concentration in the initial soil, and RV_{Hg} is the value of environmental reference for Hg (it can be defined by clean-up standards, or geochemical backgrounds, or as a result taken from risk management). A weighting factor for each of the remaining elements can be defined in a similar way. Furthermore, these coefficients must be corrected to reflect the relative importance of each element in the washing process. Therefore, in our case, for Hg the corrected weighting factor A' was defined as follows:

$$A'_{Hg} = A_{Hg} / (A_{Hg} + A_{As} + A_{Cu} + A_{Cd} + A_{Pb} + A_{Zn}) \quad (3)$$

From (1), (2) and (3) and the homologue equations for As, Cu, Cd, Pb and Zn, we obtained the index of global merit (Q^i_T), for test `i':

$$Q^i_T = Q^i_{Hg} \cdot A'_{Hg} + Q^i_{As} \cdot A'_{As} + Q^i_{Cu} \cdot A'_{Cu} + Q^i_{Cd} \cdot A'_{Cd} + Q^i_{Pb} \cdot A'_{Pb} + Q^i_{Zn} \cdot A'_{Zn} \quad (4)$$

3. Results and discussion

3.1 Multielemental characterization

Raw data of the multi-element analyses of the samples taken in the initial sampling campaign were processed with SPSS v15.0. Table 1 show the most representative statistical descriptors obtained. These data indicate significant contamination of several elements, such as As, Pb and Hg. The heterogeneous distributions of these elements (elevated coefficient of variation) probably follow a lognormal distribution typical of polluted areas [13]. In contrast, the descriptive measures for elements usually considered "natural" (Ca, Na) indicate a normal distribution [18].

Table2. 1 Statistical descriptive corresponding to the ICP-OES analysis of 21 soil samples taken in the study site.

Element	Unit	Minimum	Maximum	Average	Std. deviation	Coefficient of variation
Ag	ppm	0.1	1.20	0.41	0.36	0.88
Al	%	0.95	2.67	1.77	0.50	0.28
As	ppm	45.00	181.00	98.90	40.09	0.41
B	ppm	5.00	17.00	7.85	4.39	0.56
Ba	ppm	31.00	268.00	135.81	73.64	0.54
Bi	ppm	1.00	11.00	2.81	3.43	1.22
Ca	%	1.71	4.26	2.66	0.75	0.28
Cd	ppm	0.5	3.5	1.57	0.87	0.55
Co	ppm	7.00	33.00	13.76	6.42	0.47
Cr	ppm	19.00	436.00	96.33	116.43	1.21
Cu	ppm	62.00	266.00	121.90	61.91	0.51
Fe	%	2.35	5.66	3.83	0.92	0.24
Hg	ppm	3.00	62.00	20.67	16.16	0.78
K	%	0.13	0.53	0.24	0.11	0.46
Mg	%	0.29	0.75	0.37	0.09	0.24
Mn	ppm	207.00	1100.00	416.14	222.55	0.53
Mo	ppm	0.5	26.00	5.74	7.16	1.25
Na	%	0.03	0.07	0.05	0.01	0.20
Ni	ppm	24.00	130.00	45.00	23.08	0.51
Pb	ppm	126.00	1130.00	427.14	271.26	0.64
S	%	0.22	0.79	0.39	0.14	0.36

Regarding the multi-variant statistical analysis, a dendrogram was introduced to show results of "clustering" (Figure 2.1). The dendrogram shows three main groups of elements:

- **Group `a'**: Formed mainly by chalcophillic elements (Cu, Zn, Sb, Ag, etc.), probably associated with the sulphides toasted in the factory. The result of the furnace emissions, including waste dumping and inappropriate storage practices for sulphides and oxidized residues (pyrite ashes, etc.), affected natural soils. In addition, this group of pollutants was concerned by rapid weathering in the superior horizons of the soil, which also explains the absence of S in this group of elements. Remarkably, Fe was the only major element included in this group which results redundant in the probable origin of all of these elements (Fe-rich minerals as pyrites and maybe other sulphides). It also appears a weak correlation with Ca suggesting also a certain association of the contaminants with carbonates (the content of Ca is high, as shown in Table 2.1).

- **Group `b'**: Could be considered a sub-group of the group 'a', formed by other pollutant elements, such as Pb and Hg, mixed with other minority ones in pyrite ashes. S is included in this group and presented a good correlation with Hg. This observation may be attributed to the lower susceptibility of cinnabar (HgS) to weathering than other metallic sulphides [19].

- **Group `c'**: Regarding with the statistical treatment is distant from the preceding ones. Most of the elements included in this group are probably related to the geochemical background of the natural soil before its contamination. It comprises mainly clay aggregates, including major elements such as Al and K.

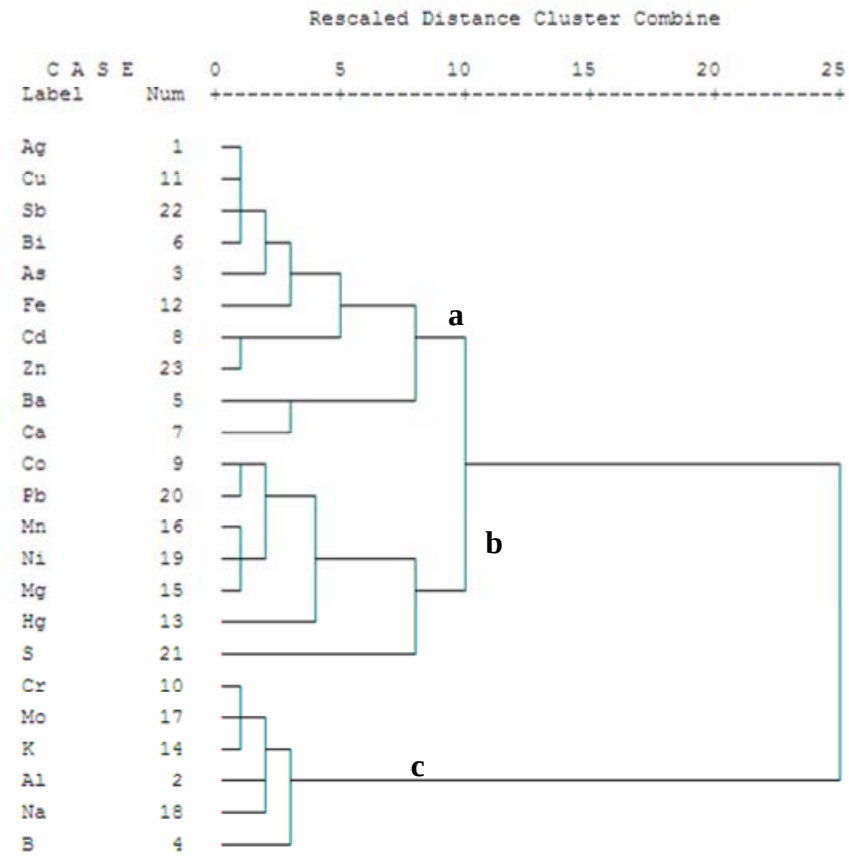

Figure 2.1 Dendrogram showing the clustering of elements associated by their geochemical affinity within the samples. Main groups are indicated based on the statistical distance between them.

We conclude that the soil presents evident although not elevated levels of contamination. The pollutants involved are mainly in the form of oxides as a result of the industrial processing of pyrites and other sulfides. There is no clear evidence of adsorption of the contaminants in clays or carbonates. Rather these contaminants are associated with Mn and Fe oxides and with the soil organic matter (see below). Finally, on the basis of the elementary concentrations and their potential toxicity, we took six elements as references for the rest of the study: As, Cd, Cu, Hg, Pb and Zn.

3.2 Pedologic and mineralogic characterization

A subsequent study was carried out with a 50-kg sample of soil from one of the zones most affected by contaminants. The representative subsamples of this area showed neutral pH (6.6), high organic matter content in the upper horizon (6 %), low electrical conductivity (EC = 0.196 dS m^{-1}), low contents of exchangeable base cations (7.13; 0.37; 0.32 and 0.59 $cmol_c$ kg^{-1} for Ca, Mg, K and Na respectively), and low ECEC (8.42 $cmol_c$ kg^{-1}). These features are consistent with the properties displayed by neutral soils in cold humid areas.

We classified the soil as a silt loam on the basis that the particle-size distribution revealed a high percentage of silt fractions (77 %). In contrast, the clay fractions (13 %) were dominated by illites (2:1 clay mineralogy) and kaolinites (1:1 clay mineralogy). The specific surface area of illites and kaolinites range from 65 to 100 m^2 g^{-1} (including the interlayer surface) and from 10 to 20 m^2 g^{-1} respectively, and the cation exchange capacity (CEC), depending on soil pH, range from 10 to 40 $cmol_c$ kg^{-1} and from 1 to 10 $cmol_c$ kg^{-1} respectively [20]. The structures of these two clays have been extensively described [21]. Furthermore, mineralogical analyses by x-ray diffraction revealed the presence of a considerable proportion of ferrihydrite - ($Fe_2O_3 \cdot 0{,}5H_2O$ - as representative of amorphous iron oxyhydroxides. With its high surface area per volumehttp://en.wikipedia.org/wiki/Ferrihydrite - cite_note-13, Ferrihydrite is a highly reactive mineral and is known to be a precursor of crystalline minerals, such as hematite and goethite [22]. Ferrihydrite interacts, either by surface adsorption or by co-precipitation, with a number of chemical species with environmental relevance, including As and heavy metals like Pb and Hg [23].

The presence of two types of low specific surface clays, together with the large amount of organic matter in the soil (6%), and the abundance of Ferrihydrite indicates that the contaminants in the study site are, to a great extent, bound to the organic matter, Fe oxyhydroxides, and secondarily carbonates [24]. This finding verifies the results of the multivariate analysis.

3.3 Grain-size characterization

Table 2.2 summarizes the result of the grain-size study for the two main fractions obtained, as well as the contaminants of interest and the concentrations of elements found. As expected, concentrations were greater in the finer fraction (-125 microns).

Table 2.2 Concentration of elements in the two grain-size fractions (the results correspond to the average of three determinations with standard error <5%).

Grain-size (microns)	Weight (%)	Trace elements of concern (ppm)					
		As	Cd	Cu	Hg	Pb	Zn
+ 125 - 4.000	9.5	48	1.0	69	10	181	162
- 125	90.5	79	1.4	106	16	359	347

However, in the case of coarse particles (+125 microns), concentrations of contaminants were also elevated. This observation indicates that it might be pertinent to undertake a physical separation treatment, which is beyond the scope of the present study (see possibilities such as MGS – multigravity separators- in [11], [25]).

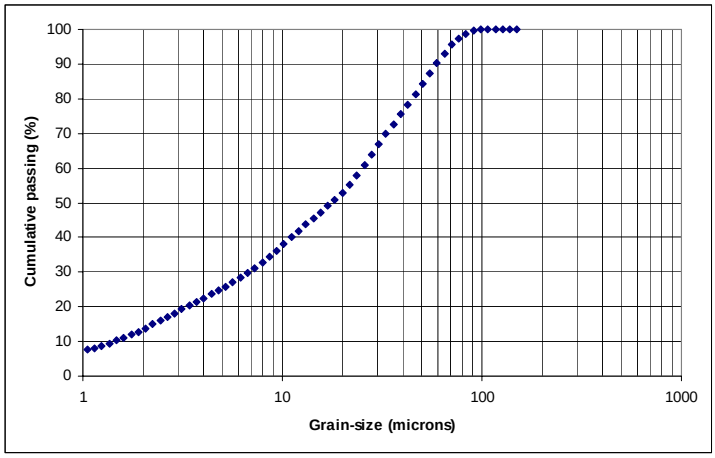

Figure 2. 2 Particle size distribution obtained by laser dispersion corresponding to a representative sample of the fraction below 125 microns.

We applied laser dispersion to focus on particle distribution in the fine fraction. Almost 40% of the material was below 10 microns and more than 10% comprised argillaceous matter (smaller than 2 microns) (Figure 2). These findings are consistent with the previous results on soil texture reported in 3.2. Given the composition of the finest materials, we propose that it is formed by a mixture of clays, organic matter and Fe oxide gels.

3.4 Hydrocycloning experiments

We completed a factorial test combining two apex diameters of the hydrocyclone (9.5 and 6.4 mm) and three levels of pressure (100, 200 and 300 kPa) for representative batches of the fraction of grain-size below 125 microns. With this starting point, the calculation of weighting factors is presented in Table 2.3. In Table 2.4 the results of the attributive analysis are shown according the definitions and parameters previously described in 2.4.2.

Table 2.3 Data required for attributive analysis of hydrocycloning tests: Initial concentrations (Co) of the soil fraction below 125 microns, reference values used as clean-up targets (RV); the weighting factors (A) and the corrected ones (A') obtained as described in 2.4.2. RV parameters were selected following an international standard [1]. Given the high Hg geochemical background in this area [26, 27], the only exception was Hg, for which 2 ppm was taken instead of 0.5 ppm.

Element	Co (ppm)	RV (ppm)	Weighting factor (A)	Corrected weighting factor (A')
As	71	20	3.55	0.16
Cd	1.3	1	1.30	0.06
Cu	104	50	2.08	0.09
Hg	14	2	7.00	0.31
Pb	359	50	7.18	0.31
Zn	358	200	1.79	0.08

It can be concluded that higher pressures are favourable only with the smaller apex diameter, i.e., there is no related general tendency with an increase in pressure. Overall, the best Q_T was obtained in test 6. We therefore studied the underflow and overflow samples of this test in further detail. First (Figure 2.3), we performed a partition curve for hydrocyclones [28] from the particle size distribution of both the underflow and overflow after laser dispersion of samples taken in stationary regime.

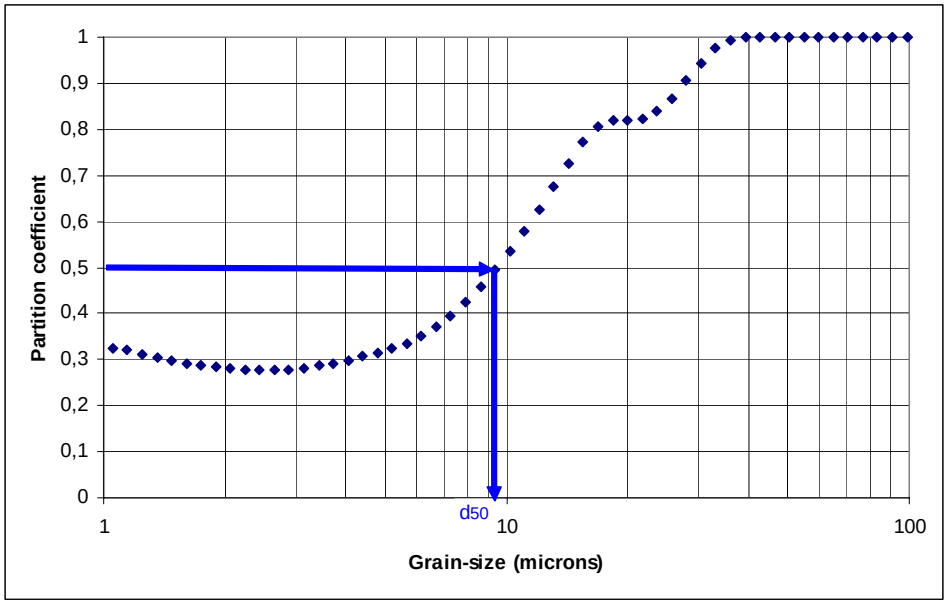

Figure 2.3 Hydrocyclone partition curve obtained in test nº6 (diameter of end 6.4 mm and 300kPa pressure). This curve plots at each grain-size the corresponding partition coefficient, which represents the fraction of total particles of a given size which reports to the underflow.

This curve was used to evaluate the effectiveness of hydrocycloning, as well as to determine some characteristic parameters of the separation, such as the cut point (denoted d_{50}) defined as the size for which 50% of the particles in the feed report to the underflow, i.e. particles of this size have an equal chance of going either with the overflow or underflow.

Table 2.4 Summary of the calculations conducted by means of attributive analysis. For all the tests and elements, the concentration effect occurred in the overflows in which a combination of fine and light fractions accumulated. The optimal conditions were found in test number 6.

Test number ('i')	Apex diameter (mm)	P (kPa)	Q^i_{As}	Q^i_{Cd}	Q^i_{Cu}	Q^i_{Hg}	Q^i_{Pb}	Q^i_{Zn}	Q_T
1	9.5	100	146.81	153.77	153.77	151.77	153.77	153.77	1.41
2	9.5	200	146.29	156.53	148.93	151.87	153.40	150.08	1.41
3	9.5	300	144.10	147.27	142.38	143.08	148.29	144.37	1.35
4	6.4	100	160.28	158.73	155.21	160.28	157.15	154.19	1.48
5	6.4	200	164.51	162.54	159.61	161.00	162.80	159.54	1.51
6	***6.4***	***300***	172.75	174.55	168.49	166.59	172.91	169.42	***1.58***

In our case the cut point was 9.5 microns. In addition, the curve demonstrates the presence of a "fish-hook" effect [29], thereby indicating that fine particles are not likely to move towards the heavy fraction, which is usually bound to the object of agglomeration. This effect could be due to the presence of organic matter that gave hydrophobic characteristics to the fine particles. Furthermore, the low slope of the curve indicates low efficiency in the separation; however, this efficiency did not impair decontamination (Table 2.5).

Table 2.5 Element concentrations in test nº 6 (results are average of three determinations). Concentration factor' was defined as the quotient between the concentration in the overflow and the feed.

	Trace elements of concern (ppm)					
	As	**Cd**	**Cu**	**Hg**	**Pb**	**Zn**
Reference value (RV)	20	1	50	2	50	200
Feed (original soil)	71	1.3	104	14	359	358
Underflow (81.5% weight)	48	0.9	72	10	247	249
Overflow (18.5% weight)	171	3.1	241	32	857	844
Concentration factor	*2.40*	*2.38*	*2.32*	*2.29*	*2.39*	*2.36*

Consequently, in spite of obtaining a deficient grain-size separation, the classification obtained appeared to be related to specific-gravity effects. Therefore a large amount of the contaminants was recovered in the overflow fraction, which was smaller in weight than the underflow. In fact, given that organometallic aggregates [30] can reach an average density of 1.4 g/cm^3 (approximately half of the mineral components of the soil), the influence of the organic matter is crucial in the separation [31].

Successive cycles of soil washing, commonly applied in full-scale processes [33], are effective in reducing metal contamination in significant fractions to acceptable levels (below the reference values). Our results support this finding, as one cycle of washing achieved notable concentration factor, as previously shown in Table 5.

4.- Conclusions

The pyrite ash, a by-product of the sulphuric acid production process during the roasting of pyrite ores, has contributed to introducing toxic elements, such as As, Pb, Cd, Ni, Cu and Hg, into the natural soils in the study site. The soil presented marked multi-component contamination. Most of the contaminants were bound to the soil organic matter and secondarily to Fe oxyhydroxides, while processes such as clay adsorption made a minor contribution.

Here we applied hydrocycloning, a physical washing procedure, to clean the fine fractions of a soil contaminated with heavy metals. Instead of the extended premise of hydrocyclones achieving separation by sizes, the separation of the contaminants by specific-gravity effects was favoured. Therefore, under these conditions, it is more appropriate to refer to cut densities rather than cutoff sizes for hydrocycloning. Furthermore, we have demonstrated attributive analysis to be an effective tool for the quantitative determination of the quality of separations, and also to establish weighting factors based on the diverse elements to be removed. Finally, optimum conditions allowed us to obtain concentration factors higher than 2.2 for all the contaminants in less than 20% of the weight of the original soil. This achievement implies that full-scale treatment with successive rewashing cycles is viable. This treatment should be considered in soil remediation programmes.

Acknowledgement

This research was funded by the CDTI (‘Centro para el Desarrollo Tecnológico e Industrial’) from the Spanish Council for Industry within the research programme named “CLEAM CENIT”.

References

[1] G.W.J. Van Linden, European soil resources, Nature and Environment nº 71. Council of Europe, Strasburg, 1995.

[2] H.D. Sharma, K.R. Reddy, Geoenvironmental Engineering: Site Remediation, Waste Containment, and Emerging Waste Management Technologies. John Wiley & Sons, 2004.

[3] G. Thornton, M. Franz, D. Edwards, G. Pahlen, P. Nathanail, The challenge of sustainability: incentives for brownfield regeneration in Europe, Environ. Sci. Policy 10 (2007) 116-134.

[4] M.J. Mann, Full scale and pilot scale soil washing, J. Hazard. Mater. 66 (1998) 119-136.

[5] R. Anderson, E. Rasor, Particle size separation via soil washing to obtain volumen reduction, J. Hazard. Mater. 6 (1998) 89-98.

[6] G. Dermont, M. Bergeron, G. Mercier, M. Richer-Laflèche, Soil washing for metal removal: A review of physical/chemical technologies and field applications, J. Hazard. Mater. 152 (2008) 1–31.

[7] J. Abumaizar, H. Smith, Heavy metal contaminants removal by soil washing, J. Hazard. Mater. 70 (1999) 71-86.

[8] D. Sverjensky, Physical surface-complexation models for sorption at the mineral–water interface, Nature 364 (1993) 776-780.

[9] B.A. Wills, T.J. Napier-Munn, Mineral Processing Technology: An Introduction to the Practical Aspects of Ore Treatment and Mineral Recovery, seventh edition, Burlington, Massachusetts, Butterworth-Heinemann, 2006.

[10] M. Pearl, M. Pruijn, J. Bovendeur, The Application of Soil Washing to the Remediation of Contaminated Soils, Land Cont. Rec. 14 (2006) 713-726.

[11] C. Sierra, F. González-Coto, R. Villa, J.M. Menéndez-Aguado, J.R. Gallego, Innovative approaches for the remediation of arsenic and mercury pollution via soil washing. Proceedings of the 3rd Internacional Meeting in Environmental Biotechnology and Engineering, Palma de Mallorca (Spain), 2008.

[12] J.R. Gallego, A. Ordóñez, J. Loredo, Investigation of trace element sources from an industrialized area (Avilés, northern Spain) using multivariate statistical methods, Environ. Int. 27 (2002) 589-596.

[13] J. Martínez, J. Llamas, E. de Miguel, J. Rey, M.C. Hidalgo, A.J. Sáez, Multivariate analysis of contamination in the mining district of Linares (Jaén, Spain), Appl. Geochem.23 (2008) 2324-2336.

[14] SPSS, SPSS for Windows, version 15. SPSS Inc, 2006.

[15] G.W. Gee, J.W. Bauder, Particle size analysis, in: A. Klute, Methods of Soil Analysis, 2nd ed, American Society of Agronomy, Madison, WI, 1996, pp. 383-411.

[16] M. Pansu, J. Gautheyrou, Handbook of soil analysis: mineralogical, organic and inorganic methods. Berlin: Springer, 2006.

[17] J.A. Pero-Sanz Elorz, Ciencia e ingeniería de materiales: estructura, transformaciones, propiedades y selección, Dossat, Madrid, 2000.

[18] J. Martínez, J. Llamas, E. de Miguel, J. Rey, M.C. Hidalgo, Determination of the geochemical background in a metal mining site: example of the mining district of Linares (South Spain), J. Geochem. Explor. 94 (2007) 19–29.

[19] C. Baldo, J. Loredo, A. Ordóñez, J.R. Gallego, J. García-Iglesias, Geochemical characterization of wastes from a mercury mine in Asturias (northern Spain), J. Geochem. Explor. 67 (1999) 377-390.

[20] B. Velde. Composition and mineralogy of clay minerals, in: B. Velde (Ed.), Origin and mineralogy of clays, Springer-Verlag, New York, 1995, pp. 8-42.

[21] S. Yariv (1992). Wettability of clay minerals. In: M.E. Schrader, G.I. Loeb (Eds), Modern approach to wettability, theory and applications vol. 11, Plenum, New York, 1992, pp. 279-326.

[22] Y. Cudennec, A. Lecerf, The transformation of ferrihydrite into goethite or hematite. J. Solid State Chem. 179 (2005) 716-722.

[23] J.L Jambor, J.E. Dutrizac, Occurrence and constitution of natural and Synthetic Ferrihydrite, a widespread iron oxyhydroxide, Chem. Rev. 98 (1998) 2549-2585.

[24] C.W. Williford, R.M. Bricka, Physical separation of metal-contaminated soils, in: I.K. Iskandar (Ed.), Environmental Restoration of Metals- Contaminated Soils, 1st ed, , CRC Press, Boca Raton, Florida, 2000.

[25] A. Traore, P. Conil, R. Houot, M. Save, An evaluation of the Mozley MGS for fine particle gravity separation, Miner. Eng. 8 (1995) 767-778.

[26] J. Loredo, C. Luque, J. García-Iglesias, Conditions of formation of Hg deposits from the Cantabrian zone (Spain), Bull. Mineral 111 (1998) 393-400.

[27] J. Loredo, A. Ordóñez, R. Álvarez, Environmental impact of toxic metals and metalloids from the Muñón Cimero mercury-mining area (Asturias, Spain), J. Hazard. Mater. 136 (2006) 455–467.

[28] L. Svarovsky. Solid-Liquid Separation, 4º Ed., Butterworth-Heinemann, Oxford, 2000, pp. 66-102.

[29] D.D. Patil, T.C. Rao, Studies on the fishhook effect in hydrocyclone classification curves, Miner. Metall. Process 18 (2001) 190–194.

[30] J. Hassink, Decomposition rate constants of size and density fractions of soil organic matter, Soil Sci. Soc. Am. J. 59 (1995) 1631-1635.

[31] M.F. Benedetti, Metal ion binding to colloids, from database to field systems, J. Geochem. Explor. 88 (2006) 81-85.

[32] R. Griffiths, Soil washing technology and practice, J. Hazard. Mater. 40 (1994) 175-189.

CHAPTER III: Feasibility study on the use of soil washing to remediate the As-Hg contamination at an ancient mining and metallurgy area

C. Sierra, J.M. Menéndez-Aguado, E. Afif, M. Carrero, J.R. Gallego

Journal of Hazardous Materials, (2011) 196, 93-100.

Abstract

Soils in abandoned mining sites generally present high concentrations of trace elements, such as As and Hg. Here we assessed the feasibility of washing procedures to physically separate these toxic elements from soils affected by a considerable amount of mining and metallurgical waste ("La Soterraña", Asturias, NW Spain). After exhaustive soil sampling and subsequent particle-size separation via wet sieving, chemical and mineralogical analysis revealed that the finer fractions held very high concentrations of As (up to 32,500 ppm) and Hg (up to 1,600 ppm). These elements were both associated mainly with Fe/Mn oxides and hydroxides. Textural and geochemical data were correlated with the geological substrate by means of a multivariate statistical analysis. In addition, the Hg liberation size (below 200 μm) was determined to be main factor conditioning the selection of suitable soil washing strategies. These studies were finally complemented with a specific-gravity study performed with a C800 Mozley separator together with a grindability test, both novel approaches in soil washing feasibility studies. The results highlighted the difficulties in treating "La Soterraña" soils. These difficulties are attributed to the presence of contaminants embedded in the soil and spoil heap aggregates, caused by the meteorization of gangue and ore minerals. As a result of these two characteristics, high concentrations of the contaminants accumulate in all grain-size fractions. Therefore, the soil washing approach proposed here includes the grinding of particles above 125 microns.

Key words: soil pollution, mercury, arsenic, ore processing, soil washing.

1. Introduction

Abandoned mining-metallurgy sites are sources of environmental pollution. This contamination is a result of mine drainage, waste disposal, subsidence and other phenomena [1, 2]. Specifically, Hg mining and processing are frequent causes of environmental concern because of the abundance of Hg and other toxic trace elements, such as As, in the ores exploited [3]. Hg participates in a number of complex environmental cycles. Geochemical studies have shown that, once in the environment, ionic Hg can be converted into organomercury compounds, which are highly toxic to most organisms [4]. Furthermore, As toxicity –specifically As (III) – has triggered severe environmental alarms throughout the world, in particular in relation to groundwater [5].

In this context, soil washing by means of physical and/or chemical procedures is a suitable technique to reduce the concentration of heavy metal contaminants in this matrix [6]. Physical processing technology in particular has been frequently used to remediate heavy metal and semi-metal pollution, including Hg and As [7, 8, 9, 10, 11]. These techniques remove contaminants from soil by concentrating them into a minor volume by means of comminution, particle size separation, specific-gravity separation, attrition scrubbing, froth flotation or magnetic separators. Thus, physical processing concentrates contaminants by exploiting differences between the characteristics of metal-bearing particles and soil particles (size, density, hydrophobic surface properties, magnetism), in much the same way as mineral ores can be treated. Given that these technologies are versatile and cost-effective when high amounts of soil are to be treated, they may be highly appropriate for the remediation of former industrial sites and old mine dumps [12]. In contrast, chemical processing usually comprises procedures such as acid or base treatment for solubilisation, or the use of specific solvents, to release pollutants into the liquid fraction [6].

The information reported in feasibility studies usually allows consideration of a range of alternatives for soil washing treatments, the final objective of which is a noteworthy reduction in the volume of contaminated soil (ideally, in a soil washing process the goal pursued for a given contaminant is to achieve a high concentration in a small fraction [6]). This broad view requires a detailed characterisation of the edaphology, mineralogy and geochemical behaviour of the grain-size soil fractions. Here we applied this work-plan to soil highly contaminated with As and Hg as a result of the physico-chemical alteration of mining-metallurgic waste [13]. In addition, specific-gravity and liberation degree studies facilitated the evaluation of the viability of applying gravimetric and/or granulometric concentrators. Concretely, the particle-size fractions obtained were used for a specific-gravity study to examine the relationship between particle size, density and contaminant content of the fractions. Milling was also considered by means of a complementary approach consisting of Bond tests to evaluate the grindability of coarse fractions in order to obtain a finer grain-size that is more appropriate for physical separation.

Following all of the preceding considerations, the main aims of the current study were as follows:

- To integrate grain size distribution, specific-gravity separation and a liberation degree study with edaphological, geochemical and mineralogical information of the study site.
- To introduce the "C800 Mozley laboratory mineral separator" and the "Bond Ball Mill Standard test" as effective tools to improve the abovementioned feasibility studies.

2. Materials and methods

2.1 Site description and soil sampling

Until the end of the 1970, extensive Hg deposits in the central zone of Asturias (northern Spain) were exploited [14, 15, 16, 17, 18]. One of the main sites was known as "La Soterraña". There, together with mining activity, ore processing and metallurgy were carried out intermittently from the middle of the XIX century in order to obtain Hg. Regarding ore geology, mining was performed through a low-temperature hydrothermal ore, which is hosted by highly fractured limestones with dispersion in the flanking sandstones and lutites of Carboniferous age. The paragenesis of this mineral deposit is constituted by cinnabar (HgS), orpiment (As_2S_3), realgar and pararealgar (AsS), As-enriched pyrite and marcasite (FeS_2), and arsenopyrite (FeAsS), in a gangue of quartz and calcite [14, 19]. These sulphides were treated at "La Soterraña" mining-metallurgic plant, where the mineral was milled and roasted to obtain Hg vapour, which was then condensed. The emissions of polluting steams and particles and the dumping of mining and smelting waste greatly affected around 80,000 m^2 of the surrounding area [14]. Currently, the distribution of the pollutants throughout the site is caused mainly by the mechanical dispersion of the spoil heap waste, together with the oxidation and lixiviation of As-Hg-rich materials, and also the processes of complexation and immobilisation related to soil particles.

In order to conduct a soil washing feasibility study, three composite and representative soil samples (labelled S1, S2 and S3, 50 kg each) were collected from the tilled depth (0-35 cm) by means of a stainless steel hand-auger and a shovel. The soil was passed through a 2-cm mesh screen *in situ* to remove rock fragments, vegetation and other large material; finally, samples were homogenised and stored in inert plastic bags.

2.2 Sample preparation

In the laboratory, the three samples were gently dried at room temperature, thoroughly disaggregated, mixed, and subsequently sieved through a 4-mm screen. Materials with a grain size greater than 4 mm were washed and rubbed off to recover fine particles adhered to gravels and pebbles. Once these gravels and pebbles had been cleaned up, they were excluded from the study. Each sample below a grain size of 4 mm was quartered by means of a channel separator to obtain representative 4-kg batches. These were then oven-dried for 48 hours at 45ºC to prevent Hg loss.

2.3 Soil characterization

Regarding pedology, the pH was measured with a glass electrode in a suspension of soil and water (1: 2.5) in H_2O and electrical conductivity was measured in the same extract (diluted 1:5). Organic matter was determined by the ignition method (weight loss at 450ºC). Exchangeable cations (Ca, Mg, K and Na) extracted with 1 M NH_4Cl, and exchangeable Al extracted with 1 M KCl were determined by atomic absorption/emission spectrophotometry [20] in an AA200 Perkin Elmer analyzer; the effective cation exchange capacity (ECEC) was calculated as the sum of the values of the latter two measurements (sum of exchangeable cations and exchangeable Al).

2.4 Wet sieving

The representative batches of each sample (S1, S2, S3) were slurried in water and then sieved (cycles of 100 g) into particle-size fractions of <63, 63–125, 125–250, 250-500, 500-1000, 1000-2000 and 2000-4000 µm. batches were passed through normalised sieves positioned in a shaker (Restch) for 5 minutes with a water flow of 0.3 l/min (ASTM D-422-63, Standard Test Method for Particle-Size Analysis of Soils).. The fractions were recovered with the help of a spray nozzle, and then dried at 50 ºC and weighed. To complete the grain size distribution, the silt-clay fraction (<63 µm) was studied using a Laser Diffraction Particle Analyser (Beckman Coulter Inc.).

Representative samples of the grain size fractions were subjected to chemical analyses by means of ICP-OES (see 2.5). However, some of these fractions were subdivided to obtain further samples for the mineralogical and specific gravity studies (see sections 2.7 and 2.8). In order to standardise the conditions used for chemical attack, samples with a grain size over 125 µm were ground at 400 rpm for 40 seconds using a vibratory disc mill (RS 100 Retsch).

2.5 Chemical analyses

For chemical analyses, 1-g representative sub-samples of the diverse origins (soils, grain size fractions, light or dense specific gravity fractions, etc.) were leached by means of an 'Aqua regia' digestion ($HCl + HNO_3$). The digested material was analysed for total concentrations of 19 major and trace elements (Ca, Mg, K, Na, Al, Fe, S, Cu, Pb, Zn, Cd, Ni, Mn, As, Sr, Sb, La, Cr and Hg) by Inductively Coupled Plasma – Optical Emission Spectroscopy (ICP-OES) in the accredited (ISO 9002) laboratories Actlabs int., Ancaster (Ontario, Canada).

2.6 Multivariate statistics

Cluster Analysis was undertaken following the Ward-algorithmic method, which maximises the variance between groups and minimises it between members of the same group [21]. A dendrogram obtained with the statistical software SPSS v18.0 was used to show the clustering of results. Groups of elements with a similar geochemical behaviour were identified on the basis of the statistical distance between them (squared-Euclidean distance was selected).

2.7 Mineralogy and liberation degree study

The mineralogical composition of the soil was estimated by means of an X-Ray diffractometer (DRX, Philips X Pert Pro, incorporating databases of the International Centre for Diffraction Data). In addition, representative samples of each wet-sieving fraction were used to prepare polished sections to be studied by an Eclipse LV 100 POL Nikon petrographic microscope. The morphology and composition of specific minerals were studied using a SEM-EDX system: Scanning Electron Microscope (Jeol JSM-6100) coupled with Energy Dispersive X-ray analyser (INCA Energy 200).

2.8 Specific gravity study

The particle-size fractions obtained were used for a specific-gravity study to examine the relationship between particle size, density and contaminant content of the fractions. A C800 Mozley laboratory mineral separator was used for this purpose. This separator, which operates using gravimetric classification, is commonly used to assess mineral processing equipment [22], although in our case it was tested for site remediation purposes.

In brief (see [22] for details), this separator comprises a riffleless shaking table; two types of table deck (trays) are available, a “V” profile for materials finer than 1,000 µm and coarser than 63 µm, and a “Flat” profile for the separation of material below 63 µm.

Physical separation is governed by the flowing film principle [23], in addition to a perpendicular movement to the tray axis, thus favouring the advance of the solids on the tray. Therefore, the separation in this equipment is only partially conditioned by Stokes force (correlated with grain-size); conversely, mass forces related to an asymmetric acceleration are enhanced (specific-gravity separation effect).

In our case, 100-g samples of the particle-size fractions of <63, 63–125, 125–250, 250-500 μm were shaken under several controlled parameters (shaking speed and amplitude, water flow, and time, see Table 3.1), in order to obtain dense and light fractions in every experiment.

Table 3.1 Parameters used in the specific gravity study performed with a C800 Mozley laboratory separator (recommendations by the manufacturer were adapted to soil properties).

Grain-size fractions (μm)	Tray	Shake speed (r.p.m.)	Amplitude (mm)	Washwater (l/min)	Feed (g)	Time (min)
< 63	'V'profile	70	2.5	3	50	3
125-63						
250-125	Flat	90	3.5	3	150	3
500-250						

However, for fractions above 63 μm, the effect of silt/clay particles physically adhered to the coarser ones should be considered; in our case, this adherence was directly linked to the efficiency of the previous wet-sieving performed. To determine the relevance of this effect, we carried out an

experiment in which three representative 50-g samples from the 63-125 µm fraction were directly treated in the C800 separator, while another three samples were pre-treated for 30 minutes in a solution of dispersing agents (3 g of sodium hexametaphosphate and 0.5 g of anhydrous sodium carbonate dissolved in 250 ml of distilled water) at 400 rpm in a Heidolph RZR 2020 shaker.

2.9 Grindability characterisation

In soil washing approaches, milling could be required to free contaminants from the matrix aggregates in which they are embedded, in order to facilitate the ulterior operation in concentrators. Therefore, we estimated the resistance of the soil samples to ball milling in terms of specific power consumption for grinding. This was done by means of the Bond Ball Mill Standard test [24, 25, 26].

In brief, with the aim to simulate closed circuit continuous operation with a recirculating load of 250%, the test [27] is carried out in a 12"x12" lab ball mill, in consecutive cycles of batch operations of grinding and sieving. In our case, the sieves selected to study the variation of the Bond work index with the milling product size were 250, 180, 125 and 80 µm. The test is useful to obtain the internal parameter named "grindability index", Gbp, in an iterative procedure. The final value of "work index" is calculated using the following equation:

$$w_i = \frac{44.5}{P_i^{0.23} \cdot Gbp^{0.82} \cdot \left(\frac{10}{\sqrt{P_{80}}} - \frac{10}{\sqrt{F_{80}}} \right)}$$

Where:

- P_i (in microns): screen size at which the test is performed.

- Gbp is the Bond's standard ball mill grindability; net weight of ball mill product passing sieve size P_i produced per mill revolution (g/rev), once the end of the test is reached.

- F_{80} and P_{80} (in microns) are the 80 % sieve opening through which 80% of the product passes (for Feed and Product respectively).

- w_i is the Bond Work index (in kWh/sht).

Once obtained the work index, the specific power consumption W [kWh/t] can be calculated using the Bond Formula:

$$W = 10 \cdot w_i \cdot \left(\frac{1}{\sqrt{P_{80}}} - \frac{1}{\sqrt{F_{80}}} \right)$$

3. Results and discussion

3.1 Pedology, grain size study and soil geochemistry

The pedological characterisation (average of three determinations over the initial bulk samples S1, S2, S3, with a standard error below 5%) revealed a slightly acid pH (6.3), low electrical conductivity (EC = 0.19 dS m^{-1}), low content of exchangeable base cations (5.42; 0.31; 0.28 and 0.47 $cmol_c$ kg^{-1} for Ca, Mg, K and Na respectively), low ECEC (sum of exchangeable cations and exchangeable Al = 7.38 $cmol_c$ kg^{-1}), and a low organic matter content in the upper horizon (0.75 %). All of these data are consistent with the geological origin of the soil and its development under particular geochemical conditions as a result of the influence of waste derived from mining activities and the metallurgy industry.

Table 3. 2 Element concentration of representative subsamples of the three initial bulk samples (results correspond to the average of three determinations with a standard error <5%).

Sample	Trace elements (mg kg^{-1})					Major elements (%)		
	Hg	As	Pb	Zn	Sb	Al	Ca	Fe
S1	805	32500	98	98	211	2.86	2.52	3.19
S2	1600	17100	49	71	111	2.08	5.6	3.09

S3	132	6350	28	46	23	2.8	5.9	2.81

Furthermore, ICP-OES analyses (Table 3.2) revealed very high concentrations of As and Hg, and a lower presence of other contaminants such as Pb. These findings are also consistent with the mineralisation-type of the ores treated at "La Soterraña". In contrast, the high concentrations of Ca, Al and Fe point to a soil matrix composed of carbonates, clay minerals and iron oxides.

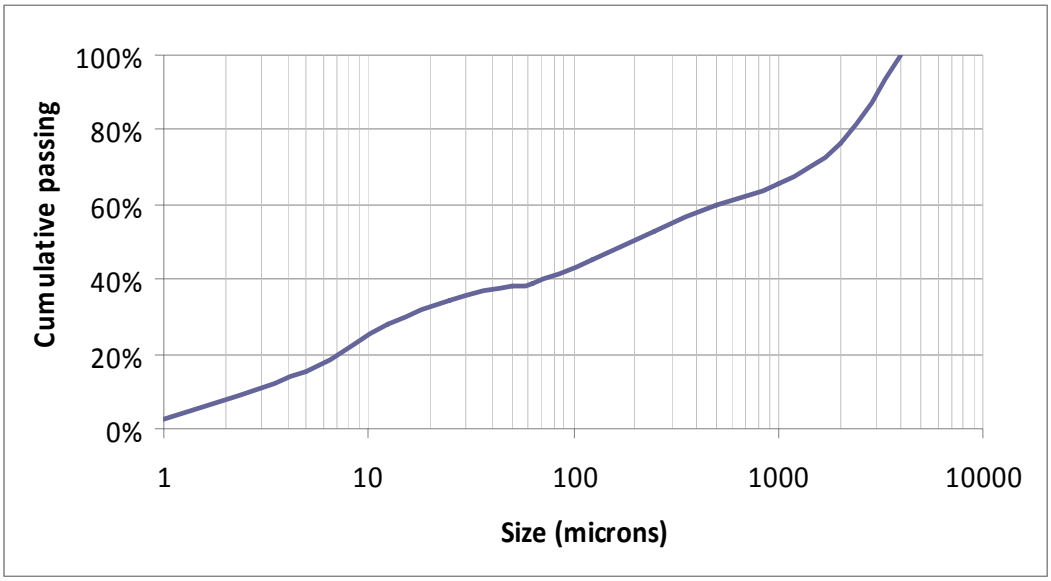

Figure 3. 1 Particle-size distribution of sample S2, obtained by compositing wet-sieving (4000-63 µm), and laser dispersion (<63 µm) data.

Regarding the grain-size analysis, the results for the three samples were very similar. For instance, the cumulative passing curve of sample S2 (Fig. 3.1) indicates that the coarsest (500-4000 µm: 39.9%) and finest fractions (<63 µm: 38.1%) were predominant, whereas intermediate fractions (250-500 µm: 1.8%; 125-250 µm: 15.7%; 63-125 µm: 4,5%) were less abundant. These data are particularly relevant given that the fineness of the material is one of the main factors impeding acceptable performance of soil washing for remediation purposes [7].

Table 3.3 Total content in grain-size fractions for major and trace elements of Sample S2 (results correspond to the average of three determinations with a standard error <5%).

Grain-size fraction (µm)	Trace elements (mg kg^{-1})					Major elements (%)		
	Hg	As	Pb	Zn	Sb	Al	Ca	Fe
4000-2000	495	15800	36	60	87	2.9	3.31	3.87
2000-1000	720	18400	44	70	101	3.25	3.42	3.74
1000-500	1000	21900	54	80	144	3.1	3.71	3.75
500-250	1920	24500	65	125	165	2.47	3.62	3.80
250-125	2030	27900	67	125	195	2.95	4.51	3.84
125-63	2520	24300	68	133	158	3.29	3.77	3.97
<63	4810	26350	76	155	212	3.31	3.42	4.39

To facilitate the study of the relationship between contaminant contents and grain-size fractions, we then measured the total content of major and trace elements in the abovementioned grain-size fractions. Hg and other trace elements showed higher contents in the fine fraction, while As showed a slightly more homogeneous distribution in all the grain-size fractions (Table 3.3). Of the major elements, only Fe showed a similar pattern to that observed for the previously mentioned trace elements, especially Hg. Therefore we hypothesised that most of the trace elements remain geochemically associated with former iron-rich sulphur minerals, which are probably oxidised in the present soil conditions. In contrast, a different profile was observed for Al and Ca, thereby suggesting a distinct behaviour of these elements to that of Hg and As. This notion was confirmed by a

multivariate approach in which a hierarchical cluster analysis and also a Principal Components Analysis (data not shown) revealed two main groups of elements, as shown in the dendrogram (Fig. 3.2).

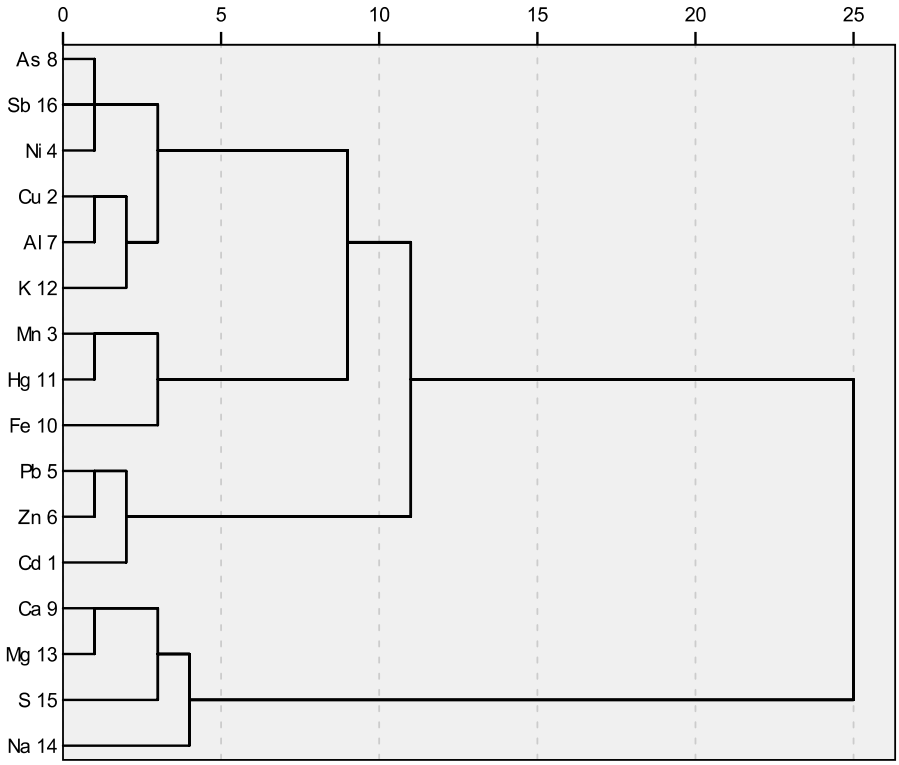

Figure 3. 2 Dendrogram showing the clustering of elements associated by their geochemical affinity within the samples (irrespective of the original sample and grain-size fraction). Main groups are indicated based on statistical distance between them.

This outcome is congruent and complementary to the mineralogical and edaphological studies, thus suggesting the following about the geochemical behaviour of As and Hg:

Group AB: Comprising mainly chalcophile trace elements and some major elements such as Fe, Al and K. This group is subdivided into two subgroups:

- **'A'** contains a clear association between Fe, Mn, Hg, As and other trace elements of concern (Sb, Ni). Consequently, and given the high contents of ultrafine materials in the soil and the low amount of organic matter, Hg and As behaviour appears to be controlled mostly by their ion binding to iron/manganese oxides-hydroxides. The presence of Al and K in this subgroup

suggests a main role of argillaceous minerals; however, the DRX data (see below) and the low ECEC suggest that phyllosilicates have little relevance.

- **'B'** includes the well-known Pb-Zn-Cd association, which probably originated from the weathering of sphalerite (ZnS, slightly enriched in Cd) and galena (PbS), both accessory minerals in La Soterraña ore.

Group C: Comprising elements linked to the alteration of the gangue rocks (for instance Ca from limestone). In addition, the presence of S in this group is linked to secondary minerals, such as gypsum ($CaSO_4 \cdot 2H_2O$), and others that can be observed in the local paragenesis of the weathered ores. According to the statistical treatment, the elements included in C are distant from the Group AB (negative correlation).

3.2 Mineralogy and liberation degree study

DRX data showed that the predominant components in the samples were quartz and secondarily, calcite, hematite, ferrihydrite, goethite and maghemite. In contrast, clay minerals were clearly minority. Mineralogical analyses, particularly microscopy observations, revealed that some of the former sulphides from the ore were undamaged in the coarse fractions, and were usually covered by gangue minerals, which shielded them from the effects of weathering (Figs. 3.3a, 3b).

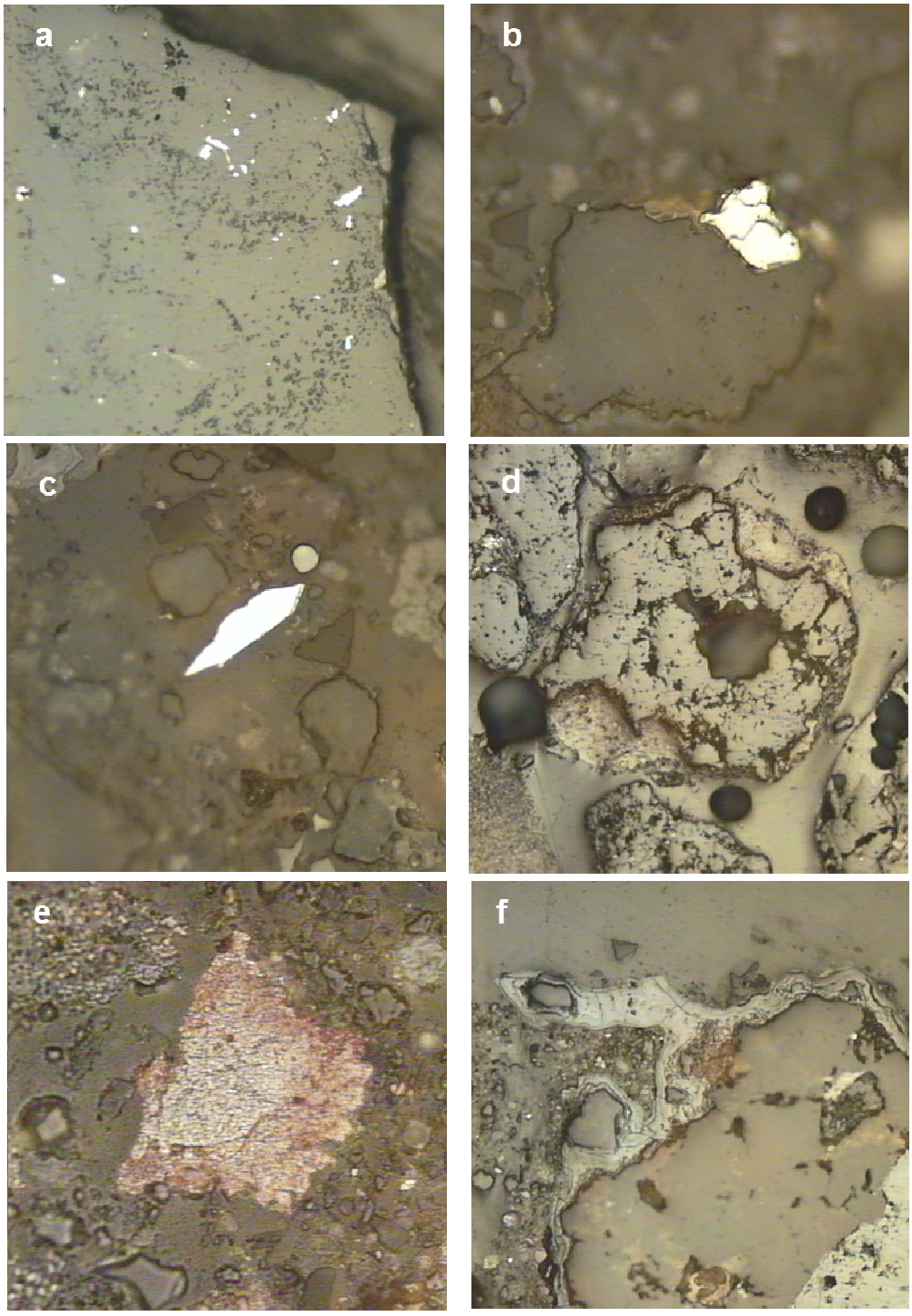

Figure 3. 3 (a) Arsenopyrite crystals within a quartz grain. (b) Pyrite inclusion in a quartz grain. (c) Unaltered free idiomorphic grain of arsenopyrite. (d) Quartz grain partially reemplaced by cinnabar (soft component). (e) Free altered cinnabar.(f) Hematite coating surrounding quartz grains. (Horizontal frame is 650 microns for Fig. 3a, 260 microns for Figs. 3b, 3c and 3e and 1.3 mm for Figs. 3d and 3f.)

Although scarce, free grains of arsenopyrite, (Fig. 3.3c), pyrite and chalcopyrite were also found. Cinnabar was the most common suphide and also appeared as inclusions in gangue minerals (Fig. 3.3d) and as free altered small grains (Fig. 3.3e, 3.3g). The texture is typical of a calcine material, the fractions below 250 microns being richer in metallic oxides and oxy-hydroxides, especially hematite (usually combined with gangue materials, Fig. 3f) and, to a lesser extent, goethite. These textures and morphologies can be attributed to the roasting process during ore treatment and also weathering. However, the most aggressive oxidising process was the former as it has the capacity to destroy As and Hg sulphides. Nevertheless, the temperature range used in the ovens (much lower than 700ºC) was not enough to destroy As-rich pyrite, arsenopyrite and chalcopyrite, irrespective of their original grain size (Fig. 3.4). In this regard, the presence and texture of cinnabar, and other mineral phases containing Hg denotes a deficient roasting procedure.

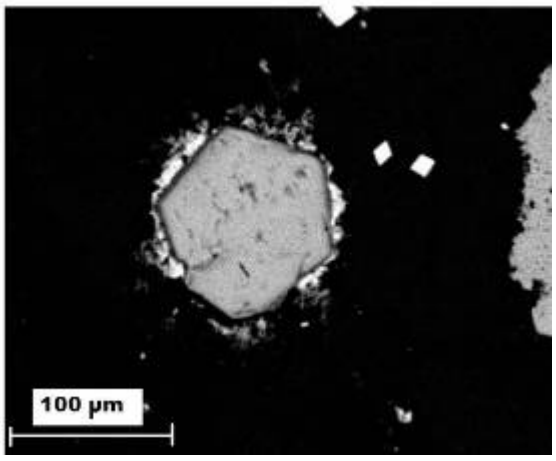

Figure 3.4 Scanning electron micrograph of a hexagonal goethite grain that preserves the original morphology of pyrite. The surrounding area contains 22% of Hg. Smaller and more reflecting grains correspond to arsenopyrite.

Therefore, the mineralogy of Hg (mainly as cinnabar) and As (mainly linked to Fe sulphides and oxides), which both show an irregular distribution within the grain-size fractions, hinders the design of an effective soil washing treatment. In fact, in the case of cinnabar (HgS), the liberation size calculated under the optical microscope (grain size for which the cinnabar grains are not mineral inclusions in other mineral phases) was below 200 µm, thus clearly limiting any physical separation equipment for fractions above this grain size. To obtain these data, we performed a complex

liberation size study composed of dozens of microphotographs with the accompanying measurements of grain sizes.

3.3 Specific-gravity study

The use of dispersants did not imply a clear improvement in the classification obtained in the C800 system (none of the chemical elements notably changed in the dense fraction concentration, see Table 3.4). Thus it can be concluded that the quality of the wet-sieving was sufficient to prevent distortions in the data described below.

Table 3.4 Major and trace elements concentrations measured in the dense fractions after experiments carried out with a C800 separator (125-63 µm fraction). Results are an average of those obtained with three samples and show a standard error <5%.

Samples	Trace elements (mg kg^{-1})					Major elements (%)		
	Hg	**As**	**Pb**	**Zn**	**Sb**	**Al**	**Ca**	**Fe**
Feed Material	785	29433	96	152	180	2,38	3.19	4,17
Dense fraction with dispersant pretreatment	925	17100	70	176	90	1,56	2.31	3,76
Dense fraction without pretreatment	897	15733	76	165	82	1,47	2.26	3,81
% Variation	*2,99*	*7,99*	*9,05*	*6,06*	*8,18*	*5,98*	*2,16*	*-1,51*

Although the liberation degree was below 200 μm for Hg, a considerable amount of contaminants might be recovered by gravity separation procedures in the grain-size interval between 500-125 microns. Initially, for the grain-size interval between 500 and 250 μm, the C800 separator was not effective as the sizes with which this equipment operates are clearly above the liberation size (Table 3.5).

Table 3. 5 Element content (percentage by weight) measured in the dense fraction for the indicated grain-size fractions. The separation between dense and light fractions was achieved in a C800 separator working as specified in Table 1. Results are an average of those obtained with three samples and show a standard error <5%.

Grain-size fraction (μm)	Textural classification	% in dense fraction		
		Hg	As	Fe
500 - 250	Medium sands	50.06	42.17	65.47
250 - 125	Fine sands	39.33	33.42	55.04
125 - 63		19.73	14.09	29.72
x<63	Silt-clay	15.65	6.82	14.06

Alternatively, for all the fractions below 250 μm, the results indicate that the dense fraction obtained in the C800 was poorer in As and Hg than the light fraction (Table 3.5). In this context, the differences in density between the two fractions were quite low (e.g., 2.5 g/cm^3 for the lighter particles and 2.8 g/cm^3 for the heavier ones in the case of the 63-125 μm fraction, both measured with a water pycnometer). This is an unexpected effect, given that the presence of 'free' As and Hg dense minerals, for instance cinnabar and arsenopyrite, arises when grain size decreases. Consequently, the concentrations in the dense fraction should be higher than those indicated in Table 5. The most probable explanation for this observation is that the size ranges used in this study were not narrow enough, and therefore a granulometric separation overlies the densimetric separation, as generally

occurs with other types of gravimetric separators [23]. In practical terms, these results imply that physical separation of this soil by means of gravity concentrators (spirals, shaking tables, etc) would be very difficult.

3.4 Grindability characterisation

The results described in the previous section indicate that the use of grain size separators or gravity concentrators is strongly hindered in fractions coarser than 200 µm; therefore milling is required to improve the liberation degree of Hg and As. This process, which normally accounts for 30% of the total costs in ore processing [23], can be significant enough to make the process unworkable. Thus, the cost of milling must also be taken into consideration in soil remediation procedures. In addition, milling would be an interesting option to address in future research into the immobilisation of trace elements [28].

Table 3. 6 Results of Bond ball mill grindability test, corresponding to the average of three determinations with a standard error <10%. F_{80} and P_{80} are the 80 % sieve opening through which 80% of the product passes (for Feed and Product respectively); P_i is the screen size at which the test is performed; Gbp is the Bond's standard ball mill grindability, w_i is the Bond index ('work index'), and W is the specific power consumption.

F_{80} [µm]	P_i [µm]	Gbp[g/rev]	P_{80}[µm]	w_i[kWh/sht]	w_i[kWh/t]	W[kWh/t]
2957	80	1.1032	72	15.01	16.54	16.45
2973	125	1.8917	109	11.22	12.37	9.69
2917	180	2.2967	154	10.97	12.09	7.50
2951	250	2.8523	194	9.90	10.91	5.82

Following the previous considerations, Bond tests were performed and the main results are presented in Table 3.6. The specific power consumption ranged from 16.45 kWh/t to 5.82 kWh/t, confirming that the finer the sieve, the greater the energy consumption. Depending on the liberation size, the power consumption in comminution operations can double from one size fraction to another. This issue should be considered when addressing the operating costs of the process. In our case, 125 microns can be considered a safe cut-off point in accordance to the results of the mineralogical study; hence the specific power consumption to take into account is 9.69 kWh/t. This value reflects a medium-high level, similar to that required for grinding an average limestone [29]. Along with the previous statements, appropriate selection of the milling machine will yield a well-balanced power efficiency process [30].

3.5 Consequences for soil washing design

The feasibility study carried out in this work should be completed by a cost analysis, highly conditioned by the huge amount of soil to be treated (80,000 m^2) and by other important questions such as cost of milling (as described above) and treatment of washing effluents. At any case, it is possible to propose a first approach to define soil washing stages, in brief:

- The grain-size fractions below 125 µm containing "free" As and Hg minerals could be treated with hydrocycloning [37] because of the demonstrated increasing concentration of the contaminants with increasing fineness. A factorial design would be required to define optimum conditions (see for example a successful application in [10]).

- The design of the strategy for the fractions coarser than 125 µm is clearly conditioned by the results of the mineralogical and specific-gravity studies. Therefore in order to improve the Hg and As liberation degree, a milling process should be required. The ground material would be below 125 µm, thereby allowing hydrocycloning.

Some other supplementary technologies might be helpful. For instance, a considerable amount of minerals such as pyrite, goethite and hematite (enriched/bound to As and Hg) could be separated prior to hydrocycloning by means of magnetic field technologies [32]. Furthermore, given that cinnabar is highly hydrophobic [33, 34], froth flotation may be an appropriate option to obtain satisfactory Hg recovery yields [35, 36].

4. Conclusions

Hg and As are primary soil pollutants, particularly in areas formerly devoted to mining activities and the metallurgy industry. In these circumstances, a proper remediation approach to reduce the volume of contamination is soil washing. This approach has been reported to be a cost-effective physical separation technique. The feasibility study at the site of "La Soterraña" shows soils with very high As and Hg content. From geochemical, edaphological and mineralogical data, we have demonstrated that Hg is concentrated mainly in fine grain fractions (below 200 microns), where it is present in the original sulphide form and bound to Fe-Mn oxyhydroxides. In contrast, As is abundant in fine-medium (below 500 μm) fractions and predominantly linked to Fe mineral phases as well.

In the context of the feasibility study, the C800 separator proved effective to study narrow grain-size intervals whenever significant differences in specific-gravity within the particles of the soil were detected. However, in our case, the results obtained were not conclusive. In fact, the mineralogical data reflected the low liberation degree of As and Hg in sandy fractions, and thus the yields of gravimetric or grain-size separation of these fractions would be unsatisfactory. Accordingly, an interesting alternative, though possibly expensive, would consist of previous milling of the medium and coarse fractions in order to allow treatment. In this context, the grindability test is a novel approach carried out to indicate the extent of power consumption and its influence on the energy efficiency and potential recovery of pollutants. This approach complemented the information from the feasibility study, and showed that in this case physical soil washing would be clearly conditioned by milling costs.

Acknowledgements

This research was funded by the CDTI ('Centro para el Desarrollo Tecnológico e Industrial'), part of the Spanish Council for Industry, within the research programme named "CLEAM CENIT". The corporations involved in this project are the final holders of the results presented here.

We thank Dr. Rodrigo Álvarez for his help with the mineralogical study. Carlos Sierra obtained a grant of the "Severo Ochoa" programme (Ficyt, Asturias, Spain).

References

[1] J.E. Gray, J.G. Crock, D.L. Fey, Environmental geochemistry of abandoned mercury mines in West-Central Nevada, USA. Appl. Geochem. 17 (2002) 1069–79.

[2] J. Martínez, J. Llamas, E. de Miguel, J. Rey, M.C. Hidalgo, A.J. Sáez, Multivariate analysis of contamination in the mining district of Linares (Jaén, Spain), Appl. Geochem. 23 (2008) 2324-2336.

[3] P. Higueras, R. Oyarzun, J. Lillo, J.C. Sánchez Hernández, J.A. Molina, J.M. Esbrí, S. Lorenzo, The Almadén district (Spain): anatomy of one of the world's largest Hg-contaminated sites, Sci. Total. Environ. 356 (2005) 112– 124.

[4] A. Davis, N.S. Bloom, S.S Que Hee, The environmental geochemistry and bioaccessibility of mercury in soils and sediments: a review, Risk Anal. 17 (1997) 557–569.

[5] A.A. Duker, E.J. Carranza, M. Hale, Arsenic geochemistry and health, Environ. Int. 31 (2005) 631-641.

[6] G. Dermont, M. Bergeron, G. Mercier, M. Richer-Laflèche, Soil washing for metal removal: A review of physical/chemical technologies and field applications, J. Hazard. Mater. 152 (2008a) 1–31.

[7] R. Anderson, E. Rasor, Particle size separation via soil washing to obtain volumen reduction, J. Hazard. Mater. 6 (1998) 89-98.

[8] R. Griffiths, Soil washing technology and practice, J. Hazard. Mater. 40 (1994) 175-189.

[9] M.J. Mann, Full scale and pilot scale soil washing, J. Hazard. Mater. 66 (1998) 119-136.

[10] C. Sierra, J.R. Gallego, E. Afif, J.M. Menéndez-Aguado, F. González-Coto, Analysis of soil washing effectiveness to remediate a brownfield polluted with pyrite ashes, J. Hazard. Mater. 180 (2010) 602-608.

[11] G. Dermont, M. Bergeron, G. Mercier, M. Richer-Laflèche, Metal-Contaminated Soils: Remediation Practices and Treatment Technologies, Practice Periodical of Hazardous, Toxic, and Radioactive Waste Management 12 (2008b) 188-209.

[12] M. Pearl, M. Pruijn, J. Bovendeur, The Application of Soil Washing to the Remediation of Contaminated Soils, Land Cont. Rec. 14 (2006) 713-726.

[13] J. Loredo, A. Ordóñez, R. Álvarez, Environmental impact of toxic metals and metalloids from the Muñón Cimero mercury-mining area (Asturias, Spain), J. Hazard. Mater. 136 (2006) 455–467.

[14] C. Luque, Las mineralizaciones de Hg de la Cordillera Cantábrica. Doct. Thesis, Universidad de Oviedo (unpublished), 1985.

[15] C. Luque, El mercurio en la Cordillera Cantábrica, Recursos minerales de España, García Guinea y Martínez Frías, (Eds.), C.S.I.C. Textos universitarios No.15, pp. 803–826, Madrid, 1992.

[16] C. Baldo, J. Loredo, A. Ordóñez, J.R. Gallego, J. García-Iglesias, Geochemical characterization of wastes from a mercury mine in Asturias (northern Spain), J. Geochem. Explor. 67 (1999) 377-390.

[17] J. Loredo, R. Álvarez, A. Ordóñez, Release of toxic metals and metalloids form Los Rueldos mercury mine (Asturias, Spain), Sci. Total Environ. 340 (2005) 247-260.

[18] R. Fernández-Martínez, J. Loredo, A. Ordóñez, M.J. Rucandio, Physicochemical characterization and mercury speciation of particle-size soil fractions from an abandoned mining area in Mieres, Asturias (Spain), Env. Pollut. 142 (2006) 217-226.

[19] J. Loredo, C. Luque, J. García-Iglesias, Conditions of formation of Hg deposits from the Cantabrian zone (Spain), Bull. Mineral. 111 (1998) 393-400.

[20] M. Pansu, J. Gautheyrou, Handbook of soil analysis: mineralogical, organic and inorganic methods. Berlin: Springer, 2006.

[21] J.R. Gallego, A. Ordóñez, J. Loredo, Investigation of trace element sources from an industrialized area (Avilés, northern Spain) using multivariate statistical methods, Environ. Int. 27 (2002) 589-596.

[22] M.G. Cordingley, M.P. Hallewell, J.W. Turner, Release analysis and its use in the optimisation of the comminution and gravity circuits at the Wheal Jane Tin concentratror, Min. Eng. 7 (1994) 1517-1526.

[23] B.A. Wills, T.J. Napier-Munn, Mineral Processing Technology: An Introduction to the Practical Aspects of Ore Treatment and Mineral Recovery, seventh edition, Burlington, Massachusetts, Butterworth-Heinemann, 2006.

[24] F.C. Bond, Third theory of comminution, Min. Eng. Trans. AIME. 193 (1952) 484-494.

[25] N. Magdalinovic, A procedure for rapid determination of the Bond work index, Int. J. Miner. Process. 27 (1989) 125-132.

[26] J.M. Menéndez-Aguado, B.R. Dzioba, A.L. Coello-Valazquez, Determination of work index in a common laboratory mill, Miner. Metal. Proc. 22 (2005), 173-176.

[27] R.J. Deister, How to determine the Bond work index using lab ball mill grindability tests, Eng. Min. J. 188 (1997) 42-45.

[28] S. Montinaro, A. Concas, M. Pisu, G. Cao, Remediation of heavy metals contaminated soils by ball milling, Chemosphere 67 (2007), 631-639.

[29] V. Deniz, H. Ozdag, A new approach to Bond grindability and work index: dynamic elastic parameters. Min. Eng. 16 (2003) 211-217.

[30] H.T. Ozkahraman, A meaningful expression between bond work index, grindability index and friability value, Min. Eng. 18 (2005), 1057-1059.

[31] C.W. Williford, R.M. Bricka, Physical separation of metal-contaminated soils, in: I.K. Iskandar (Ed.), Environmental Restoration of Metals- Contaminated Soils, 1st ed, , CRC Press, Boca Raton, Florida, 2000.

[32] R.A. Rikers, P. Rem, W.L. Dalmijn, Improved method for prediction of heavy metal recoveries from soil using high intensity magnetic separation (HIMS), Int. J. Miner. Process. 54 (1998), 165–182.

[33] E.G. Erspamer, R.R.Wells, Selective extraction of mercury and antimony from cinnabar-stibnite ore. Bureau of Mines Report of Investigations 5243 (1956), United States Department of the Interior.

[34] P. Cauwenberg, F. Verdonckt, A. Maes, Flotation as a remediation technique for heavily polluted dredged material. A feasibility study, Sci. Total. Environ. 209 (1999) 113-119.

[35] M. Vanthuyne, A. Maes, P. Cauwenberg, The use of flotation techniques in the remediation of heavy metal contaminated sediments and soils: an overview of controlling factors, Miner. Eng. 16 (2003), 1131–1141.

[36] G. Dermont, M. Bergeron, M. Richer-Lafleche, G. Mercier, Remediation of metal-contaminated urban soil using flotation technique, Sci. Total Environ. 408 (2010) 1199-1211.

CHAPTER IV: High intensity magnetic separation for the clean-up of a site polluted by lead metallurgy.

C. Sierra[(a)], J. Martínez [(b)], J.M. Menéndez-Aguado[(a)], E. Afif[(c)], J.R. Gallego[*(a)]

Journal of Hazardous Materials, (2013) 248–249, 194-201.

Abstract

The industrial history in the district of Linares (Spain) has had a severe impact on soil quality. Here we examined soil contaminated by lead and other heavy metals in "La Cruz" site, a brownfield affected by metallurgical residues. Initially, the presence of contaminants mainly associated with the presence of lead slag fragments mixed with the soil was evaluated. The subsequent analysis showed a quasi-uniform distribution of the pollution irrespective of the grain-size fractions. This study was accompanied by a characterization of the lead slag behaviour under the presence of a magnetic field. Two main magnetic components were detected: first a ferromagnetic and/or ferrimagnetic contribution, second a paramagnetic and/or antiferromagnetic one. It was also established that the slag was composed mainly of lead spherules and iron oxides embedded in a silicate matrix. Under these conditions, the capacity of magnetic separation to remove pollutants was examined. Therefore, two high intensity magnetic separators (dry and wet devices respectively) were used. Dry separation proved to be successful at decontaminating soil in the first stages of a soil washing plant. In contrast, wet separation was found effective as a post-process for the finer fractions.

Key words: Soil pollution; Lead; Slag; Magnetic separation; Soil washing.

1. Introduction

Lead mining and primary lead metallurgical facilities usually generate large volumes of waste, the storage of which may cause serious damage to the environment. This waste is a source of potentially toxic trace elements (Pb, As, Cd, Zn, Cu, Mn) that can be released into soils, the atmosphere, surface waters and groundwater [1, 2].

Lead-slag is the main waste generated in lead metallurgy. Initially, metals in slags are fused together and bound, thus they cannot be easily released or leached into the environment [3]. However, slag heaps also hold alterable components such as secondary minerals and by-products of lead production; both are a source of a range of elements that can make waste chemically active. In fact, slag often holds impure Pb, speiss (formed if enough S and Cu is available) and matte (formed if enough As is present, but also Fe, Co, and Ni, among others). In addition, sulphides present in the slag can be slowly oxidized by weathering (Pb has the capacity to replace K, Ba, Sr, and even Ca on clay surfaces and in their interlayer), thereby co-precipitate metals in the form of metal oxides and sorbed on organic matter [4]. Finally, blast furnace flue dust is another source of pollutants that is generally responsible for heavy metal accumulation in soils. It has been concluded that lead slags are not always inert residua [5, 6] and, consequently, they can release dangerous metals and semi-metals, thus promoting soil pollution.

In metal-polluted sites, soils used to be remediated by means of conventional approaches such as excavation of the impacted soil and subsequent disposal of the material at a landfill, or by means of on-site stabilization treatments based on pH and Eh modifications in order to avoid lixiviation [7]. However, in recent years, governmental policies and applied research have fostered less intrusive technologies [8]. In this sense, soil washing, although it modifies soil structure and geochemical

equilibriums, can be very cost-effective when dealing with great volumes of contaminated soil; in particular, the physical separation approaches that guarantee a minimum of secondary waste The basic principle of physical soil washing consists of the removal of contaminants by exploiting differences between the characteristics of metal-bearing particles and soil particles (size, density, hydrophobic surface properties, and magnetism). Among these technologies, magnetic separation is a physical separation process that segregates materials on the basis of their magnetic susceptibility [9]. All materials have magnetic susceptibility, which can be either positive (ferro-, ferri-, para-, and antiferro-magnetic) or negative (diamagnetic). When a particle with a positive susceptibility encounters a non-uniform magnetic field, it is pushed in the direction in which the field gradient increases, whereas diamagnetic particles are affected in the opposite manner. When the field gradient is low, ferro- and ferri-magnetic particles can be separated, whereas higher intensities are required for para- and antiferro-magnetic particles in order to be physically captured and separated from extraneous diamagnetic material [10].

Minerals and pollutants present in soil have susceptibilities that vary from negative (organic) and intermediate (paramagnetic minerals and organometallics), to largely positive (ferro and ferri minerals), thereby making magnetic separation of these soil fractions feasible [11]. The magnetic separation of heavy metals from the soil matrix is not the most widely used technique, although it has been applied when metal contaminants are associated with ferromagnetic fractions [12]. Consequently, a number of strategies have been proposed; for instance LIMS (low intensity magnetic separation) has been used to recover spent ammunition debris and other kinds of debris while HIMS (high intensity magnetic separation) has been applied to remove metals from a range of soils [13]. Furthermore, when slags (Fe alloys) hold diamagnetic mineral-forming elements, the removal of these compounds is still possible [14]. The magnetic properties of slags are variable and dependent on many parameters, such as chemical heterogeneity, depositional and/or crystallization conditions, and post-deformational stress. In fact, magnetic susceptibility values for Pb-slag depends on the grain size, on the Fe content (particularly when magnetite (Fe_3O_4) has been formed as a result of imperfect reduction of Fe_2O_3, or by the presence of pyrrhotite), on the Mn content (able to form highly ferro- and ferri-magnetic alloys), and finally on the presence of dislocations, lattice vacancies, impurities, among others [15].

The first step in the design of a full-scale washing treatment is a viability analysis [16]. This involves several analytical measurements in order to examine the main characteristics of the soil. The viability study presented here was carried out on a soil contaminated with Pb and other metals and semi-metals derived from metallurgical activities. The major challenge was to analyze the properties and components of the slag affecting the soil.

The main specific aims of the study were the following:

- To integrate grain-size distribution, with geochemical and mineralogical information of a highly Pb-polluted site (La Cruz foundry, Linares, Spain) in which the presence of fine waste of lead slag is one of the main environmental risks.

- To characterize chemically and magnetically the Pb-slag, in order to identify the main properties conditioning a possible soil washing treatment by means of magnetic separation.

- To evaluate the recoveries of heavy metals via both dry and wet HIMS (High-Intensity Magnetic Separation).

2. Materials and methods

2.1 Site description and sampling

In the Linares district (NE Andalucía, Spain) a large mining and mineral extraction industry based on the exploitation and transformation of galena (PbS), associated with sphalerite (ZnS), chalcopyrite ($CuFeS_2$) and barite ($BaSO_4$), thrived for centuries [17, 18]. This activity produced a large amount of waste material, which accumulated in the vicinity of the exploitations and mineral processing sites. The minerals obtained were then treated in various metallurgical factories, a process that generated large Pb-slag heaps. These deposits exposed local people to a heavy atmospheric dust load and contaminated extensive areas used for crop cultivation (Linares is an important agricultural area) by releasing heavy metals as a result of natural weathering. In recent years, several geochemical characterizations of these soils have been conducted in order to assess the environmental impact that mining/metallurgy activities have caused [19, 20, 21].

Of the metallurgical industries that operated in the area, we highlight La Cruz lead foundry (38º 8' 20.493'' N, 3º 37' 59.893'' W), which was finally shut down in 1994 after functioning for 160 years. This factory generated numerous Pb residues as a consequence of a range of metallurgical processing systems in operation throughout its history: reverberatory furnaces, shaft-furnaces, and blast furnaces. With nearby 23.000 mg/kg Pb at selected location [22] La Cruz foundry is an important reference location for Pb pollution in Europe. The activities undertaken at La Cruz produced a brownfield of around 20 ha of polluted soils, in which there are several randomly distributed slag heaps with a total surface area of 4.7 ha and an accumulated volume of approximately 1,345,000 m^3. These materials lie directly on Triassic substrate, and substantial surface erosion by

water and wind has been reported, along with local landslides, excavated slopes (by extraction of the material for cement production), crusts, exudations and leachates at the foot of the deposits [22].

Geologically, two groups of materials can be differentiated in the studied area: the Palaeozoic basement and the sediment cover [17]. The sedimentary cover is formed by Triassic, Neogene and Quaternary materials. The Quaternary materials are primarily made up of alluvial silts, with embedded discontinuous levels of sand and conglomerates.

In this context, three representative bulk samples of soil (25 kg each) were taken by compositing sub-samples collected at ten random locations in the brownfield. These samples were collected from a tilled depth (0-35 cm) by means of a stainless steel hand-auger and a shovel; the soil was passed through a 2-cm mesh screen *in situ* to remove rock fragments, vegetation and other large material. Finally, samples were homogenized and stored in inert plastic bags at room temperature; further preparation and analyses were carried out before fifteen days after the sampling.

Regarding lead-slag samples, these were obtained by directly collecting 3 representative bulk samples (3 Kg each) from the heaps.

2.2 Solid-phase study

2.2.1 Pedology and mineralogy

Soil pH was measured with a glass electrode in a suspension of soil and deionized water (1: 2.5) and electrical conductivity was measured in the same extract (diluted 1:5). Organic matter was determined by the ignition method (weight loss at 450ºC). Exchangeable cations (Ca, Mg, K and Na), extracted with 1 M NH_4Cl, and exchangeable Al, extracted with 1 M KCl, were determined by

atomic absorption/emission spectrophotometry (AA200 Perkin Elmer). The effective cation exchange capacity (ECEC) was calculated as the sum of concentrations in exchangeable cations and Al. Particle-size distribution was determined by the pipette method while sodium hexametaphosphate and Na_2CO_3 were used to previously disperse the samples.

A first approach to the mineralogical composition of the soil was obtained by means of an X-Ray diffractometer (XRD, Philips X Pert Pro, incorporating databases of the International Centre for Diffraction Data); then, a Nikon Stereoscopic Zoom Microscope SMZ1000 coupled to a Nikon DS-Ri1 color high resolution camera and NIS-elements Software BR (Nikon Instruments, Inc) were used to perform stereomicroscopic observations of the samples in order to estimate the percentages of slag vs. soil, and to define semi-quantitatively soil mineralogy by means of petrographic point-count analysis.

2.2.2 Grain-size fractioning

Representative batches of each sample were slurried in deionized water and then sieved (cycles of 100 g) into particle-size fractions of > 4000 µm (A), 4000 – 2000 µm (B), 2000 – 1000 µm (C), 1000 – 500 µm (D), 500 – 250 µm (E), 250 – 125 µm (F), 125 – 63 µm (G), < 63 µm (H) using normalized sieves positioned in a sieve shaker (Restch) for 5 minutes with a water flow of 0.3 l/min (ASTM D-422-63, Standard Test Method for Particle-Size Analysis of Soils). The fractions were recovered with the help of a spray nozzle, dried at 50 ºC for 48h and weighed.

2.2.3 Geochemical analysis

Representative samples of the grain-size fractions were digested and subjected to chemical analyses by means of ICP-OES. In order to standardize the conditions used for chemical attack,

samples with a grain size over 125 μm were ground using a vibratory disc mill (RS 100 Retsch) at 400 rpm for 40 seconds to obtain <125 um samples. For chemical analyses, 1-g representative sub-samples of the diverse origins (soils, grain-size fractions, etc.) were digested by means of an 'Aqua regia' digestion (HCl + HNO_3). This method, although not total, was considered effective enough given the nature of the samples [23, 24, 25]; in fact, the relevance of the quantity of pollutants hard to digest is very low, given that this fractions are nearly impossible to be lixiviated in natural conditions. In addition, all the samples were equally extracted and thus the recovery extents can be compared on a relative basis. The digested material was analyzed for total concentrations of 19 major and trace elements (Ca, Mg, K, Na, Al, Fe, S, Cu, Pb, Zn, Cd, Ni, Mn, As, Sr, Sb, La, Cr and Hg) by ICP-OES in the accredited (ISO 9002) laboratories Actlabs Int., Ancaster (Ontario, Canada).

2.2.4 Slag composition

Representative slag sub-samples were used to prepare polished sections to be studied under an Eclipse LV 100 POL Nikon petrographic microscope. As a second step, the mineralogical composition of the slag was estimated by means of a PANalytical X'Pert Pro MPD X-ray diffractometer after an exposure time of 7.5 hours (incorporating databases of the International Centre for Diffraction Data). Regarding chemical analyses, lithium borate was used to fuse the 3 slag samples. These were then cast into a disc and analyzed by X-ray fluorescence (Philips PW2404) to determine concentrations of major, minor and trace elements (Cd content was determined by means of ICP-OES from another set of 3 representative samples previously ground as described above).

Scanning Electron Microscope and Energy Dispersive X-Ray Spectrometer (SEM/EDS, Jeol JSM-6100) was used to study the microstructure of the slag and to evaluate the chemical composition of the materials (accelerating voltage BEC 20KV, EDS measurement time: 340 sec).

2.2.5. Magnetic properties of the slag

Three representative samples of about 30g of slag each were ground in an agate mortar and then subjected to magnetic characterization in a vibrating sample magnetometer VSM EV9 (Microsense, LLC) at laboratory temperature (20 °C). Data were analyzed by means of the software EasyVSM ®. The virgin curve was obtained after demagnetizing the samples using oscillating magnetic fields (dumped from 796 kA/m up to 0 kA/ m). The hysteresis loop was, subsequently measured with a maximum applied field of 1592 kA / m. The specific or mass magnetic susceptibility, χ_{mass}, is defined as the ratio of the material magnetization M (per unit mass) to the applied external field H_a [9].

2.3 Magnetic washing

Before HIMS studies, the bulk sample was passed through a dry-LIMS apparatus (KHD Humboldt Wedag). This first step was performed in order to simulate the normal mineral dressing procedure, wherein dry LIMS is performed as a previous step [12] in order to prevent highly magnetic particles from disturbing the magnetic field.

After this, fractions were treated following the manufacturer's instructions regarding feeding sizes for the HIMS apparatus used: Grain-sizes intervals between 4-2, 2-1, and 1-0.5 mm were treated in a dry-HIMS device (see section 2.4.1), while those ranging from 500-250, 250-125 and 125-63 µm were treated in a wet-HIMS module (see section 2.4.2). Fractions below 63 µm were not treated, given that they would require operative changes in the configuration of the separation chamber of the wet-HIMS apparatus, thereby hindering the comparison of the results.

2.3.1 Dry-HIMS

Dry-HIMS is a technique based on rare earth permanent magnets that provides high recovery yields with low operating costs. This method efficiently removes weak magnetic pollutants and can achieve precise separations because of the absence of drag forces [26]. The particularities of this technique (it can be used only on dry soils) make it generally uneconomical in soil washing operations. Nevertheless, given the climatic characteristics of Linares (dry and warm Mediterranean weather), this technique is appropriate for the study site and thus circumvents one of the main problems in soil washing, i.e. the generation of liquid wastes.

The rare earth magnetic separator used was the high force magnetic separator Model Nº L/p 10:30 of International Process Systems Inc. (US PATENT) [27]. The separator consists of a support frame, a magnetic roller, an idler roller and a conveyor belt. This induced magnetic roll separator uses gravity and magnetic force (centripetal force) to separate particles on the basis of their magnetic properties, since the particles are affected by a magnetic force, which keeps them attached to the conveyor belt, thereby resulting in a different discharge trajectory. The velocity of the roller in factorial tests was set at 20, 60, 100 rpm. The fractions obtained in each experiment were observed and classified by hand sorting, and under a stereoscopic microscope assisted by NIS-elements Software BR (Nikon Instruments, Inc) when needed.

2.3.2 Wet-HIMS

For the finer fractions, dry-HIMS is not effective. However wet-HIMS is suitable with ease of operation, providing that there is a large concentration and beneficiation ratio [13, 28].

The equipment used was an OUTOTEC Laboratory WHIMS 3X4L, which has the capacity to separate paramagnetic (weakly magnetic) from non-magnetic materials.

Feed slurry was accomplished by pulping 50 g of soil with 200 g of water. This mixture was then passed through the separating chamber, called a matrix canister, in this case selecting a soft Fe sphere media composed of spheres of 12.7 mm in diameter. The magnetic flux density was 2.16 T (max) according to the manufacturer's specifications. The water and non-magnetic components pass through the cell after flushing with water and are collected in a pan, while the magnetic components are efficiently retained and finally washed out by reducing the magnetic field to zero.

The variable magnetic field intensity of the equipment is adjusted through control of the coil input amperage (0-6 amps) [29]. The voltages used in factorial tests were 30, 60 and 90 % of the maximum output voltage. The fractions obtained in each experiment were observed under a stereoscopic microscope assisted by NIS-elements Software BR (Nikon Instruments, Inc); Eclipse LV 100 POL Nikon petrographic microscope was used only for the fraction below 63 μm.

3. Results and discussion.

3.1. Soil characterization.

The representative subsamples of the study area showed neutral pH (6.9), low organic matter content in the upper horizon (1%), high electrical conductivity (EC = 1.3 dS m^{-1}), low contents of exchangeable base cations (6.3; 1.2 and 0.3 $cmol_c\ kg^{-1}$ for Ca, Mg and K respectively), high Na (3.6 $cmol_c\ kg^{-1}$), and moderate ECEC (11.5 $cmol_c\ kg^{-1}$). The mineral soil texture of the samples was sandy loam, the particle-size distribution of which revealed a high percentage of sand fractions (85.5 %). These features are consistent with the properties displayed by neutral soils in Mediterranean areas.

Concerning mineralogical analyses, X-ray diffraction indicated the presence of the six main mineral phases that were ordered by their relative abundances, after optical point-counting determination, as follows: Quartz, feldspar, illite, calcium carbonate, trioctahedral vermiculite and gypsum. The presence of two types of clays –illite and vermiculite– and carbonates determined the adsorption of contaminants [30]. Paired to the referred main minerals in the soil, we also observed various metallic minerals, such as hematite, magnetite, chalcopyrite, pyrite, sphalerite and galena. Interestingly, lead slag fragments were abundant in various grain-sizes (estimated 10 % in weight) and were also found pulverized and coating soil particles on some occasions.

Table 4.1 Particle-size distribution and element concentration of representative subsamples of the three initial bulk samples (results correspond to the average of three determinations with a standard error <5%; aqua-regia digestion and ICP-OES).

Grain-size (µm)	Weight (%)	Elements (mg·Kg^{-1})					Elements (%)			
		Cd	Cu	Mn	Zn	As	Pb	Ca	Fe	Al
2,000 to 4,000	11.86	11.1	280	1482	302	30	0.21	4.33	1.76	0.37
1,000 to 2,000	16.95	7.0	374	1206	816	42	0.36	3.02	1.90	0.43
500 to 1,000	16.95	5.5	303	898	754	47	0.29	2.03	1.58	0.40
250 to 500	18.64	5.5	215	568	312	40	0.23	1.23	0.92	0.76
125 to 250	13.56	7.5	276	566	333	55	0.30	1.20	0.94	0.97
63 to 125	8.47	14.0	498	794	567	104	0.54	1.76	1.39	1.28
- 63	13.56	11.6	870	853	870	300	0.49	1.85	2.56	1.75
Bulk sample	-	*8.9*	*405*	*903*	*565*	*86*	*0.35*	*2.12*	*1.54*	*0.85*

Furthermore, ICP-OES analyses revealed very high concentrations of Pb and a lower presence of As, Cd, Cu and Zn. As previously stated, grain-size classification is a normal stage in soil washing; however, in this case, since all grain-sizes showed elevated pollutant concentrations (Table 4.1), we considered it necessary to subject most of the fraction to a soil washing procedure (magnetic separation in our study).

3. 2 Chemical and mineral composition of the slag.

The main slag appeared as a dense, opaque, glassy, with a color ranging from black to grayish black, and occasional brown tones that can be associated with Fe hydroxides. Fresh cuts had a metallic shine with the presence of some golden tones, these probably corresponding to complex intermetallic compounds (Fig. 4.1). The larger fragments had significant alveolar porosity, a conchoidal surface and braided morphologies, typical of rapid solidification. The general appearance was similar to that of air-cooled slag.

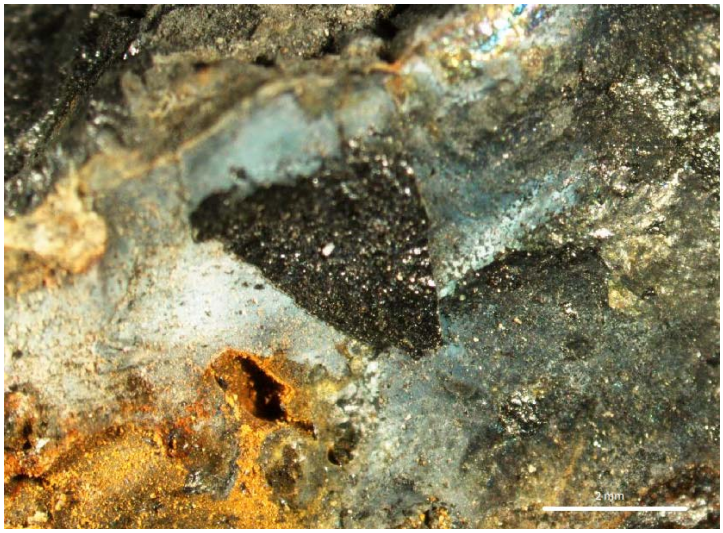

Figure 4. 1 Macrostructure corresponding to a selected lead slag fragment.

The stoichiometric transformation of analyses shown in Table 4.2 evidence that the slag consisted mainly of Fe (24%), Si (13.59 %), and Ca (13.99 %), which, summed together and expressed as weight percentage of the most probable oxides, constituted 82.97 % of the slag.

Table 4. 2 Major components of the slag obtained by X-ray fluorescence. Results are an average of those obtained with three samples and with a standard error <5%.

Component	SiO_2	Al_2O_3	Fe_2O_3	CaO	MgO	K_2O	MnO	TiO_2	P_2O_5	Cr_2O_3	V_2O_5
wt %	29.07	6.75	34.32	19.58	1.82	1.35	1.13	0.3	0.45	0.011	0.031
Component	**As**	**Ba**	**Co**	**Cu**	**Ni**	**Pb**	**S**	**Sn**	**Sr**	**Zn**	**Zr**
$mg \cdot kg^{-1}$	230	21,490	70	1,350	160	12,490	12,790	190	1,000	29,450	80

Regarding the chemical composition in elements of environmental concern, Pb, Zn and also Cu were present in significant concentrations in the samples. In contrast, the concentration of As was low (230 mg/kg); this observation could be attributable to the fact that this semi-metal tends to accumulate in the condensing chamber during the smelting process. Likewise, the Cd concentration (not included in the table), which was analyzed by ICP-OES was low value (2.85 mg/Kg). High concentrations of Al, Mn, Mg, and C were also found, these corresponding to the ore, flux and reducing agent.

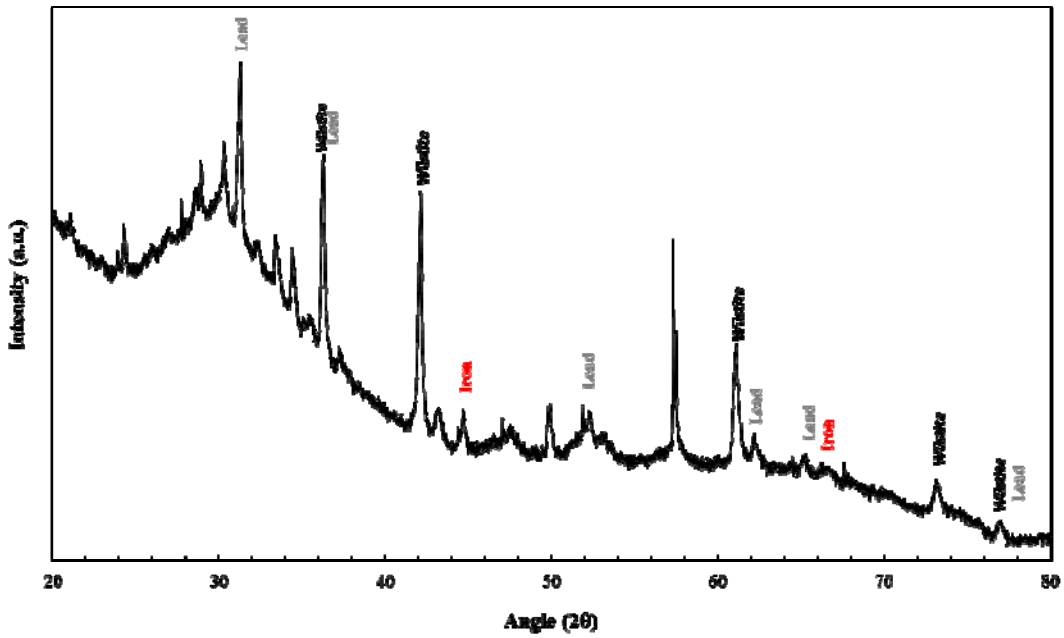

Figure 4.2 XRD pattern obtained from a representative lead slag sample. Only most probable peaks (iron, Wüstite and lead) are shown. Note the prominent amorphous silica hump on the left side of the diagram. Intensity is expressed in arbitrary units (a.u).

Results from the optical light microscopy and SEM/EDS allowed the identification of the following three main constituents (also confirmed by the XRD pattern (Fig. 4.2)): i) an intermetallic matrix composed of Si and Fe, and traces of Ca, Mn, and Zn in the form of a vitreous phase that suggests relatively fast cooling; ii) Fe oxides, which were represented mainly by Wüstite (Fig. 4.3a), an anti-ferromagnetic iron oxide formed as a result of the alteration of other iron-bearing minerals at high temperatures in a highly reducing environment; as well as by the possible presence of discreet amounts of magnetite in the form of small elongated crystals; and iii) lead, which appeared in the form of spherules (Fig. 4.3b) of vitreous nature and heterogeneous size ranging from 5 to 60 µm, sometimes coming together with galena, then developing elongated ex-solution textures. These spherules were sometimes accompanied by other metallic minerals, which coated the bullion and could be partially transformed into secondary minerals, surely as a result of years of weathering. In addition, As was also found associated with the bullion but in concentrations below 4% for all the samples (higher amounts would have caused its immiscibility).

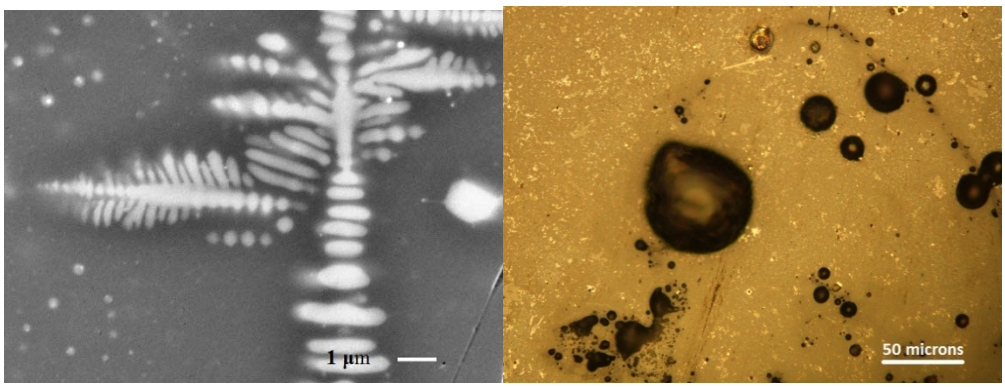

Figure 4.3 a) Backscattered scanning electron micrograph of the slag (1000x). Higher reflectance corresponds to Wüstite. b) Microphotograph from optical microscope (in reflected light) of several lead spherules within the slag.

This study suggested mineralogical homogeneity that contrasts with other cases [31, 32, 33]. This finding is consistent with the low concentrations and narrow range of trace elements present in the samples, the long-exposure to weathering, and mainly the low stability of many of the possible phases found i.e., sulphides (galena, wurtzite, pyrrhotite, etc.), arsenides, complex intermetallic compounds and natural alteration products (oxides and hydroxides, sulphates, hydroxysulphates and carbonates) [34]. No remains of speiss (corroborated by the low As content, and absence of significant amounts of Sb, Ni and Co) were found; presence of metallic sulphides, principally of Cu and Fe, was observed in some samples (Fig. 4.4a and 4.4b).

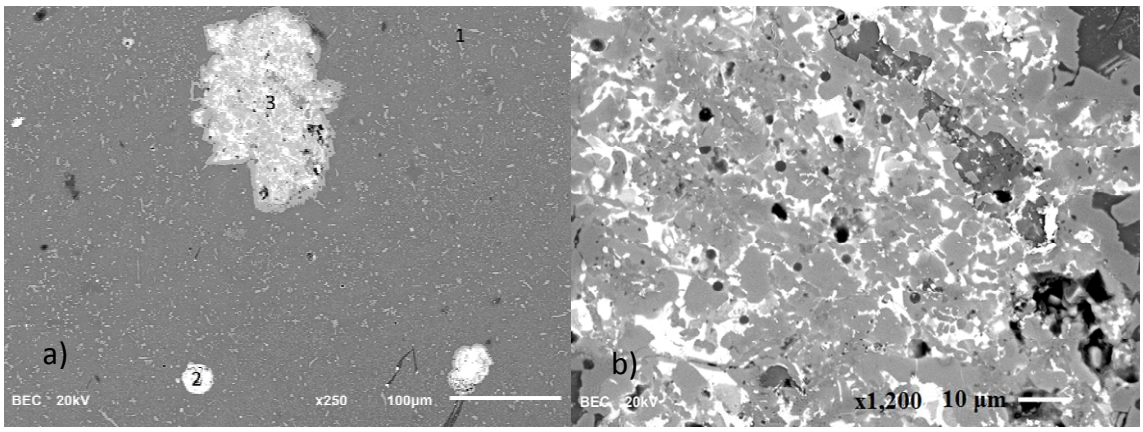

Figure 4. 4 Backscattered scanning electron micrograph of the slag. a) Reflects the general petrography where the major component is an intermetallic matrix composed of Si and Fe, and traces of Ca, Mn, and Zn. Three phases can be distinguished embedded in a siliceous glass matrix (dark grey): 1-Wüstite (elongated forms); 2- Pb-spherules (higher reflectivity) with a very small size generated by the rapid cooling and with low abundance by weight and; 3- complex intermetallic compounds principally composed of metallic sulphides, of Cu and Fe (zoom shown in b)).

The magnetic characterization of one representative sample is shown in Fig. 4.5, in which the main plot corresponds to both the virgin curve (blue) and the hysteresis loop (red). The incremental susceptibility plot was obtained by derivation of the virgin curve and is shown in the bottom right corner. Its maximum corresponds to 1.48×10^{-6} m^3/kg (1.38×10^{-6} m^3/kg was the average value for the three samples studied), which drops off with the increasing magnetic field applied to a final value of 7.64×10^{-8} m^3/kg (8.01×10^{-8} m^3/kg average of three samples), corresponding to the mass susceptibility of the para- and/or antiferro-magnetic phases (applied magnetic field above 1194 kA/m). This para- and/or ferro-magnetic contribution was subtracted from the measured hysteresis loop and is represented in the top left corner, showing that the ferro- and/or ferri-magnetic phases have a coercive field of 24.11 kA/m (17.77 kA/m average of three samples) and a specific saturation magnetization of 0.472 Am^2/kg (0.489 Am^2/kg average of three samples).

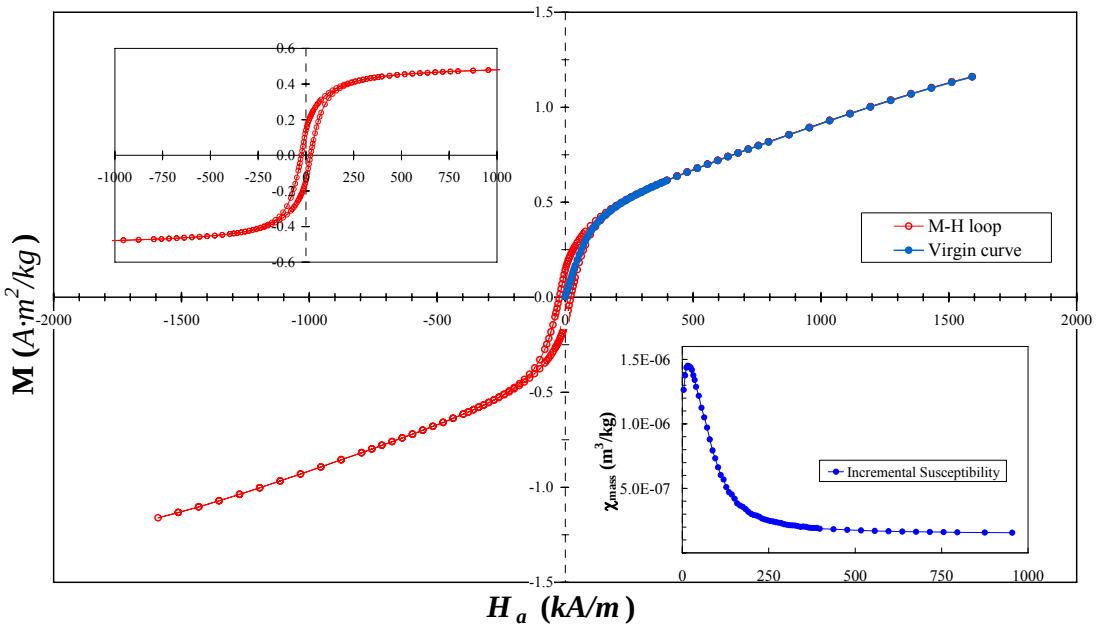

Figure 4. 5 Hysteresis curve (red) and virgin curve (blue) obtained for one of the samples analyzed in the magnetometer. Top left, corrected hysteresis loop. Bottom right, incremental susceptibility. M is the specific magnetization, H_a is the applied magnetic field, and χ_{mass} is the mass magnetic susceptibility.

These data are compatible with the presence of para- and antiferro-magnetic Fe oxides and, moreover, according to the value obtained for the specific saturation magnetization (very low for a ferro- and/or ferri-magnetic material), it may be considered that the percentage of the ferro- and/or ferri-magnetic phases is very low (< 2%). Therefore, we can conclude that Fe is mostly in antiferro- and/or para-magnetic ordering.

3.3 Magnetic separation experiments.

As mention above, all the experiments described in the following section were preceded by a pre-treatment step using LIMS equipment.

3.3.1 Dry high intensity magnetic separation.

The factorial test was completed by combining three rolling speeds (20, 60 and 100 rpm) for the three grain-size fractions, these ranging from a very fine gravel (<4mm) to coarse sand (>0.5 mm), namely 0.5-1, 1-2, and 2-4 mm fractions. The following two parameters were used to evaluate the results of the tests [26]: i) Ratio of concentration: namely the ratio of the weight of a specific grain size fraction that feeds the separator to the weight of the magnetically trapped product, expressed in percent; and ii) Recovery: namely the percentage of the total metal in the magnetically trapped product that is recovered from a feed composed of an specific grain size fraction.

Table 4. 3 Dry-HIMS results for major, minor and trace elements of environmental concern present in the soil. The magnetically separated fraction is referred to as the "mags". Results are an average of those obtained with three samples and with a standard error <5% (aqua-regia digestion and ICP-OES).

Grain-size fraction	Roll speed	Ratio of concentration	Recovery in the "mags" (%)						
(mm)	(rpm)	in the "mags" (%)	Cd	Cu	Mn	Pb	Zn	As	Fe
0.5 - 1	20	24.9	63.1	77.3	90.6	56.0	85.9	56.8	86.0
	60	19.1	57.7	81.0	89.6	34.4	83.8	50.1	84.5
	100	14.6	48.5	73.0	85.1	45.4	74.6	40.1	77.5
1- 2	20	25.2	56.9	81.6	84.9	37.9	84.1	55.2	84.9
	60	21.4	57.0	79.3	83.2	57.2	86.3	55.4	84.9
	100	17.7	49.2	47.6	83.0	30.3	80.0	45.5	80.7
2 - 4	20	23.3	25.2	68.0	74.6	67.8	40.4	47.3	80.1
	60	20.7	60.8	71.5	78.6	67.5	71.5	55.8	78.4
	100	15.9	42.9	20.0	62.2	44.8	63.5	31.9	70.3

Our results (Table 4.3) show that concentration occurred since the recovery in the magnetic fraction was greater than the ratio of concentration of the magnetic fraction, which varied from 15.9% up to 25.2%. On the whole, recoveries ranged from 30.3 % to 67.8% in the case of Pb, whereas the highest recoveries were obtained for Cu and Zn. No significant improvement in the recovery yields was obtained when roll speed was modified, with the single exception of the finer grain-size fraction. Conversely, the poorest performance was obtained for the largest grains; this can be explained by the fact that large grains produce irregular feeds, with diverse magnetic susceptibility, amount of middlings, and/ or particle size distribution, thus causing irregularities in the results.

These results were coherent with stereomicroscopic observations that showed that the separation process was partially dependant on the presence of slag grains but also by the presence of Fe-bearing minerals. Thus, separated fractions of non-magnetic nature were dominated by the presence of diamagnetic minerals such as quartz (χ_{mass} tabulated between $-0.5\cdot10^{-8}$ and $-0.6\cdot10^{-8}$ m^3kg^{-1} [35]) and carbonates (calcite, χ_{mass} tabulated between $-0.3\cdot10^{-8}$ to $-1.4\cdot10^{-8}$ m^3kg^{-1}), which gave the samples clear colors. In addition, there were extremely low concentrations of slag and Fe oxides, all together in small amounts of around 5%, even appearing to a lesser extent when smaller sizes were treated, thus implying greater efficiency of the separation at the finest grain-size (Table 4.3). In contrast, separated fractions of magnetic nature were dominated by a similar proportion of Fe oxides and slags, ranging from 15 up to 25%, depending on the grain-sizes treated. This composition resulted in colored concentrates, particularly in the smaller fractions. Other diamagnetic and/or paramagnetic minerals present in the soil, like galena ($\chi_{mass} = -0.44\cdot10^{-8}$ m^3kg^{-1}) and sphalerite (χ_{mass} tabulated between $-0.77\cdot10^{-8}$ m^3kg^{-1} and $19\cdot10^{-8}$ m^3kg^{-1}), did not show a clear tendency, as demonstrated by their occasional presence in the non-magnetically trapped fraction.

3.3.2 Wet high intensity magnetic separation

Another factorial test was completed by combining three voltages (expressed as % of the maximum output voltage: 30, 60 and 90 %) for three representative batches of grain sizes, these ranging from a medium sand (<500 µm) up to a very fine sand (>63 µm), namely: 63-125, 125-250, and 250-500 mm fractions (Table 4.4).

Table 4.4 Wet-HIMS results for major, minor and trace elements of environmental concern present in the soil. The magnetically separated fraction is referred to as the "mags". Results are an average of those obtained with three samples and with a standard error <5% (aqua-regia digestion and ICP-OES).

Grain-size fraction (microns)	Voltage (% of the maximum output voltage)	Ratio of concentration in the "mags" (%)	Recovery in the "mags" (%)						
			Cd	Cu	Mn	Pb	Zn	As	Fe
63-125	30	11.7	28.7	36.1	55.5	28.1	32.0	28.8	55,5
	60	12.7	28.9	37.0	66.4	29.3	35.2	30.2	61,3
	90	13.4	30,4	39.4	68.5	28.9	35.5	31.7	62,1
125-250	30	8.4	27.5	38.0	63.7	25.5	34.1	26.1	59,2
	60	9.6	32.5	44.1	73.9	28.6	36.8	29.0	65,0
	90	10.6	33.6	43.8	76.2	29.3	38.8	31.2	66,9
250-500	30	8,5	32.0	46.3	66.7	27.1	42.9	25.9	64,8
	60	9.9	36.4	52.0	80.2	29.9	48.8	31.3	70,7
	90	10.3	39.3	56.9	80.3	31.3	50.0	34.1	72,7

As occurred in the dry-HIMS tests, concentration of heavy metals also took place, but to a lesser extent, probably because of competition between magnetic and hydraulic forces. The ratio of concentration of the magnetically trapped fraction varied from 8.4% to 13.4%. For all the grain-size

fractions, both the ratio of concentration and recovery of heavy metals and metalloids in the magnetic fraction rose with increasing intensity, whilst only a slight correlation between the increase in the recovery and the increase in the intensity was observed. These values ranged between 25.5% and 80.35 % as a maximum; the best recoveries were obtained for Fe and Mn, which may indicate the presence of Fe-Mn oxides with magnetic properties.

The differences between the separation methods may be attributable to the mode in which the contaminants are present in the different grain sizes, thus these fractions are influenced, among other factors, by the adsorptive properties of the negatively charged and greater specific surface anionic sites of phylosilicates **(**clay: χ_{mass} 10-15 10^{-8} m^3kg^{-1}) and organic matter.

4. Conclusions

The study in the brownfield of La Cruz site showed soils with anomalous contents of Cd, Cu, Mn, Zn, As, and especially Pb in the polluted area surrounding the abandoned smelter. Geochemical and mineralogical data revealed that most of the pollutants are regularly distributed in all the grain-size fractions.

Lead-slag, a common waste generated by lead metallurgy, was directly mixed with soil and is therefore the most important source of anthropogenic accumulation of heavy metals at the study site, which is also affected by ore stockpiling and particulate emissions from both lead slag heaps and lead slag chimneys. The major constituents of the lead slag were Fe, Si, Ca, Al and Mg, as well as marked concentrations of Zn, Pb, Mn, As and Cu. From a mineralogical view, Pb spherules, Fe oxides (Wüstite), and complex intermetallic compounds were present in the slag.

The abundance of Fe in the slag, and in the other sources of soil contamination, pointed to the feasibility of applying magnetic separation. A magnetism study showed that the magnetic properties of the slag mainly correspond to a para- and /or antiferro- magnetic material; evidencing a weak ferro- and/or ferri- magnetic contribution, which was not caused mainly by the presence of ferro-magnetic Fe. Therefore, in this case, HIMS equipment is required for a magnetic soil washing treatment.

Dry-HIMS proved to be an effective tool for the decontamination of this soil in the coarser fractions (between 0.5 and 4 mm), while the recoveries by wet-HIMS were lower for finer fractions (between 63 and 500 microns). However, in this sort of soil (sandy, arid and combined with slag particles), both separation techniques demonstrated their effectiveness at processing a wide range of grain-size fractions. This implies that a significant and cost-effective reduction of the volume of contaminated soil could be obtained in a single real-scale step, something non-usual in a soil washing process.

Acknowledgements

We thank Dr. David Martínez Blanco from the "Servicio Cientifico-Técnico de Medidas Magnéticas" of the University of Oviedo for the assistance provided. Carlos Sierra obtained a grant of the "Severo Ochoa" programme (Ficyt, Asturias, Spain).

References

[1] J.R. Gallego, A. Ordóñez, J. Loredo, J., Investigation of trace element sources from an industrialized area (Avilés, northern Spain) using multivariate statistical methods, Environ. Int. 27 (2002) 589–596.

[2] J.S. Casas, J. Sordo, Lead Chemistry, Analytical Aspects, Environmental Impacts and Health Effects, Elsevier Sci Ltd, UK, 2006.

[3] L.R.P. de Andrade Lima, L.A. Bernardez, Characterization of the lead smelter slag in Santo Amaro, Bahia, Brazil, J. Hazard. Mater. 189 (2001) 692–699.

[4] A. Violante, V. Cozzolino, L. Perelomov, A.G. Caporale1e, M. Pigna, Mobility and bioavailability of heavy metals and metalloids in soil environments, J. Soil. Sci. Plant Nutr. 10 (2010) 268 – 292.

[5] H. Kucha, A. Martens, R. Ottenburgs, W. De Vos, W. Viaene, Primary minerals of Zn–Pb mining and metallurgical dumps and their environmental behavior at Plombiéres, Belgium, Envir. Geol. 27 (1996) 1-15.

[6] M. Manz, L.J. Castro, The environmental hazard caused by smelter slags from the Sta. Maria de la Paz mining district in Mexico, Environ. Pollut. 98 (1997) 7–13.

[7] H.D. Sharma, K.R. Reddy, Geoenvironmental Engineering: Site Remediation,Waste Containment, and Emerging Waste Management Technologies, John Wiley & Sons, 2004.

[8] C. Sierra, J.R. Gallego, E. Afif, J.M. Menéndez-Aguado, F. González-Coto, Analysis of soil washing effectiveness to remediate a brownfield polluted with pyrite ashes, J. Hazard. Mater. 180 (2010) 602–608.

[9] J. Svoboda, Magnetic Techniques for the Treatment of Materials, Kluwer Academic Publishers, 2004.

[10] A.R. Schake, L.R. Avens, D. Hill, D. Padilla, F.C. Prenger, D.A. Romero, T.L. Tolt, L.A. Worl, Magnetic Separation for Environmental Remediation, in: Proceedings of the ACS Symposium on F-Elements Separation. The 207th American Chemical Society National Meeting, San Diego, CA, (USA), 1994.

[11] G. Dermont, M. Bergeron, G. Mercier, M. Richer-Laflèche, Soil washing for metal removal: a review of physical/chemical technologies and field applications, J. Hazard. Mater. 152 (2008) 1–31.

[12] R.A. Rikers, P. Rem, W.L. Dalmijn, Improved method for prediction of heavy metal recoveries from soil using high intensity magnetic separation (HIMS), Int. J. Miner. Process, 54 (1998) 165–182.

[13] L.R. Avens, L.A. Worl, K.J. de Aguero, D.D. Padilla, F.C. Prenger, W.F. Stewart, D.D. Hill, T.L. Tolt, 1993. Magnetic separation for soil decontamination. Los Álamos National Lab. NM (USA), 1993.

[14] M.I. Kuhlman, T.M. Greenfield, Simplified soil washing processes for a variety of soils, J. Hazard. Mater. 66 (1999) 35-41.

[15] H. Kronmuller, S. S. P. Parkin, Handbook of magnetism and advanced magnetics materials, John Wiley & Sons, 2007.

[16] C. Sierra, J.M. Menéndez-Aguado, E. Afif, M. Carrero, J.R. Gallego, Feasibility study on the use of soil washing to remediate the As–Hg contamination at an ancient mining and metallurgy area, J. Hazard. Mater. 196 (2011) 93– 100.

[17] J. Lillo, Geology and Geochemistry of Linares-La Carolina Pb-Ore field (Southeastern border of the Hesperian Massif). Ph.D. Thesis, Univ. Leeds, 1992.

[18] J. Lillo, Hydrothermal alteration in the Linares-La Carolina Ba–Pb–Zn–Cu–(Ag) vein district, Spain: mineralogical data from El Cobre vein, Applied Earth Science, 111 (2003) 114-118.

[19] J. Martínez, Caracterización geoquímica y ambiental de los suelos en el sector minero de Linares. Ph.D. Thesis, Univ. Politécnica de Madrid, 2002.

[20] J. Martínez, J. Llamas, E. De Miguel, J. Rey, M.C. Hidalgo, Application of the Visman method to the design of a soil sampling camping in the mining district of Linares (Spain), J. Geochem. Explor. 92 (2007) 73–82.

[21] J. Martínez, J. Llamas, E. De Miguel, J. Rey, M.C. Hidalgo, Determination of geochemical background in a metal mining site: example of the mining district of Linares (south Spain), J. Geochem. Explor. 94 (2008) 19–29.

[22] J. Martínez, J. Rey, M.C. Hidalgo, J. Benavente, Characterizing Abandoned Mining Dams by Geophysical (ERI) and Geochemical Methods: The Linares-La Carolina District (Southern Spain), Water Air Soil Pollut. 223 (2012) 1-14.

[23] J. Sastre, A. Sahuquillo, M. Vidal, G. Rauret Determination of Cd, Cu, Pb and Zn in environmental samples: microwave-assisted total digestion versus aqua regia and nitric acid extraction, Anal. Chim. Acta 462 (2002) 59–72.

[24] M. Bettinelli, G.M. Beone, S. Spezia, C. Baffi, Determination of heavy metals in soils and sediments by microwave-assisted digestion and inductively coupled plasma optical emission spectrometry analysis, Anal. Chim. Acta 424 (2000) 289-296.

[25] G.S. Camm, H. J. Glass, D. W. Bryce, A. R. Butcher, Characterisation of a mining-related arsenic-contaminated site, Cornwall, UK, J. Geochem. Explor. 82 (2004) 1-15.

[26] B.A. Wills, T.J. Napier-Munn, Mineral Processing Technology: An Introduction to the Practical Aspects of Ore Treatment and Mineral Recovery, 7th ed., Butterworth-Heinemann, Burlington, MA, 2006.

[27] Magnetic Separator Assembly for Use in Material Separator Equipment. Patent number 5,101,980. United States Patent. 1992.

[28] G. Mercier, J. Duchesne, D. Blackburn, Prediction of the efficiency of physical methods to remove metals from contaminated soils. J. Environ. Eng. 127 (2001) 348–358.

[29] Carpco Wet High-Intensity Magnetic Separator model 3X4L. Available at: http://www.outotec.com/18470.epibrw (accessed April 2012).

[30] C.W. Williford, R.M. Bricka, Physical separation of metal-contaminated soils, in: I.K. Iskandar (Ed.), Environmental Restoration of Metals- Contaminated Soils, 1st ed., CRC Press, Boca Raton, FL, 2000.

[31] V. Ettler, O. Legendre, F. Bodenan, J.C. Touray, Primary phases and natural weathering of old lead–zinc pyrometallurgical slag from Pribram, Czech Republic, Can. Mineral, 39 (2001) 873–888.

[32] N. Seignez, A. Gauthier, D. Bulteel, M. Buatier, D. Damidot, J.L. Potdevin, Leaching of lead metallurgical slag and pollutant mobility far from equilibrium conditions, Appl. Geochem, 23 (2008) 3699–3711.

[33] M. Scheinert, H. Kupsch, B. Bletz, Geochemical investigations of slags from the historical smelting in Freiberg, Erzgebirge (Germany), Chem. Erde. 69 (2009) 81–90.

[34] V. Ettler, Z. Johan, Natural alteration products of sulphide mattes from primary lead smelting. C. R. Geoscience 335 (2003) 1013–1020.

[35] C.P. Hunt, B.M. Moskowitz, S.K. Banerjee, in: T.J. Ahrens (Ed.), Rock Physics and Phase Relations 189-204, AGU, Washington DC, 1995.

CHAPTER V: Optimisation of magnetic separation: A case study for soil washing

C. Sierra[(a)], D. Martínez-Blanco[(b)], Jesús A. Blanco[(c)], J.R. Gallego[*(a)]

[a] Environmental Biotechnology and Geochemistry Group. University of Oviedo. C/Gonzalo Gut. S/N, 33600-Mieres (Asturias), Spain. Phone:+34 985458064 - 651043415. Fax +34 985458182.[b] Servicio Científico-Técnico de Medidas Magnéticas. University of Oviedo. C/Gonzalo Gut. s/n, 33600 Mieres (Asturias), Spain.

[c] Departamento de Física, University of Oviedo, c/Calvo Sotelo s/n, 33007 Oviedo, Spain

Abstract

Soil polluted with heavy metals from an ancient Pb mining and metallurgy site was treated by means of wet high-intensity magnetic separation to remove some of the pollutants therein. The separated fractions were subjected to magnetic characterisation, which determined the high-field specific (mass) magnetic susceptibility (κ) and the specific (mass) saturation magnetisation (σ_S) through isothermal remanent magnetisation (IRM) curves. An additional magnetic characterisation by means of thermal demagnetisation of the saturation isothermal remanent magnetisation (SIRM) and thermal dependence of saturation magnetisation was also performed in order to identify and quantify, respectively, the magnetic phases involved in the separation. From the specific values of κ and σ_S, an expression to assess the performance of the magnetic separation operation was formulated and verified. The procedure proved effective for the treatment of the contaminated soil. The magnetic study provided valuable information for the exhaustive explanation of the operation, and the deduced mathematical expression was found to be appropriate to estimate the performance of the separation operation.

Key words: Magnetic separation; Soil washing; Soil contamination; Mineral processing.

1.Introduction

The magnitude that specifies the degree of magnetisation of a substance when a magnetic field is applied is called magnetic susceptibility [1]. All substances are magnetic to some extent, and from an engineering point of view, minerals are usually classified on the basis of this property. Thus, substances with a highly positive magnetic susceptibility are usually termed “magnetic” while those with a lower positive magnetic susceptibility are referred to as “weakly magnetic”. The former include ferri- and ferro-magnetic materials, which are characterised by their capacity to multiply the magnetic flux density (B) inside them, while the latter usually refer to the para- and antiferro-magnetic materials, which barely increase the magnetic flux density in their surroundings. In contrast, substances usually designated as “non-magnetic”, which weaken the magnetic field when present, that is to say they show a negative magnetic susceptibility, are termed diamagnetic [2]. All materials show some degree of diamagnetism, but in general, it is a weak effect that can be either ignored or is a small correction to a large effect.

From a practical point of view, this implies that materials with positive magnetic susceptibility are attracted by a magnetic field, whilst those with a negative value are weakly repelled from the magnet. Thus, ferro- and ferri-magnetic materials can be easily separated from others by means of low-intensity magnetic separators. In contrast, fine para- and antiferro-magnetic particles require high-intensity magnetic separation in order to be removed from a mixture containing diamagnetic particles [3].

In this regard, magnetic separation is a mechanical procedure that applies a magnetic force to segregate substances from a mixture on the basis of their magnetic susceptibility [4]. This technique has been widely used in mineral processing to concentrate Fe ores, for instance magnetite (Fe_3O_4),

pyrrhotite (FeS), hematite (Fe_2O_3), siderite ($FeCO_3$), and other Fe-containing minerals, such as ilmenite ($FeTiO_3$) and chromite ($FeCr_2O_4$) [5]. Moreover, it has been used in soil washing to remove pollutants from contaminated soils, exploiting the differences in the magnetic susceptibility of the constituents of a soil to concentrate them into the smallest fraction [6-9].

The performance of a mineral dressing operation has generally been defined based on the quality, quantity, features, and the component's name, mass, volume, population, or number of moles of the separated fractions [3]. Thus expressions to estimate the performance of a concentration process have been proposed based on parameters (recovery, ratio of concentration, separation efficiency) obtained from chemical, grain size (imperfection, cut of sizes, partition coefficient) and density (settling ratios) characterisation [3, 4]. However, few studies have addressed magnetic separation efficiency indexes. In this work, we propose an index that allows the classification of the tests from a magnetic separation process on the basis of the magnetic properties of the separated materials.

In order to define a new efficiency index, it is important to set the appropriate magnetic parameters for the study. Ferri- and ferro-magnetic materials are usually characterised by means of their hysteresis loops. Some magnitudes or intrinsic parameters of the hysteresis loop, namely remanence (residual magnetisation after the maximum applied magnetic field is removed) and coercivity (the intensity of magnetic field require to reduce the magnetisation to zero after the material has reached saturation), are sensitive to microstructure and also depend on the shape and magnetic history of the sample [10]. Others, such as saturation magnetisation (when an increase in the magnetisation of the material is not possible unless there is an increase in the external magnetising field applied), and Curie temperature (the temperature above which a ferro- or ferri-magnetic body loses its ordering, behaving as purely paramagnetic), are intrinsic magnitudes and are thus characteristic of each material [11]. In this regard, our work formulates an expression to characterise the concentration operation with some of these intrinsic parameters determined within the high magnetic field region of the hysteresis loop, thus attempting to avoid any possible extrinsic influence.

Here we applied this knowledge to a highly Pb-polluted soil (Linares, Spain) after an upgrading process via wet-HIMS (High-Intensity Magnetic Separation). Thus, the main aims of the study were as follow:

- To magnetically characterise the separation process by means of the high-field magnetic susceptibility, κ, and the saturation magnetisation, σ_S, parameters.

- To identify the magnetic phases involved in the separation process by means of measuring magnetic phase transition temperatures.
- To formulate an expression to evaluate the performance of the separation on the basis of the results from the magnetic study.

2. Materials and methods

2.1 Site description

The district of Linares (NE Andalucía, Spain) is an old mining and metallurgical area dedicated to the extraction of Pb from galena (PbS), which is accompanied by other minerals such as sphalerite (ZnS), chalcopyrite ($CuFeS_2$) and barite ($BaSO_4$) [12, 13]. The activity in this area started in Roman times and expanded greatly in the nineteenth century and early twentieth century, until the last mines and industrial facilities finally closed at the beginning of the 90s. Samples were taken in an olive grove field in the vicinity of the San Genaro mining shaft (38º 8´ 31.23´´ N, 3º 37´ 29.50´´ W). The soil is moderately developed, and the geological substrate is composed of shales and sandstones. The emissions of dust released during mining and waste dumping caused soil contamination.

2.2 Soil sampling

Samples were collected from the tilled depth (0-35 cm) by means of a stainless steel hand-auger and a shovel in random locations in the polluted area. These samples were then mixed in order to obtain a single representative sample of 20 Kg, which was screened *in situ* in order to discard materials larger than 2 cm. Finally, the samples obtained were homogenised and stored in inert plastic bags.

2.3 Grain-size fractioning

Representative lots of the initial sample were slurried in water and then sieved (cycles of 100 g) using a normalised 250-µm sieve positioned in a sieve shaker (Restch) for 5 min with a water flow of 0.3 l/min (ASTM D-422-63, Standard Test Method for Particle-Size Analysis of Soils). The fraction obtained was subsequently dried at 35 ºC.

2.4 Wet-HIMS

The fractions were treated in a batch-type wet-HIMS unit (OUTOTEC Laboratory, WHIMS 3X4L [14]). The apparatus was fed a pulp composed 50 g of soil in 200 g of water. The feed was passed through the separating chamber, which comprised soft Fe spheres of 12.7 mm in diameter. Particles of the initial feed were separated on the basis of their magnetic properties; thus, some of them remained in the water stream passing through the chamber ("non-mags"). The separator was then flushed with water and the product was collected in a tray. Other particles were attracted to the Fe balls, overcoming the hydrodynamic drag force ("mags"), and were washed out by setting the voltage to zero. The separator was flushed again, and the material was recovered in another tray.

The magnetic field intensity of the equipment is controlled by varying the coil input amperage (0-6 amps). We tested a range of output voltages: 5, 10, 20, 30, 60 and 90 % in a wet-HIMS to optimise of the separation process. According to the manufacturer's specifications, the magnetic flux density quickly decreases in the air gap between the balls, its value on the surface of the sphere media reaching the maximum input voltage of 2.16 T, a value close to the saturation value for Fe [15].

2.5. Magnetic properties

Using an agate mortar, we ground 0.5 g of each sample. The powder was then quartered and then three selected specimens were subjected the corresponding magnetic characterisation using a Vibrating Sample Magnetometer (VSM), model EV9 VSM from Microsense LLC. Specimens of approximately 50 mg of powder mass were encapsulated in a cylindrical sample holder, which was then attached to the quartz rod of the VSM using scotch tape. After demagnetisation of each specimen by a dumped oscillate field from 1580 kA/m to 0, the mass isothermal remanent magnetisation (IRM), σ, was determined after removing the applied magnetic field, H, at room temperature. The IRM curves were measured from 0 to 1750 kA/m, where the room temperature of the tests was approximately 290 K, and were then analysed using the software EasyVSM ®.

In addition, the evolution of the mass magnetisation with temperature for a representative specimen was also determined. In this case, a quartz sample holder was attached to a vibrating rod inside a cylindrical oven open on one side, where the sample was at thermal equilibrium with N_2 or Ar gas at controlled temperatures below or above room temperature, respectively. Continuous data acquisition of the mass magnetisation was performed between 100 and 1000 K for a heating rate of 10 K/min. The samples were first heated to 1000 K for 15 min and then cooled to 100 K at an applied magnetic field of 795 kA/m. Subsequently, after removing the magnetic field at 77 K, the samples were monitored at zero-field warming from 100 to 1000 K. The temperature dependence of the saturation magnetisation was obtained during cooling, whereas the second measurement is known as thermal demagnetisation of the saturation isothermal remanent magnetisation (SIRM) [16]. The

number of ferri- and/or ferro-magnetic phases was estimated from the values determined for the saturation magnetisation, while the SIRM curve allowed us to distinguish the type of ferri- and/or ferro-magnetic minerals present in the sample through their Curie temperatures [17], T_C, defined by the minimum of the numerical derivate of the data.

2.6 Estimation of the relative magnetic force

The intensity of the magnetic force, F_m, on a particle with mass m and specific (mass) magnetic susceptibility, κ , moving in water medium can be expressed by [4]:

$$F_m = \frac{(\kappa - \kappa_w)m}{\mu_0} \left| B\vec{\nabla}B \right| \tag{1}$$

where $\vec{B}$ is the magnetic flux density, $\mu_0 = 4\pi \times 10^{-7}\ \mathrm{T{\cdot}m/A}$ is the magnetic permeability of vacuum (relative permeability of air is assumed to be 1), and $\kappa_w = -9.05 \times 10^{-9}\ \mathrm{m^3/kg}$ is the specific (mass) magnetic susceptibility of water [18]. This expression establishes that the magnitude of a magnetic force is proportional to the product of magnetic flux density and its gradient. Figure 5.1 shows the relative "force", $\left|B\vec{\nabla}B\right| \Big/ \left|B_{\max}\vec{\nabla}B_{\max}\right|$, for the magnetic separation unit as function of the output voltage, estimated using a portable GM8 gaussmeter coupled to a Hall sensor (Hirst Magnetic Instruments LTD). Accordingly, linear correlation with the input voltage is observed only for inputs over 25 % of the maximum output voltage.

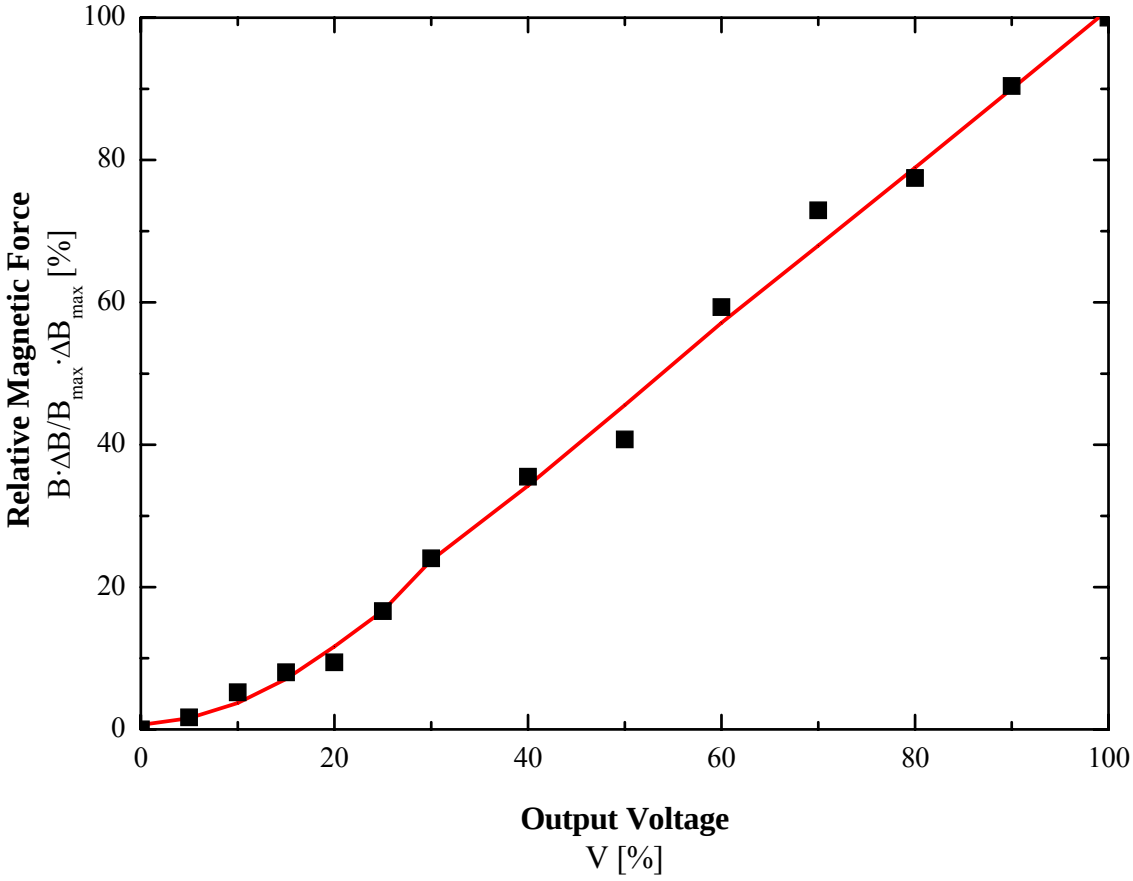

Figure 5. 1 Variation of the relative magnetic force with the output voltage in the magnetic separator.

2.7 Generation of the parameter to evaluate the efficiency of the concentration operation

The specific (mass) susceptibility for non-oriented dia-, para- or antiferro-magnetic powder materials is a scalar, κ_P, such that

$$\sigma = \kappa_p H \tag{2}$$

The relation between specific (mass) magnetisation and magnetic field for a ferri- or ferro-magnetic equivalent substance is more complex, but in the high-field region it can be described by the following law of approach-to-saturation

$$\sigma = \sigma_S^F \left(1 - \frac{a}{H} - \frac{b}{H^2} \right) + \kappa_F H \tag{3}$$

where *a* and *b* are constants related to defects and anisotropy, κ_F is the high-field mass susceptibility, which is small at a temperature well below T_C [19], and σ_S^F is the mass saturation magnetisation. Combining (2) and (3), it can be concluded that, at high magnetic fields, specific magnetisation can be described by

$$\sigma = \sigma_S \left(1 - \frac{a}{H} - \frac{b}{H^2} \right) + \kappa H \tag{4}$$

$\sigma_S = \sum_F f_F \sigma_S^F$ and $\kappa = \sum_F f_F \kappa_F + \sum_P f_P \kappa_P = \kappa_F + \kappa_P$ being the magnetisation saturation and the susceptibility at high fields of the sample, respectively, and f_F and f_P the mass fraction of each ferro- and para-magnetic phase present in the sample.

In order to verify the adequacy of this equation to describe the behaviour of the samples, we tested the feed sample (M_0). Figure 5.2 shows a significant correlation between equation (4) and the data measured at magnetic fields over 200 kA/m (R^2=0.99997).

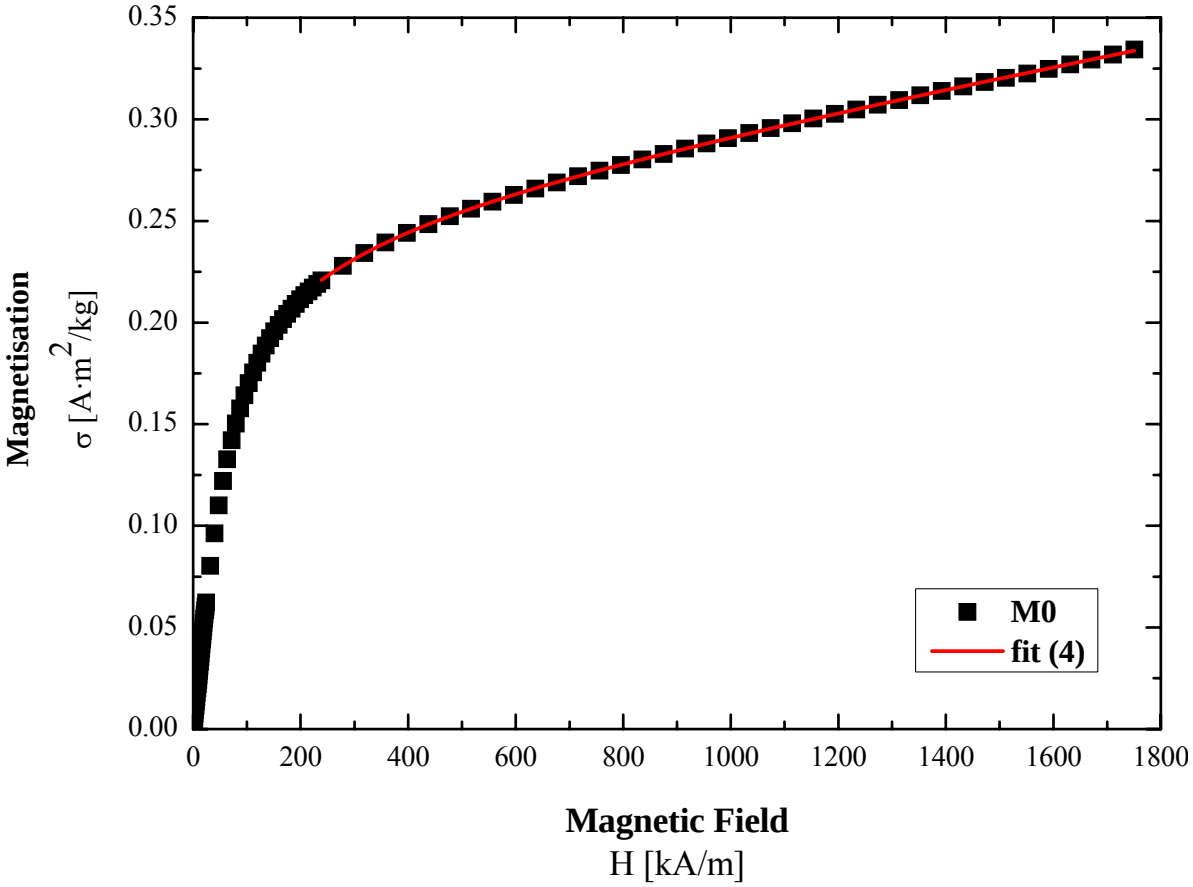

Figure 5. 2 Mean isothermal remanent magnetisation (IRM) curve for the feed sample M_0.

If the mass of ferri- and ferro-magnetic phases in the "mags" and "non-mags" fractions is denoted by *x* and *y* respectively, the following expressions must be satisfied

$$x\sigma_S^M + y\sigma_S^{NM} = z\sigma_S^0 \tag{5a}$$

$$x\kappa_F^M + \left(m^M - x\right)\kappa_P^M + y\kappa_F^{NM} + \left(m^{NM} - y\right)\kappa_P^{NM} = z\kappa_F^0 + \left(m^0 - z\right)\kappa_P^0 \tag{5b}$$

where superindexes are used to identify the parameters corresponding to "mags", M, "non-mags", NM, and initial feed soil, 0. Therefore, m^M and m^{NM} indicate the masses of "mags" and "non-mags" fractions, respectively, and *z* is the mass of ferri- and/or ferro-magnetic materials in the soil samples with mass m^0.

Moreover, conservation of mass along the magnetic separation process enforces that:

$$x + y = z \tag{6}$$

From (5a) and (6), the relative percentages of ferri- and/or ferro- magnetic material in the "mags" and "non-mags" fractions, with respect to the initial mass in the feed sample (usually defined as recoveries [3]), can be determined by:

$$\frac{x}{z} = \frac{\sigma_S^0 - \sigma_S^{NM}}{\sigma_S^M - \sigma_S^{NM}} \tag{7a}$$

$$\frac{y}{z} = \frac{\sigma_S^M - \sigma_S^0}{\sigma_S^M - \sigma_S^{NM}} \tag{7b}$$

Thus, the amount z of ferri- and/or ferro- magnetic material present in the initial feed soil can also be obtained by combining the expressions (5b), (7a) y (7b), thus leading to

$$z = \frac{m^M\left(\kappa^M - \kappa_F^M\right) + m^{NM}\left(\kappa^{NM} - \kappa_F^{NM}\right) - m^0\left(\kappa^0 - \kappa_F^0\right)}{\frac{\sigma_S^0 - \sigma_S^{NM}}{\sigma_S^M - \sigma_S^{NM}}\left(\kappa^M - 2\kappa_F^M\right) + \frac{\sigma_S^M - \sigma_S^0}{\sigma_S^M - \sigma_S^{NM}}\left(\kappa^{NM} - 2\kappa_F^{NM}\right) - \left(\kappa^0 - 2\kappa_F^0\right)} \tag{8}$$

Two cases simplify the latter equation in the same way. First, it is postulated that the mass fraction of ferri- and/ or ferro-magnetic phases is similar in the "mags" and "non-mags" fractions and in the soil sample ($\kappa_F^{NM} = \kappa_F^M = \kappa_F^0$); second, when the IRM curves are measured at a lower temperature than the Curie temperatures of all ferri- and/or ferro-magnetic phases, it is known that their high-field susceptibility is negligible, ($\kappa_F^{M,NM,0} \approx 0 \Rightarrow \kappa^{M,NM,0} = \kappa_P^{M,NM,0}$). In both cases, expression (8) is reduced to the following equation:

$$z = \frac{m^M\kappa^M + m^{NM}\kappa^{NM} - m^0\kappa^0}{\frac{\sigma_S^0 - \sigma_S^{NM}}{\sigma_S^M - \sigma_S^{NM}}\kappa^M + \frac{\sigma_S^M - \sigma_S^0}{\sigma_S^M - \sigma_S^{NM}}\kappa^{NM} - \kappa^0} \tag{9}$$

Consequently, by means of equations (7-9), the amount of ferri- and/or ferro- magnetic phases in the fractions and feed can be directly established on the basis of their magnetic contribution from para- and/or antiferro-magnetic substances. To the best of our knowledge [20], to date, no similar methods have been reported to carry out the separation of magnetic contributions in this straightforward manner. On the contrary, conventional analyses usually involve combined measurements at low and high magnetic fields with thermal dependence of the magnetic susceptibility to distinguish between both contributions [21].

If the expression for the determination of separation efficiency proposed by Schulz [22] is particularised for the mass of ferri- and/ or ferro- magnetic phases in the "mags", "non-mags" fractions and soil samples previously determined, then:

$$\zeta\,[\%] = \left(\frac{m^0 \frac{x}{z} - m^M}{m^0 - z} \right) \cdot 100 \tag{10}$$

This equation contemplates the following extreme conditions:

- First, when the "mags" is composed only of ferri- and/ or ferro- magnetic material, and there is no presence of these kinds of phases in the "non-mags" (i.e., $x = m^M$ and $x = z$), the parameter yields 100%, thus indicating the perfect separation.
- Second, when the percentage of ferri- and/ or ferro- magnetic phases in the "mags" is the same as in the feed soil $\left(\frac{x}{m^M} = \frac{z}{m^0} \right)$, the expression yields 0%, indicating the absence of separation.

2.8 Chemical analysis

All samples subjected to chemical analyses were ground in an agate mortar. The milled samples were shipped to the accredited (ISO 9002) ACME laboratories (Vancouver, Canada). There, 1-g representative sub-samples of the ground product were leached by means of an 'Aqua regia' digestion ($HCl + HNO_3$), and the concentrations of 19 major, minor and trace elements (Ca, Mg, K, Na, Al, Fe, S, Cu, Pb, Zn, Cd, Ni, Mn, As, Sr, Sb, La, Cr and Hg) were analysed for the digested material by inductively coupled plasma optical emission spectrometry (ICP-OES).

3. Results and Discussion

3.1 Magnetic characterisation

3.1.1 Determination of the magnetic parameters

Figure 3 shows the mean IRM curves corresponding to the "mags" and "non-mags". In general, the smaller the magnetic field applied by the separator, the higher the magnetisation signal. Notwithstanding, this tendency was broken by the curves measured at 90 % of the maximum output voltage. This exception will be discussed later (see section 3.1.3). Particularising for the "mags", all samples tended to have a higher magnetisation signal in the high-field region than the initial feed sample. Conversely, the IRM curves for the "non-mags" were lower than the initial feed.

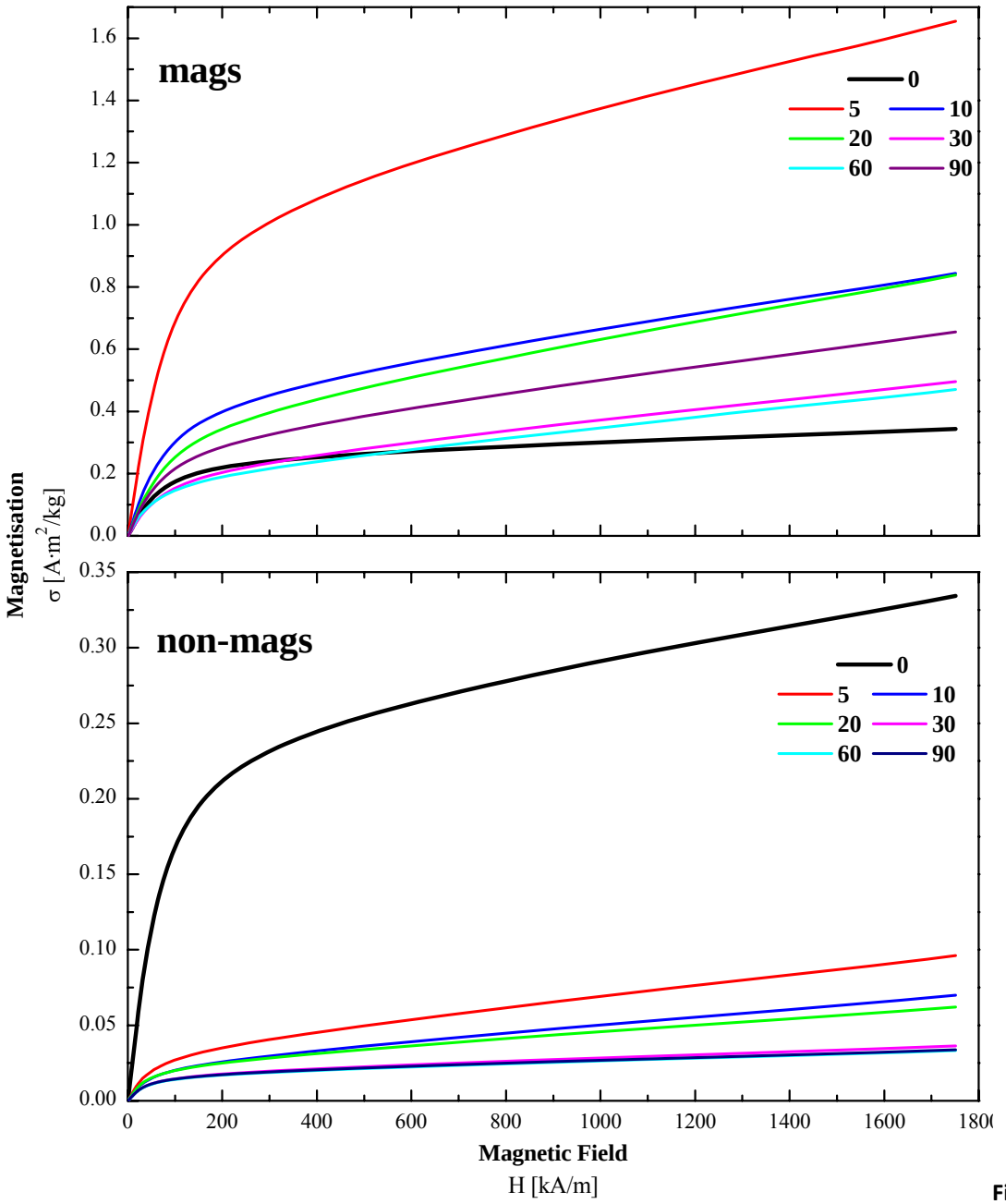

Figure 5. 3 Mean isothermal remanent magnetisation (IRM) curves for the magnetically (mags) and non-magnetically separated fractions (non-mags). Results correspond to the average of three determinations. The numbers indicate the percentage of the maximum output voltage applied to the separator.

In this way, data from the high-magnetic field region were fitted using equation (4) for each measurement. The corresponding average magnetic parameters and their fitting equations are shown in Table 5.1. Both saturation magnetisation, σ_S, and high-field magnetic susceptibility, κ, followed the same behaviour as their mass magnetisation curves for the studied voltages.

Table 5. 1 Magnetic parameters obtained from the fitted high-field region (up 200 kA/m) of mean isothermal remanent magnetisation (IRM) curves following equation 4 for the magnetically (mags) and non-magnetically separated fractions (non-mags). Results correspond to the average of three determinations.

Voltage	*Mass*	*Rel. Magn. Force*	*Saturation Magnetisation*	*High-field susceptibility*
0	50	-	0.25	5.0
		Mags		
5	1.5	0.02	1.07	31.7
10	4.2	0.05	0.64	24.8
20	4.8	0.09	0.42	26.6
30	10.8	0.24	0.32	17.4
60	11.3	0.59	0.29	18.0
90	10.9	0.90	0.34	19.7
		Non-Mags		
5	45.3	0.02	0.038	3.4
10	44.4	0.05	0.027	2.5
20	44.4	0.09	0.027	2.0
30	37.9	0.24	0.020	1.0
60	37.6	0.59	0.019	0.83
90	38.6	0.90	0.019	0.84

The relative weight percentages of ferri- and/ or ferro- magnetic phases in the "mags" and "non-mags" were derived from expression (7) through the values of the data arranged in Table 1. Figure 4 summarises the results that prove that upgrading takes place gradually. The results are presented in terms of concentration of ferri- and/or ferro-magnetic phases in the "mags" (dark grey) and "non-mags" (light grey) relative to $\frac{x}{z}$ $\frac{y}{z}$ the initial feed sample ("recovery"), and respectively, for increasing output voltages. According to this, a linear tendency between these recoveries in the "mags" and their diminution in the "non-mags" was observed as the input voltage increased. In contrast, when high magnetic fields were applied (above 60% of the maximum input voltage), the relative percentage of ferri- and/ or ferro- magnetic phases in the "mags" decreased. Again, this exception will be discussed later in section 3.1.3.

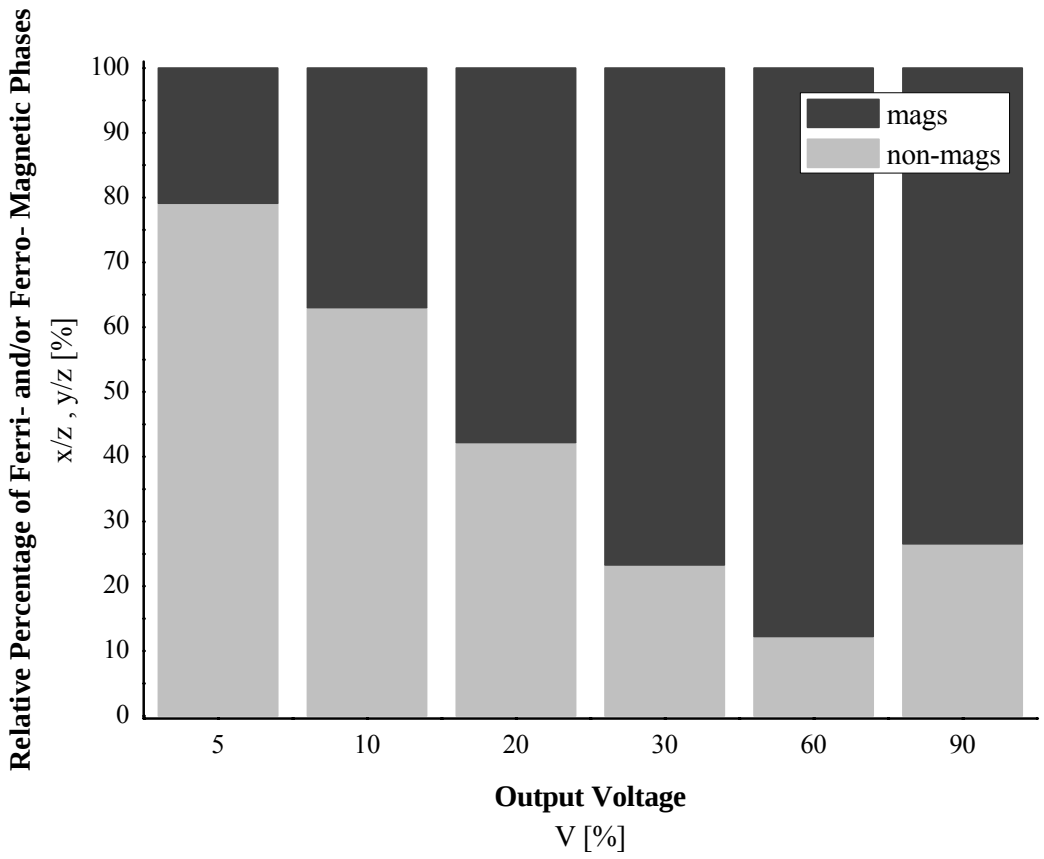

Figure 5. 4 Percentages of ferri- and/or ferro-magnetic phases in the magnetically (mags) (dark grey) and non-magnetically (non-mags) (light grey) separated fractions relative to feed sample for a range of output voltages. Results correspond to the average of three determinations.

3.1.2 Determination of the magnetic phases: quantification

Figure 5 (a) shows the evolution of mass magnetisation with temperature for one of the samples ("mags"10%). The blue curve corresponds to the thermal dependence of saturation magnetisation while the red one represents the thermal demagnetisation of the SIRM. The numerical derivate of the SIRM signal exhibited at least six characteristic minima at the following temperatures: 115, 290, 400, 590, 795 and 840 K (Fig. 5(b)).

At the first temperature, a significant drop in the SIRM was caused by the structural phase transition of magnetite from monoclinic to cubic crystal structures [23]. The following temperature corresponds to a setup exchange at room temperature, the result of the distinct thermal properties of each temperature driven gas, which produces a step-like demagnetisation that cannot be avoided in the continuous acquisition of data. At around 400 K, SIRM showed a local maximum, which could be attributed to the appearance of a weak ferrimagnetism in the anti-ferromagnetic ordering of the goethite. This effect may be caused by unbalanced spins (located in crystal imperfections and/or impurities), which disappeared above its Néel temperature, $T_N \approx 395\,\mathrm{K}$ [24]. A similar effect was observed at $T_C \approx 595\,\mathrm{K}$, which could be attributed to the onset of the ferromagnetism of the sulphides, mainly pyrrohotite [25]. Finally, above 840 K, the SIRM signal dropped to zero as a result of the magnetic transition of magnetite, whose Curie temperature is 851 K. However, partial substitution of Fe with divalent and/or trivalent cations in its composition can modify this point and cause the different minima observed around 795 K, which have been attributed to the Curie temperatures of several ferrites [26].

Furthermore, the behaviour of saturation magnetisation clearly proves that the major contribution of the magnetic signal comes from these magnetite-type minerals, whose total mass accounted for about 7.2 % of the studied sample, according to the value of saturation magnetisation measured at room temperature [27]. From this estimated value and through the information shown in Figure 5.4 and Table 5.1, the average concentration of ferrimagnetic phases in the soil was around 1.6 %.

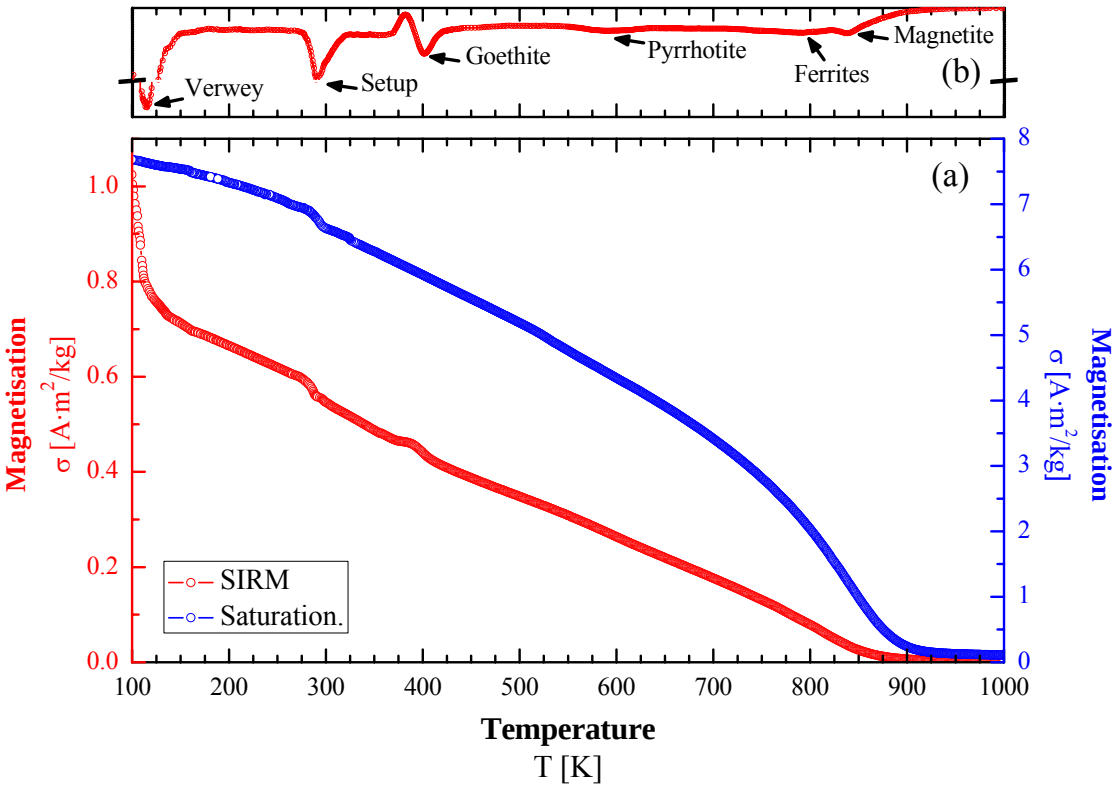

Figure 5.5 Temperature dependence of saturation isothermal remnant magnetisation (SIRM) and mass magnetisation at 795 kA/m (saturation) for the magnetically separated fraction (mags) at 10% of the maximum output voltage. SIRM signal (a) and numerical derivate (b), where arrows indicate the characteristic temperatures of the magnetic phases.

3.1.3 Determination of the efficiency of the magnetic separation

The corresponding efficiency of the magnetic separation, ζ, for each output voltage was calculated using expression (10), where the recovery for the ferri- and/or ferro-magnetic phases in the "mags", $\frac{x}{z}$, was already determined in section 3.1.1 (see Fig. 4), and the mean mass of ferri- and/or ferro-magnetic phases included in the original soil, $z \approx 0.8\,\mathrm{g}$, was also estimated in the former section. The efficiency of the magnetic separation was higher at 60 % of the maximum output voltage (Fig. 5.6). Moreover, a linear trend of the magnetic separation efficiency was detected when the

voltage rose from zero to this output value; however, an increasing voltage beyond this point led to a perceptible decrease in efficiency (80 % of its maximum value).

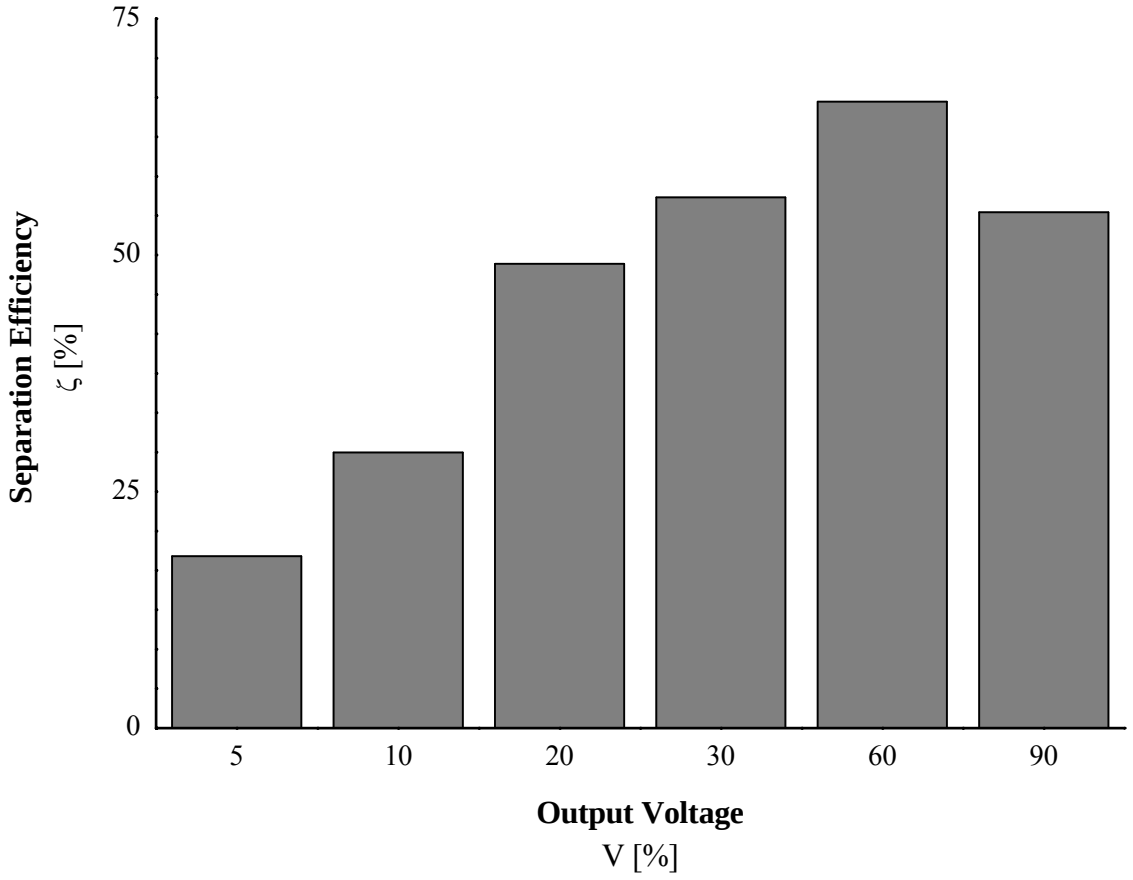

Figure 5. 6 Magnetic separation efficiency (ζ) as a function of output voltage.

In order to understand the behaviour shown in Figure 6 (as well as the aforementioned exceptions depicted in Figs. 5.3 and 5.4), the details of equation (1) require further explanation. If it is assumed that the hydrodynamic drag force (depending on the medium viscosity, velocity, and grain diameter), the product $\left|B\vec{\nabla}B\right|$ (depending on the module and shape of the magnetic field), and the gravity forces are basically similar on average for all the substances (para-, antiferro-, ferri- and ferro-magnetic phases), then the performance observed must be related only to the dependence of magnetic susceptibility on the magnetic field applied for each mineral phase.

In this regard, it is important to note that the magnetic susceptibility of the ferro- and ferri-magnetic phases increases with the applied magnetic field up to a maximum. After this point, it decreases, becoming insignificant in the region of the high fields (note that temperatures in the separator are not close to the Curie points of these materials), where saturation of magnetisation is achieved (Stoletov curve [28]). In contrast, the para- and antiferro-magnetic phases have constant magnetic susceptibilities over the entire range of magnetic field strengths applied in the separator. These susceptibilities are several orders of magnitude lower than those of the initial ferro- and ferri-magnetic phases [29].

Thus, a magnetic induction, *B*, of at least 0.8 T on the surface of the Fe balls (minimum value conditioned by the difficulty to provide an accurate value with the Hall sensor) was measured at 60% of the maximum output voltage. This magnetic field was high enough to saturate some of the ferro and/or ferri-magnetic phases [30]. Consequently, the magnetic susceptibility of the para- and antiferro-magnetic phases exceeded that of the ferro- and ferri-magnetic phases, thus reducing the performance of the operation in terms of the recovery of ferro- and/ or ferri-magnetic particles.

3.2 Chemical characterisation

In view of the results shown in Table 5.2, the total concentration for most of the elements analysed (major and minor) was more than three times higher in the “mags” than in the “non-mags”. This was particularly evident for Zn, Fe and S, whereas other elements, for instance Pb and Ba, were more abundant in the “non-mags”.

Table 5.2 Weight percentage of some major and minor elements in the magnetically (mags) and non-magnetically (non-mags) separated fractions. Voltage corresponds to % of the maximum output.

Voltage	*Cu*	*Mn*	*Fe*	*Ca*	*P*	*Mg*	*Ba*	*Ti*	*Al*	*Na*	*K*	*S*	*Pb*	*Zn*
							%-w							
0	0.05	0.23	3.22	3.17	0.26	0.46	0.15	0.03	1.17	0.09	0.26	0.20	2.17	0.28
Mags														
5	0.16	0.25	15.99	5.89	0.17	0.74	0.02	0.09	1.96	0.45	0.53	1.07	1.70	2.70
10	0.15	0.32	13.22	6.27	0.19	0.88	0.02	0.08	1.92	0.39	0.52	0.91	1.95	2.13
20	0.13	0.43	13.49	6.11	0.22	1.21	0.04	0.09	2.12	0.38	0.54	0.72	1.93	1.95
30	0.12	0.44	10.19	5.85	0.27	1.20	0.04	0.08	1.97	0.28	0.49	0.56	1.99	1.29
60	0.13	0.53	10.70	6.29	0.30	1.45	0.04	0.09	2.12	0.26	0.53	0.54	2.14	1.22
90	0.14	0.53	10.99	6.36	0.29	1.47	0.04	0.09	2.11	0.27	0.53	0.58	2.04	1.22
Non-mags														
5	0.04	0.23	2.65	2.96	0.28	0.44	0.15	0.03	1.14	0.07	0.25	0.15	2.20	0.17
10	0.04	0.22	2.19	2.81	0.26	0.40	0.16	0.03	1.08	0.06	0.24	0.13	2.17	0.11
20	0.04	0.21	1.90	2.63	0.30	0.34	0.18	0.02	1.14	0.06	0.24	0.12	2.12	0.07
30	0.03	0.18	1.45	2.63	0.25	0.27	0.19	0.02	0.94	0.05	0.20	0.12	2.24	0.04
60	0.03	0.14	1.12	2.33	0.23	0.18	0.19	0.02	0.87	0.04	0.18	0.11	2.23	0.03
90	0.03	0.15	1.16	2.44	0.24	0.19	0.20	0.02	0.90	0.04	0.19	0.12	2.27	0.03

These results were evaluated again on the basis of the relation of two parameters, namely the ratio of concentration, γ, and recovery, ε. The former indicates the weight percentage of the original feed sample recovered in the "mags", while the latter designates the weight percentage of a specific metal from the feed that is retained in the same fraction.

Table 3 shows the recoveries in the "mags" for five elements (Fe, Zn, S, Pb and Ba) considered of interest in the decontamination. The ratio of concentration in this fraction ranged between 3.21% to 23.11%, while recovery varied between 0.46% and 92.44 %. The best recoveries were observed for Zn, while the worst were for Ba. In general, it can be concluded that the greater the recovery and the lower the ratio of concentration, the better the performance of the concentration operation. Consequently, it can be stated that the first three elements concentrated in the "mags", since recovery for these elements was superior to their ratio of concentration; in contrast, Pb and Ba were recovered mostly in the "non-mags".

Table 5.3 Ratio of concentration and recovery for Fe, Zn, Pb, S and Ba in the in the magnetically separated fraction (mags).

Voltage	*Ratio of concentration* γ *[%]*	*Recovery Zn* ε **[%]**	*Recovery Fe* ε **[%]**	*Recovery S* ε **[%]**	*Recovery Pb* ε **[%]**	*Recovery Ba* ε **[%]**
5	3.21	34.47	16.65	19.11	2.49	0.46
10	8.64	64.69	36.35	39.84	7.83	0.97
20	9.76	75.07	43.43	39.34	8.96	2.10
30	22.18	90.19	66.70	57.08	20.20	5.24
60	23.11	92.44	74.17	59.60	22.38	5.69
90	22.02	91.99	72.79	57.71	20.24	5.14

Finally, we also determined the separation efficiency (S.E.), following the definition given by Schulz [22]. Figure 5.7 shows the relative S.E. for the selected elements, as a function of the output voltage in the separator. In general, it was observed that this was achieved for S, Fe and Zn, while this was not the case for Ba and Pb. These observations indicate, as stated above, that the concentration for the latter elements took place in the "non-mags".

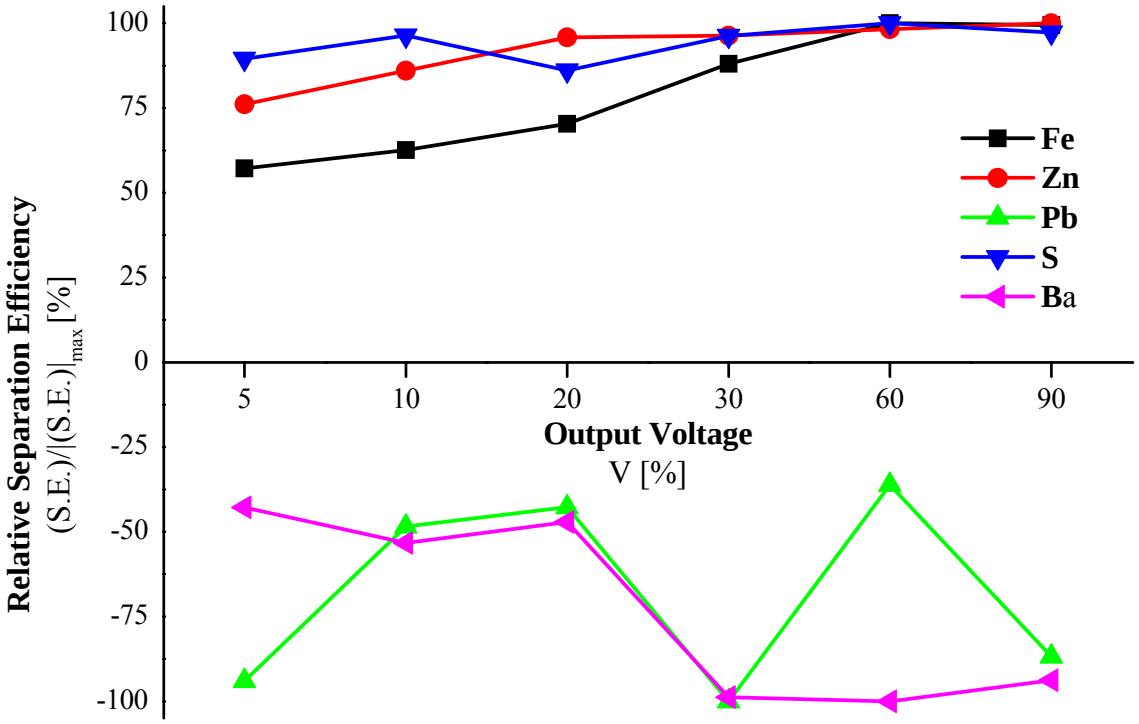

Figure 5. 7 Relative chemical separation efficiency for Fe, Zn, Pb, S and Ba as a function of output voltage.

Moreover, the dependence of the relative S.E. on the output voltage followed the behaviour observed for the magnetic S.E. (see Fig. 5.6), especially for Fe. This element was present mainly in the chemical formulae of the ferromagnetic phases identified in the magnetic characterisation (see section 3.1.2), and combined with Zn (connected with the majority of doped ferrites) or S (related with iron sulphides), probably formed the ferro- and/ or ferri-magnetic minerals of the soil. As in the previous case, S.E. peaked at 60 % of maximum output voltage for all these elements (see Table 5.3).

4. Conclusions

Pb metallurgy and mining facilities located in the San Genaro mining shaft (Linares, Spain) introduced anomalous concentrations of toxic elements into the surrounding area. A physical soil washing procedure via magnetic separation proved effective at removing a significant amount of the contaminants present in the soil.

The exhaustive magnetic characterisation performed allowed us to propose a general formulation for the quantification of the ferri- and ferro- magnetic phases in the soil. This magnetic characterisation detected the presence of ferri- or canted antiferro-magnetic minerals such as pyrrhotite, doped magnetites and goethite, which were identified over thermomagnetic curves.

Moreover, taking into consideration the total masses of ferri- and/ or ferro-magnetic phases in the "mags" and the "non-mags", we formulated a new expression to determine the yield of the magnetic separation operation on the basis of the properties of the materials separated at high magnetic fields.

The expression was used to study the magnetic yield as a function of the input voltage in the magnetic separator. We determined that higher efficiency is reached at 60% of the maximum input voltage. This finding allowed us to estimate the separation threshold for the different components of the soil treated in the magnetic separator. These results were consistent with those of the chemical characterisation. In summary, the findings reported in this study may be relevant for the implementation of strategies to separate hazardous materials that pose a risk to public health and safety.

Acknowledgements

Carlos Sierra obtained a grant from the "Severo Ochoa" programme (Ficyt, Asturias, Spain). The authors thank the "Servicio Cientifico-Técnico de Medidas

Magnéticas" of the University of Oviedo, and Dr. Julián Martínez, at the University of Jaén, for assistance provided in the elaboration of this paper.

References

[1] S. Blundell, Magnetism in Condensed Matter, Oxford Master Series in Physics, 2001.

[2] B.D. Cullity, C.D. Graham, Introduction to Magnetic Materials, John Willey & sons, 2008.

[3] J. Drzymala, Mineral Processing, Foundations of Theory and Practice of Minerallurgy, Oficyna Wydawnicza PWr., 2007. Available at: www.ig.pwr.wroc.pl/minproc (accessed January 2013).

[4] J. Svoboda, Magnetic Techniques for the Treatment of Materials, Kluwer Academic Publishers, 2004.

[5] B.A. Wills, T.J. Napier-Munn, Mineral Processing Technology: An Introduction to the Practical Aspects of Ore Treatment and Mineral Recovery, 7th ed., Butterworth-Heinemann, Burlington, MA, 2006.

[6] R.A. Rikers, P. Rem, W.L. Dalmijn, Improved Method for Prediction of Heavy Metal Recoveries from Soil Using High Intensity Magnetic Separation (HIMS), Int. J. Miner. Process, 54 (1998) 165–182.

[7] G. Dermont, M. Bergeron, G. Mercier, M. Richer-Laflèche, Soil Washing for Metal Removal: a Review of Physical/Chemical Technologies and Field Applications, J. Hazard. Mater., 152 (2008) 1–31.

[8] L.R. Avens, L.A. Worl, K.J. de Aguero, D.D. Padilla, F.C. Prenger, W.F. Stewart, D.D. Hill, T.L. Tolt, Magnetic Separation for Soil Decontamination. Los Álamos National Lab. NM (USA), 1993.

[9] C. Sierra, J. Martínez, J.M. Menéndez-Aguado, E. Afif, J.R. Gallego, High Intensity Magnetic Separation for the Clean-up of a Site Polluted by Lead Metallurgy, J. Hazard. Mater., 248–249 (2013) 194–201.

[10] J.M.D. Coey, Magnetism and Magnetic Materials, Cambridge University Press, 2010.

[11] Y. Liu, D.J. Sellmyer, D. Shindo (Eds), Handbook of Advanced Magnetic Materials, Springer, 2005.

[12] J. Martínez, J. Llamas, E. De Miguel, J. Rey, M.C. Hidalgo, Application of the Visman Method to the Design of a Soil Sampling Camping in the Mining District of Linares (Spain), J. Geochem. Explor. 92 (2007) 73–82.

[13] J. Martínez, J. Llamas, E. De Miguel, J. Rey, M.C. Hidalgo, Determination of Geochemical Background in a Metal Mining Site: Example of the Mining District of Linares (south Spain), J. Geochem. Explor. 94 (2008) 19–29.

[14] Carpco Wet High-Intensity Magnetic Separator model 3X4L. Available at: http://www.outotec.com/18470.epibrw (accessed April 2012).

[15] D. Martínez-Blanco, P. Gorria, J.A. Blanco, Nanostructured Fe Obtained by High-Energy Ball Milling170, J. Magn. Magn. Mater. 300 (2006) e339-e341.

[16] D. Gubbins, E. Herrero-Bervera E. (Eds), Encyclopedia of Geomagnetism and Paleomagnetism, Springer (2007).

[17] J.T. Ahrens (Ed), Rock Physics & Phase Relations: A Handbook of Physical Constants, American Geophysical Union Books Board (1995).

[18] G.P. Arrighini, M. Maestro, R. Moccia, Magnetic Properties of Polyatomic Molecules: Magnetic Susceptibility of H_2O, NH_3, CH_4, H_2O_2, J. Chem. Phys., 49 (1968) 882–889.

[19] É. du Trémolet de Lacheisserie, D. Gignoux, M. Schlenker (Eds.) Magnetism: Fundamentals. Grenoble Sciencies (2005).

[20] F. Martín-Hernández, E.C. Ferré, Separation of Paramagnetic and Ferromagnetic Anisotropies: A Review", J. Geophys. Res., 112 (2007) B03105.

[21] C. Richter, B.A. van der Pluijm, Separation of Paramagnetic and Ferrimagnetic Susceptibilities using Low Temperature Magnetic Susceptibilities and Comparison with High Field Methods", Phys. Earth Planet. Int., 83 (1994) 113-123.

[22] N.F. Schulz, Separation Efficiency, Transaction SME-AIME., 247 (1970) 81-87.

[23] Ö. Özdemir, D.J. Dunlop, Low-Temperature Properties of a Single Crystal of Magnetite Oriented Along Principal Magnetic Axes", Earth Planet. Sci. Lett., 165 (1999) 229–239.

[24] Ö. Özdemir, D.J. Dunlop, "Thermoremanence and Néel Temperature of Goethite", Geophys. Res. Lett., 23 (1996) 921–924.

[25] L. Néel , "Some New Results on Antiferromagnetism and Ferromagnetism", Rev. Mod. Phys., 25 (1953) 58–63.

[26] T. Nagata, Rock magnetism, Maruzen (1961).

[27] D. Martínez-Blanco, P. Gorria, J.A. Blanco, M.J. Pérez, J. Campo, Analysis of the diffraction-line broadening on nanostructured Fe: size-strain effects induced by milling and heating, J. Phys.: Condens. Matter 20 (2008) 335213 1-10.

[28] A. Stoletow, "Ueber die Magnetisirungsfunction des weichen Eisens, insbesondere bei schwächeren Scheidungskräften", Annalen der Physik, 222(7) (1872) 439–463.

[29] W. O´Reilly , Rock and mineral magnetism, Blackie (1984).

[30] E.C. Ferré, F. Martín-Hernández, C. Teyssier, M. Jackson, Paramagnetic and Ferromagnetic Anisotropy of Magnetic Susceptibility in Migmatites: Measurements in High and Low Fields and Kinematics Implications", Geophys. J Int., 157 (2004) 1119–1129.

CONCLUSIONS

1. Soil washing relevance

The existence of Brownfields, former contaminated industrial and/or mining sites located in the vicinity of major cities, often generates environmental, social, economic and urban planning problems. These are the reasons why much of the legislation in modern countries advocates the adoption of sustainable development principles.

In this connection, soil washing techniques area a good alternative, for at least reducing the amount of pollution in these sites. These procedures remove contaminants from soils, by concentrating them in a smaller volume, usually in a finer fraction. For this purpose, a combination of size separation, gravity, attrition or other processes is employed, with or without the use of chemical additives. The advantages are obvious: these techniques are well established in the chemical industry; the implementation is relatively simple; the operation is low in cost; and the equipment involved is well-known.

These procedures were tested in 3 different locations, after an exhaustive investigation of the soils. The conclusions obtained were as follows:

2. Soil washing tests at Nitrastur (Asturias, Langreo)

The roasting of pyrite ores contributed towards introduction of toxic elements, such as As, Pb, Cd, Ni, Cu and Hg, into the natural soils, causing a marked multi component contamination. Most of these pollutants were bound to the soil organic matter and, secondarily, to Fe oxyhydroxides, while processes, such as clay adsorption,

made a minor contribution. The decontamination process by means of hydrocyclones proved a marked effect of the soil organic matter into the separation process, to such an extent as to say that in this case, rather than achieving separation by sizes, the separation of the contaminants occurred through specific gravity. The process allowed us to obtain concentration factors higher than 2.2 for all the contaminants in less than 20% of the weight of the original soil. This proved that full-scale treatment with successive rewashing cycles was feasible.

3. Soil washing tests at La Soterraña (Pola de Lena, Asturias)

Hg and As were the primary soil pollutants found in the mining and metallurgy area. From geochemical, edaphological and mineralogical data, we have demonstrated that Hg is mainly concentrated in fine grain fractions (below 200 μm), where it is present in the original sulphide form and bound to Fe–Mnoxyhydroxides. In contrast, As is abundant in fine-medium (below 500 μm) fractions and predominantly linked to Fe mineral phases as well. In fact, the mineralogical data reflected the low liberation degree of As and Hg in sandy fractions, and, thus, the yields of gravimetric or grain-size separation of these fractions would be unsatisfactory.

In the context of the feasibility study, the C800 separator proved effective for studying narrow grain-size intervals whenever significant differences in specific-gravity within the particles of the soil were detected. Accordingly, an interesting alternative, though possibly expensive, consisted of prior milling of the medium and coarse fractions in order to allow treatment. In this context, the grindability test is a novel approach carried out to indicate the extent of power consumption and its influence on the energy efficiency and potential recovery of pollutants.

4. Soil washing tests at Linares mining and metallurgy sites

4.1 La Cruz lead foundry

The study in the Brownfield of La Cruz site showed soils with anomalous contents of Cd, Cu, Mn, Zn, As and especially Pb in the polluted area surrounding the abandoned smelter. Geochemical and mineralogical data revealed that most of the pollutants are evenly distributed in all the grain-size fractions.

Lead-slag, a common waste generated by lead metallurgy, was directly mixed with soil and is, therefore, the most important source of anthropogenic accumulation of heavy metals at the study site, which is also affected by ore stockpiling and particulate emissions from both heaps of lead slag and lead slag chimneys.

The major constituents of the lead slag were Fe, Si, Ca, Al and Mg, as well as marked concentrations of Zn, Pb, Mn, As and Cu. From a mineralogical point of view, Pb spherules, Fe oxides (Wüstite) and complex inter-metallic compounds were present in the slag. The abundance of Fe in the slag and in the other sources of soil contamination pointed towards the feasibility of applying magnetic separation.

A magnetism study showed that the magnetic properties of the slag mainly corresponded with a para- and/or antiferromagnetic material; evidencing a weak ferro- and/or ferri-magnetic contribution, which was not caused mainly by the presence of ferromagnetic Fe. Therefore, in this case, HIMS equipment is required for a magnetic soil washing treatment.

Dry-HIMS proved to be an effective tool for the decontamination of this soil in the coarser fractions (between 0.5 and 4 mm). The recoveries by wet-HIMS were lower in case of finer fractions (between 63 and 500 microns). However, in this sort of soil

(sandy, arid and combined with slag particles), both the separation techniques demonstrated their effectiveness for processing a wide range of grain-size fractions. This implies that a significant and cost-effective reduction of the volume of contaminated soil could be obtained in a single real-scale step, something unusual in a soil washing process.

4.2 San Genaro mining shaft

The kinds of pollutants in this case were similar to the ones in the previous case. The performance of exhaustive magnetic characterization enabled the quantification of the ferri- and ferro- magnetic phases contained in the soil. This magnetic characterization enabled detecting the presence of ferrimagnetic or canted antiferromagnetic minerals, such as pyrrhotite, doped magnetites and goethite, which were identified over thermomagnetic curves. The separation of the contaminated fractions via wet-HIMS proved to be feasible. The higher separation efficiency was reached at 60% of the maximum input voltage, according to the chemical characterization. This enabled establishing an estimation of the separation threshold for the different components of the soil treated in the magnetic separator.

5. Conclusions regarding obtaining the optimal concentration conditions

It has been demonstrated that attributive analysis can be an effective tool for the quantitative determination of the quality of separations and also for establishing weighting factors, based on the diverse elements to be removed.

The equation for obtaining the optimal concentration conditions can be summarized as follows:

$$Q_T{}^j = \frac{\sum_{i=1}^{n} Ai\left(\frac{\mathrm{Re}\,nd^{\min}}{\mathrm{Re}\,nd^{j}} + \frac{\mathrm{Re}\,c_i^{j}}{\mathrm{Re}\,c_i^{\max}}\right)}{\sum_{i=1}^{n} Ai}$$

$$\left\{\forall N, \mathrm{Re}c, \mathrm{Re}nd, Vo : n \in \mathrm{N}, \mathrm{Re}c''i''\mathrm{Re}nd \in [0,100], Vo \in [VLA, 10^6], Q_i \in (0,2n)\right\}$$

Wherein:

Rec= Recovery

Rend =Ratio of concentration

Vo = Initial concentration of the pollutants in the soil

VLA= Maximum value accepted by the Administration

n = Number of pollutants

i= Considered pollutant

j= Number of the test

Additional tests performed on the basis of this equation indicate that it is preferable to standardize the concentration of the pollutants before introducing the data into the equation. Moreover, a new expression to determine the yield of the magnetic separation operation, based on the magnetic properties of the separated materials, has been formulated, taking into consideration the total masses of ferri- and/ or ferro- magnetic phases contained in the mags and in the non-mags, which were calculated according to

$$z = \frac{m^M \kappa^M + m^{NM} \kappa^{NM} - m^0 \kappa^0}{\frac{\sigma_S^0 - \sigma_S^{NM}}{\sigma_S^M - \sigma_S^{NM}} \kappa^M + \frac{\sigma_S^M - \sigma_S^0}{\sigma_S^M - \sigma_S^{NM}} \kappa^{NM} - \kappa^0}$$

Thus, if the expression for the determination of the separation efficiency proposed by Schulz is particularized for the mass of ferri- and/ or ferro- magnetic phases in the mags, non-mags and soil samples determined according to the preceding equation, it is obtained that:

$$\zeta\,[\%] = \left(\frac{m^{0}\,\frac{x}{z} - m^{M}}{m^{0} - z} \right) \cdot 100$$

Wherein:

- m^{0} = mass of the initial feeding sample.
- m^{M} = mass of the mags.
- x = mass of ferrimagnetic materials in the mags.
- z = mass of ferri- and/or ferro-magnetic materials in initial feeding sample.

The expression was used to study the magnetic yield as a function of the input voltage in the magnetic separator. This finding enabled us to estimate the separation threshold for the different components of the soil treated in the magnetic separator. These results were consistent with those obtained from the chemical characterization.

In summary, soil washing proved to be an effective tool for the removal of heavy metals, at both industrial and mining and metallurgy Brownfields. All the findings reported in this study can be relevant for implementing strategies to separate hazardous materials that pose a risk to public health and safety.

ANNEX I: Tool to obtain the optimal concentration conditions in soil washing processing by means of attributive analyses.

The ensuing lines correspond to the algorithm of attributive analysis, programmed in java, as they have been registered in the Intellectual Property Registry of the Principality of Asturias by Resolution of June 19, 2012 (registration entry: 05/2012/255) as part of the software COS which is provided in an CD attached to the thesis.

Authors: C. Sierra, J. L. R. Gallego,

S.Gutiérrez Rodríguez, J. M. Menéndez-Aguado.

```
package experiment;

public class Experiment {
	private double[][] weightsAssaysTable;
	private double[][] ratioRecoveryTable;
	private double[][] ratioRecoveryDiscardTable;
	private double[] totalAssaysValues;
	private double[] referenceValues;
	private double[] AFactors;
	private double[] BFactors;
	private double[][] maxRecoveryMinRatioTable;
	private double[][] unponderatedMeritIndexTable;
	private double[][] ponderatedMeritIndexTable;
	private double[] unponderatedEssayMeritIndex;
	private double[] globalEssayMeritIndex;
	private double[][] maxMinGeneralTable;
	private int maxProperties;
	private double[][] unponderatedGeneralTable;
	private double[] generalReferenceValues;
	private double[][] ponderatedGeneralTable;
	private double[] ponderatedElementsValues;
	private double[] unponderatedElementsValues;

	/**
	 * Set the general reference values(General module)
	 *
```

```
       * @param generalReferenceValues
       */
      public         void         setGeneralReferenceValues(double[]
generalReferenceValues) {
            this.generalReferenceValues = generalReferenceValues;
      }

      /**
       *  Set  the  refenrence  values(Soil  Washing/Mineral  Dressing
module)
       *
       * @param referenceValues
       */
      public void setReferenceValues(double[] referenceValues) {
            this.referenceValues = referenceValues;
      }

      /**
       * Set the bulk sample values
       *
       * @param totalAssaysValues
       */
      public  void  setTotalAssaysValues(double[]  totalAssaysValues)
{
            this.totalAssaysValues = totalAssaysValues;
      }

      /**
       * Set The data from the weights assays.
       *
```

```
       * @param weightsAssaysTable
       */
      public          void          setWeightsAssaysTable(double[][]
weightsAssaysTable) {
            this.weightsAssaysTable = weightsAssaysTable;
      }


      /**
       * Set the data from the elements properties panel
       *
       * @param maxProperties
       * @param maxMinGeneralTable
       */
      public void setMaxMinGeneralTable(int maxProperties,
                  double[][] maxMinGeneralTable) {
            this.maxMinGeneralTable = maxMinGeneralTable;
            this.maxProperties = maxProperties;
      }


      /**
       * Calcs the ratio recoveries data.
       */
      private void calcRatioRecoveryTable() {
            double[][]           tempTable           =           new
double[weightsAssaysTable.length][weightsAssaysTable[0].length];
            for (int i = 0; i < tempTable.length; i++) {
                  calcRatio(i, tempTable);
            }
            for (int i = 0; i < tempTable.length; i++) {
```

```
                for (int j = 1; j < tempTable[0].length; j++) {
                      calcRecovery(i, j, tempTable);
                }
          }
          ratioRecoveryTable = tempTable;
     }

     /**
      * calc the ratios
      *
      * @param pos
      * @param tempTable
      */
     private void calcRatio(int pos, double[][] tempTable) {
          int mod = pos % 2;// the module to know the sample that
the value
                                    // belongs
          if (mod == 0) {// it's from L sample
                tempTable[pos][0] = weightsAssaysTable[pos][0]
                          /     (weightsAssaysTable[pos][0]     +
weightsAssaysTable[pos + 1][0]);
          }
          if (mod != 0) {
                tempTable[pos][0] = weightsAssaysTable[pos][0]
                          /     (weightsAssaysTable[pos][0]     +
weightsAssaysTable[pos - 1][0]);
          }
     }

     /**
```

```
       * calc the recoveries

       *

       * @param row

       * @param column

       * @param tempTable

       */

      private void calcRecovery(int row, int column, double[][]
tempTable) {

            int mod = row % 2;

            if (mod == 0) {

                  tempTable[row][column]                              =
(weightsAssaysTable[row][column] * weightsAssaysTable[row][0])

                              /  ((weightsAssaysTable[row][column]  *
weightsAssaysTable[row][0]) + (weightsAssaysTable[row + 1][column]
* weightsAssaysTable[row + 1][0]));

            }

            if (mod != 0) {

                  tempTable[row][column]                              =
(weightsAssaysTable[row][column] * weightsAssaysTable[row][0])

                              /  ((weightsAssaysTable[row][column]  *
weightsAssaysTable[row][0]) + (weightsAssaysTable[row - 1][column]
* weightsAssaysTable[row - 1][0]));

            }

      }



      /**

       * calc a table discarding the values recovery<ratio

       */

      private void calcDiscardTable() {

            // if(ratioRecoveryTable==null)

            calcRatioRecoveryTable();
```

```
            double[][]             temp             =             new
double[ratioRecoveryTable.length][ratioRecoveryTable[0].length];

            for (int i = 0; i < temp.length; i++) {

                  for (int j = 0; j < temp[0].length; j++) {

                        if (j == 0)

                              temp[i][j] = ratioRecoveryTable[i][j];

                        else    if    (ratioRecoveryTable[i][j]    <
ratioRecoveryTable[i][0])

                              temp[i][j] = 0;

                        else

                              temp[i][j] = ratioRecoveryTable[i][j];

                  }

            }

            ratioRecoveryDiscardTable = temp;

      }



      /**

       * Calc the unweighted index table

       */

      private void calcUnponderatedMeritIndexTable() {

            // if(ratioRecoveryDiscardTable==null);

            calcDiscardTable();

            double[][]           tempTable           =           new
double[ratioRecoveryDiscardTable.length][ratioRecoveryDiscardTable[
0].length - 1];

            double[] minRatio = findMinRatio();// for each element

            double[]  maxRecovery  =  findMaxRecovery();//  for  each
element

            for (int j = 0; j < tempTable[0].length; j++) {

                  for (int i = 0; i < tempTable.length; i++) {

                        if (ratioRecoveryDiscardTable[i][j + 1] != 0)
```

```
                              tempTable[i][j]                          =
calcMaxRecovery(maxRecovery[j],

      ratioRecoveryDiscardTable[i][j + 1])

                                      + calcMinRatio(minRatio[j],

      ratioRecoveryDiscardTable[i][0]);

                  }

            }

            unponderatedMeritIndexTable = tempTable;

      }


      /**

       * find the maximum recovery

       *

       * @param maxRecovery

       * @param recovery

       * @return

       */

      private  double  calcMaxRecovery(double  maxRecovery,  double
recovery) {

            return recovery / maxRecovery;

      }


      /**

       * find the minimum ratio

       *

       * @param minRatio

       * @param ratio

       * @return
```

```
	 */
	private double calcMinRatio(double minRatio, double ratio) {
		return minRatio / ratio;
	}

	private double[] findMinRatio() {
		double[] min = new double[ratioRecoveryDiscardTable[0].length - 1];
		for (int i = 0; i < min.length; i++) {
			min[i] = Double.MAX_VALUE;
		}

		for (int i = 0; i < ratioRecoveryDiscardTable.length; i++) {
			for (int j = 1; j < ratioRecoveryDiscardTable[0].length; j++) {
				if (ratioRecoveryDiscardTable[i][j] != 0) {
					if (ratioRecoveryDiscardTable[i][0] < min[j - 1])
						min[j - 1] = ratioRecoveryDiscardTable[i][0];
				}
			}
		}
		return min;
	}

	private double[] findMaxRecovery() {
		double[] max = new double[ratioRecoveryDiscardTable[0].length - 1];
		for (int i = 0; i < max.length; i++) {
```

```
                max[i] = Double.MIN_VALUE;
            }
            for (int j = 0; j < max.length; j++)
                for (int i = 0; i < ratioRecoveryDiscardTable.length; i++)
                    if (ratioRecoveryDiscardTable[i][j + 1] > max[j])
                        max[j] = ratioRecoveryDiscardTable[i][j + 1];
            return max;
      }

      /**
       * calc the weighted merit index table
       */
      private void calcPonderatedMeritIndexTable() {
            calcUnponderatedMeritIndexTable();
            calcBFactors();
            double[][] temp = new double[unponderatedMeritIndexTable.length][unponderatedMeritIndexTable[0].length];
            for (int j = 0; j < temp[0].length; j++) {
                for (int i = 0; i < temp.length; i++) {
                    temp[i][j] = BFactors[j] * unponderatedMeritIndexTable[i][j];
                }
            }
            ponderatedMeritIndexTable = temp;
      }

      /**
```

```
       *Calc the A weighting coefficients A=initial/reference.
       */
      private void calcAFactors() {
            AFactors = new double[this.totalAssaysValues.length];
            for (int i = 0; i < AFactors.length; i++) {
                  AFactors[i]    =    this.totalAssaysValues[i]    /
this.referenceValues[i];
            }
      }

      /**
       * Calc the B weighting coefficients=A/sum(A).
       */
      private void calcBFactors() {
            calcAFactors();
            BFactors = new double[AFactors.length];
            double AFactorsSum = 0;

            for (int i = 0; i < AFactors.length; i++) {
                  AFactorsSum += AFactors[i];
            }

            for (int i = 0; i < BFactors.length; i++) {
                  BFactors[i] = AFactors[i] / AFactorsSum;
            }
      }

      /**
       * calc the unweighted merit index table;
```

```
       */
      private void calcUnponderatedMeritIndex() {
            calcUnponderatedMeritIndexTable();
            double[] temp = new
double[unponderatedMeritIndexTable.length];
            for (int i = 0; i < unponderatedMeritIndexTable.length;
i++) {
                  for (int j = 0; j <
unponderatedMeritIndexTable[0].length; j++) {
                        temp[i] += unponderatedMeritIndexTable[i][j];
                  }
            }
            unponderatedEssayMeritIndex = temp;
      }

      /**
       * calc the globla essay merit index
       */
      private void calcGlobalEssayMeritIndex() {
            calcPonderatedMeritIndexTable();
            double[] temp = new
double[ponderatedMeritIndexTable.length];
            for (int i = 0; i < temp.length; i++) {
                  for (int j = 0; j <
ponderatedMeritIndexTable[0].length; j++) {
                        temp[i] += ponderatedMeritIndexTable[i][j];
                  }
                  globalEssayMeritIndex = temp;
            }
      }
```

```
	/**
	 * calc the unweigthed general table.
	 */
	private void calcUnponderatedGeneralTable() {
		double[][] temp = new
double[maxMinGeneralTable.length][maxMinGeneralTable[0].length];
		double[] maxPropertiesMaxValues =
findMaxPropertiesMaxValues();
		double[] minPropertiesMinValues =
findMinPropertiesMinValues();
		int offset = maxPropertiesMaxValues.length;
		for (int j = 0; j < maxMinGeneralTable[0].length; j++) {
			for (int i = 0; i < maxMinGeneralTable.length;
i++) {
				if (j < maxPropertiesMaxValues.length)
					temp[i][j] = maxMinGeneralTable[i][j]
							/ maxPropertiesMaxValues[j];
				else
					temp[i][j] = minPropertiesMinValues[j -
offset]
							/ maxMinGeneralTable[i][j];
			}
		}
		unponderatedGeneralTable = temp;
	}

	/**
	 * calc the unweighted elements values
	 */
	private void calcUnponderatedElementsValues() {
		calcUnponderatedGeneralTable();
```

```
            double[]             temp             =             new
double[unponderatedGeneralTable.length];

            for  (int  i  =  0;  i  <  unponderatedGeneralTable.length;
i++) {

                  for      (int      j      =      0;      j      <
unponderatedGeneralTable[0].length; j++) {

                        temp[i] += unponderatedGeneralTable[i][j];

                  }

            }

            unponderatedElementsValues = temp;

      }


      private double[] findMaxPropertiesMaxValues() {

            double[] max = new double[maxProperties];

            for (int i = 0; i < max.length; i++) {

                  max[i] = Double.MIN_VALUE;

            }

            for (int j = 0; j < max.length; j++) {

                  for  (int  i  =  0;  i  <  maxMinGeneralTable.length;
i++) {

                        if (maxMinGeneralTable[i][j] > max[j])

                              max[j] = maxMinGeneralTable[i][j];

                  }

            }

            return max;

      }


      private double[] findMinPropertiesMinValues() {

            double[] min = new double[maxMinGeneralTable[0].length -
maxProperties];

            int offset = maxProperties;
```

```
            for (int i = 0; i < min.length; i++) {
                  min[i] = Double.MAX_VALUE;
            }
            for (int j = 0; j < min.length; j++) {
                  for (int i = 0; i < maxMinGeneralTable.length;
i++) {
                        if (maxMinGeneralTable[i][j + offset] <
min[j])
                              min[j] = maxMinGeneralTable[i][j +
offset];
                  }
            }
            return min;
      }


      /**
       * calc the weighted general table
       */
      private void calcPonderatedGeneralTable() {
            calcUnponderatedGeneralTable();
            double[][] temp = new
double[unponderatedGeneralTable.length][unponderatedGeneralTable[0]
.length];
            for (int i = 0; i < temp.length; i++) {
                  for (int j = 0; j < temp[0].length; j++) {
                        temp[i][j] = generalReferenceValues[j]
                                    * unponderatedGeneralTable[i][j];
                  }
            }
            ponderatedGeneralTable = temp;
      }
```

```
	/**
	 * calc the weighted elements values
	 */
	private void calcPonderatedElementsValues() {
		calcPonderatedGeneralTable();
		double[] temp = new double[ponderatedGeneralTable.length];
		for (int i = 0; i < ponderatedGeneralTable.length; i++) {
			for (int j = 0; j < ponderatedGeneralTable[0].length; j++) {
				temp[i] += ponderatedGeneralTable[i][j];
			}
		}
		ponderatedElementsValues = temp;
	}

	public double[] getGlobalQualityIndex() {
		calcGlobalEssayMeritIndex();
		return globalEssayMeritIndex;
	}

	public double[] getUnponderatedGlobalQualityIndex() {
		calcUnponderatedMeritIndex();
		return unponderatedEssayMeritIndex;
	}

	public double[][] getRatioRecoveryDiscardTable() {
		calcDiscardTable();
```

```
        return ratioRecoveryDiscardTable;
    }

    public double[][] getUnponderatedMeritIndexData() {
        calcUnponderatedMeritIndexTable();
        return unponderatedMeritIndexTable;
    }

    public double[][] getPonderatedMeritIndexData() {
        calcPonderatedMeritIndexTable();
        return ponderatedMeritIndexTable;
    }

    public double[][] getRatioRecoveryTable() {
        calcRatioRecoveryTable();
        return ratioRecoveryTable;
    }

    public double[] getTotalAssaysValues() {
        return totalAssaysValues;
    }

    public double[] getReferenceValues() {
        return referenceValues;
    }

    public double[][] getWeightsAssaysData() {
        return weightsAssaysTable;
```

```
	}

	public double[][] getUnponderatedGeneralTable() {
		calcUnponderatedGeneralTable();
		return unponderatedGeneralTable;
	}

	public double[][] getPonderatedGeneralTable() {
		calcPonderatedGeneralTable();
		return ponderatedGeneralTable;
	}

	public double[] getPonderatedElementsValues() {
		calcPonderatedElementsValues();
		return ponderatedElementsValues;
	}

	public double[] getUnponderatedElementsValues() {
		calcUnponderatedElementsValues();
		return unponderatedElementsValues;
	}
}
```

ANNEX II: Published works

Index

Index of figures

Index of tables